Journal of the OPTICAL SOCIETY *of* AMERICA

VOLUME 38
No. 6

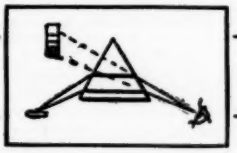

JUNE
1948

Reflection and Transmission Interference Filters. Part II. Experimental, Comparison with Theory, Results . . . . . L. N. HADLEY AND D. M. DENNISON 483

Projection Screens for Home Television Receivers . . . . . R. R. LAW AND I. G. MALOFF 497

Case of Unilateral Deuteranopia . . . . . LOUISE L. SLOAN AND LORRAINE WOLLACH 502

Industrial Application of Geiger-Müller Counters to the Analysis of Phosphorus in Steels . . . . . FORD R. BRYAN AND GEORGE A. NAHSTOLL 510

Quantitative Spectrographic Analysis of the Rare Earth Elements. I. Determination of Samarium in Neodymium. II. Determination of Europium in Samarium . . . . . VELMER A. FASSEL AND HARLEY A. WILHELM 518

Normal Probability Curve as an Approximation to the Distribution Curve of the High Intensity Searchlight . . . . . FRANK BENFORD AND JOHN E. BOCK 527

Illuminant-Stable Color Vision Test, I . . . . . ELLIS FREEMAN 532

Quantitative Spectrochemical Determination of Barium, Strontium, and Calcium . . . . . WERNER HARTMANN AND BETTY E. PRESCOTT 539

Athermalization of Optical Systems . . . . . DAVID S. GREY 542

Erratum: Reflection and Transmission Interference Filters. Part I. Theory . . . . . L. N. HADLEY AND D. M. DENNISON 546

Condensed Arc Source Unit for Spectrochemical Analysis . . . . . D. A. SINCLAIR 547

Color Variations in Glasses Containing Iron . . . . . JOHN W. FORREST, NORBERT J. KREIDL, AND TYLER G. PETT 554

Book Review 560

Published monthly
at Prince and Lemon Sts., Lancaster, Pa.
by the
AMERICAN INSTITUTE OF PHYSICS
Incorporated
57 East 55 Street, New York 22, New York
FOR AND UNDER THE EDITORIAL SUPERVISION OF THE
OPTICAL SOCIETY OF AMERICA

THE OPTICAL SOCIETY OF AMERICA

Officers of the Society

RUDOLF KINGSLAKE, *President*
Eastman Kodak Company
Rochester, New York

WILLIAM F. MEGGERS, *Vice President*
National Bureau of Standards
Washington 25, D. C.

ARTHUR C. HARDY, *Secretary*
Massachusetts Institute of Technology
Cambridge 39, Massachusetts

W. W. GRAEPER, *Treasurer*
Bausch & Lomb Optical Company
Rochester 2, New York

The Board of Directors consists of the above officers; the Editor of the Journal; the Past President; and five directors-at-large.

G. R. HARRISON, *Editor and Past President*
Massachusetts Institute of Technology
Cambridge 39, Massachusetts

Directors-at-Large

FRANK BENFORD
General Electric Company
Schenectady, New York

F. M. BISHOP
Eastman Kodak Company
Rochester 4, New York

WALLACE R. BRODE
Ohio State University
Columbus 10, Ohio

A. H. BENNETT
American Optical Company
Buffalo 11, New York

E. H. LAND
Polaroid Corporation
Cambridge, Massachusetts

Local Sections

STANLEY S. BALLARD, *Secretary for Local Sections*

Rochester Section

ARTHUR F. TURNER, *President*
ROBERT N. WOLFE, *Vice President*
PAUL W. STEVENS, *Secretary*
HOMER C. IMES, *Treasurer*

Detroit Section

GERALD M. RASSWEILER, *Chairman*
JOHN SCHUCH, *Vice Chairman*
DANIEL L. HARMON, *Secretary*
HENRY TUTTLE, *Treasurer*

Niagara Frontier Section

ALLEN B. FUHR, *President*
GUY H. FETTERLEY, *Secretary*
HOYT G. THOMPSON, *Treasurer*

Patrons

AMERICAN OPTICAL COMPANY — BAUSCH & LOMB OPTICAL COMPANY
EASTMAN KODAK COMPANY

Corporation Members

ALLIED CHEMICAL AND DYE CORPORATION, NATIONAL ANILINE DIVISION, Buffalo, New York
AMERICAN CYSTOSCOPE MAKERS, INC., New York, New York
AMERICAN OPTICAL COMPANY, Southbridge, Massachusetts
ARGUS, INCORPORATED, Ann Arbor, Michigan
BAUSCH & LOMB OPTICAL COMPANY, Rochester, New York
BELL & HOWELL COMPANY, Chicago, Illinois
BELL TELEPHONE LABORATORIES, INC., New York, New York
CENTURY LIGHTING, INC., New York, New York
CORNING GLASS WORKS, Corning, New York
R. R. DONNELLEY & SONS COMPANY, Chicago, Illinois
E. I. DUPONT DE NEMOURS & COMPANY, INC., Chemical Department, Experimental Station, Wilmington, Delaware
EASTMAN KODAK COMPANY, Rochester, New York
EDMUND SALVAGE COMPANY, Oaklyn-Audubon, New Jersey
FAIRCHILD AVIATION CORPORATION, Jamaica, New York
FARRAND OPTICAL COMPANY, INC., New York, New York
FISH-SCHURMAN CORPORATION, New York, New York
GAERTNER SCIENTIFIC CORPORATION, Chicago, Illinois
W. & L. E. GURLEY, Troy, New York
INTERCHEMICAL CORPORATION, New York, New York
KEUFFEL & ESSER COMPANY, Hoboken, New Jersey
KOLLSMAN INSTRUMENT DIVISION OF SQUARE D COMPANY, Elmhurst, New York
NATIONAL CARBON COMPANY, Cleveland, Ohio
NATIONAL TECHNICAL LABORATORIES, South Pasadena, California
PERKIN-ELMER CORPORATION, Glenbrook, Connecticut
POLAROID CORPORATION, Cambridge, Massachusetts
PORTMAN MACHINE TOOL COMPANY, New Rochelle, New York
SIMPSON OPTICAL MANUFACTURING COMPANY, Chicago, Illinois
SOCONY-VACUUM LABORATORIES, Paulsboro, New Jersey
ARTHUR H. THOMAS COMPANY, Philadelphia, Pennsylvania
UNIVIS LENS COMPANY, Dayton, Ohio
ZENITH OPTICAL COMPANY, Huntington, West Virginia

THE OPTICAL SOCIETY OF AMERICA was organized in 1916 *"to increase and diffuse the knowledge of optics in all its branches, pure and applied, to promote the mutual interests of investigators of optical problems, of designers, manufacturers and users of optical instruments and apparatus of all kinds and to encourage cooperation among them."* It aims to serve the interests of all who are engaged in any branch of optics from fundamental research to the manufacture of optical goods.

MEMBERSHIP

Regular Members: "Any person who has contributed materially to the advancement of optics is eligible for regular membership."

Associate Members: "Any person who is interested in optics is eligible for associate membership."

Corporate Members: "Any corporation desirous of encouraging the work of the Society is eligible for corporation membership."

Patrons: The payment, within any one year, of $1000 or more toward the expenses of the Society by any corporation or individual entitles such corporation or individual to the rank of patron.

The Society cordially invites to membership all who are interested in any branch of optics, either in research, in instruction, in optical or illuminating engineering, in the manufacture and distribution of optical goods of all kinds, or in physiological and medical optics.

ANNUAL DUES

Regular members, $8.50; Associate members, $6.00; Corporate members, $50.00. These dues include subscription to the Society's official journal, the *Journal of the Optical Society of America.*

CHANGES OF ADDRESS

All changes of address of members of the Optical Society of America should be communicated to the Secretary, Professor Arthur C. Hardy, Massachusetts Institute of Technology, Cambridge 39, Massachusetts.

Journal of the
OPTICAL SOCIETY
of AMERICA

VOLUME 38, NUMBER 6 JUNE, 1938

Reflection and Transmission Interference Filters

Part II. Experimental, Comparison with Theory, Results

L. N. HADLEY* AND D. M. DENNISON
University of Michigan, Ann Arbor, Michigan

(Received November 24, 1947)

Reflection and transmission filters have been constructed by the evaporation process, and their properties have been measured and shown to conform with the theory developed in Part I of this paper. A more extended set of curves of the reflection and transmission coefficients and the phase shift angles of a single metal film are given. From these curves, and from measurements made on the transmission filter, the optical constants of silver films are deduced and shown to be in agreement with other published data. A typical spectrogram of an infra-red reflection filter is also given, showing a minimum reflection coefficient of less than one percent at the odd overtones of the fundamental frequency.

INTRODUCTION

IN Part I of this paper[1] the theory of reflection and transmission interference filters was developed. This development was based on the optical properties of a single metallic layer sandwiched between two dielectric layers. It was shown that the characteristics of each of the two types of filters could be expressed in terms of the reflection and the transmission coefficients, R and T, of a single metal film, the phase shift angles which occur in reflection and in transmission, y and u, and other parameters, which included the thickness Δ of the separating dielectric layer, the index of refraction n_3 of the dielectric layer involved, the angle of incidence θ, and the wave-length λ.

It will be convenient to rewrite here the two filter equations. The transmission coefficient T_F of the transmission filter is given by

$$T_F=\frac{T^2}{(1-R^L)^2+4R^L\sin^2\left[\frac{2\pi\Delta(n_3^2-\sin^2\theta)^{\frac{1}{2}}}{\lambda}+y^L\right]}.$$

The reflection coefficient of the reflection filter is (in the infra-red region)

$$R_F=\frac{(1-f)^2+n^2\cot^2(2\pi n\Delta/\lambda)}{(1+f)^2+n^2\cot^2(2\pi n\Delta/\lambda)}.$$

It will be recalled that the superscripts R and L over T, R, and y indicate an asymmetry in these quantities because of the different indices of refraction of the two dielectric media on either side of the metal film. The value of R^L, for example, is the value determined when a wave is

* Now at Wilder Laboratory of Physics, Dartmouth College, Hanover, N. H.

[1] L. N. Hadley and D. M. Dennison, J. Opt. Soc. Am. 36, 451 (1947).

being propagated from the dielectric n_3 toward the dielectric n_1. It will also be recalled that a very great simplification occurs for the reflection coefficient of the reflection filter when the incident radiation is in the infra-red region: namely, both R and T of the single metal film can be expressed in terms of a quantity f which is a measure of the d.c. resistance of the film.

One further item to be mentioned here is that the reflection and transmission coefficients of the single metal film were expressed in terms of the index of refraction η, the extinction coefficient κ, and the thickness s of the metal film, the two indices of refraction n_1 and n_3 of the dielectric media on either side of the film, the angle of incidence θ, and the wave-length λ. The phase angle y was also expressed in terms of these same parameters. In a later section of Part II, curves of R, T, and y as functions of these parameters will be given in some detail.

It is the purpose of Part II of the paper to describe the production of experimental filters and to show how the theory previously developed applies to these filters. As a consequence, from measurements made on experimental filters, we may determine the optical constants of the components of the filter.

APPARATUS AND MANUFACTURE OF FILTERS

All filters were produced by the vacuum evaporation method. In each case the supporting substrate (region V of Fig. 11, and the supporting layer for region IV of Fig. 9, Part I) was ordinary plate glass. The vacuum system used consisted of two bell jars of diameter 12″ and height 18″, whose base plates were connected by means of a large T to a 4″ oil diffusion pump. Pressures of the order of 10^{-5} mm of Hg were maintained during evaporation. The speed of the system was such that this pressure was attained in about 20 minutes after the pumps were turned on.

Electrical connections for the various filaments and crucibles used in the evaporation were brought in through the base plates. These connections were made sufficiently vacuum tight by the use of rubber gaskets. The power source for the filaments was capable of supplying up to about 10 volts at 100 amperes. Continuous variation of the supply voltage was achieved by a type S649 Powerstat operating through a 110 v-11 v, 1500-kva filament transformer. A smaller auxiliary power supply was available for the few instances in which it was desired to have two filaments operating simultaneously. A 15000-v neon sign transformer, with suitable connections into each vacuum chamber, was used for outgassing. Pressures were measured by means of an ionization gauge inserted in the T mentioned above.

Satisfactory techniques for the evaporation of most of the metals used are described in an article by Olsen, Smith, and Crittenden.[2] The technique for evaporation of dielectric layers is very similar, and a number of variations were tried. Of the various dielectric materials used, successful evaporations were obtained from a helical tungsten filament, a conical tungsten basket (wound from 0.020″ or 0.030″ tungsten wire), a crucible made by painting a conical tungsten basket with a solution of levigated alumina in water, a "boat" made from a flat tantalum strip, and finally by placing the dielectric material in a small alundum crucible and heating the dielectric by radiation from a flat spiral tungsten filament placed in the opening of the crucible.

One of the major difficulties was that of obtaining layers (both metal and dielectric) of uniform thickness. Best results were obtained for the metal layers by making the distance between source and filter as large as possible. This distance was usually from 30 to 40 cm. If the filament is considered as a point source of radiation and radiates uniformly over all space, then the computed variation in thickness over a three-inch square at a distance of 30 cm from the source is about 3 percent. For the metal layers this was considered sufficiently uniform. For experimental layers the variation in thickness was probably more nearly 5 percent, which is still reasonably good. Such a variation in the dielectric layer was considered undesirable. For example, a transmission filter which has its transmission band at 6000A at the center and 5700A at the corners of the filter is not a good filter if the transmission band is 100A wide, and if the whole area of the filter is to be used at once. It is

[2] L. O. Olsen, C. F. Smith, and E. C. Crittenden, Jr., "Techniques for evaporation of metals," J. App. Phys. 16, 425 (1945).

possible, however, to arrange a multiple-source system to obtain greater uniformity of the dielectric layer, and this was done for most of the filters constructed.

Since each type of filter required the evaporation of three successive layers of material, a shutter and a filament reload system were used in making some of the filters, so that the entire process could be done in a single evacuation. In the study of transmission filters it was necessary to obtain the transmission of each of the metal films separately. Test filters were made on a 1″ by 3″ microscope slide. The center part of the slide contained the complete filter, one end had the first metal layer only, and the other end the second metal layer only. The shutter system was thus arranged so that first one end and the center of the slide were exposed during the evaporation of the metal. Next, the center region only was exposed during the evaporation of the dielectric, and finally, the center and the other end of the slide were exposed during the second metal evaporation. The shutter was pivoted on conical bearings and operated by a small permanent magnet outside the chamber.

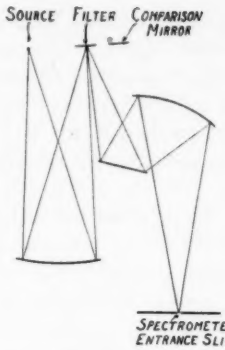

FIG. 1. Diagram of experimental arrangement used in obtaining reflection coefficient of reflection filter.

MATERIALS

In the construction of the reflection filter, which we will consider to be chiefly an infra-red device, there are four components whose properties are to be considered. First, the substrate, which must be optically smooth for the wave-length region considered. For our purposes (determining the optical properties of the filter) ordinary plate glass is sufficiently smooth and flat. For use in a spectrograph it might be desirable to have a more nearly perfect optical surface. Second, the mirror material must have a high reflection coefficient. Aluminum was used as the mirror layer on all reflection filters constructed here, and in all measurements of reflection coefficient comparison was made with an aluminum mirror. Third, the dielectric layer must be transparent in the region in which the filter is used, and must present a smooth surface on which to deposit the thin metal layer (region II of Fig. 9, Part I). Magnesium fluoride seems to be satisfactory in these respects out to wave-lengths of 8 or 10 mμ. How much further the wave-length can be pushed, using MgF_2 as a dielectric, is not certain. Other dielectrics which were tried were LiF, KBr, and TlI. None of these proved very satisfactory, however. The surmise is that the surface becomes too rough, so that the final thin metal layer no longer has the proper optical properties. It is well known that in the evaporation of materials of relatively low melting temperatures the films produced consist of rather large clumps of material, and that the size of these clumps decreases as materials with higher and higher melting points are used.

Fourth, the semiconducting metal layer must have a resistance of 377 ohms/square, and with this resistance must, by itself, have a reflection coefficient of 1/9 and a transmission coefficient of 4/9. Rhodium gave satisfactory results as a material for this layer. Other metals tried were chromium, bismuth, and palladium. Filters made with the last metals named had minimum reflection coefficients of around 10 percent. Attempts to measure the reflection and transmission coefficients of these metal films by themselves were not very definitive. It may be significant, however, that evaporated rhodium films appear to be amorphous as studied by electron diffraction, while the other metals named have high crystallinity.[3]

For the transmission filter the same remarks hold as before concerning the substrate (except that the substrate must also be transparent here) and the dielectric layer. The only materials tried for the dielectric layer were LiF, which was

[3] H. Levinstein, doctoral thesis, University of Michigan, January 1947.

unsatisfactory for apparently the same reasons as given above, and MgF_2, which gave excellent results. The requirements for the metal layer are that it possess a high reflection coefficient and a low absorption coefficient for the wave-length region considered. Generally speaking, a further requirement is that the transmission coefficient be equal to or larger than the absorption coefficient. Silver satisfies these requirements in the visible region and, as mentioned above, it will be one of the purposes of this paper to deduce from the properties of the transmission filter the optical constants of silver films.

MEASUREMENTS

There were essentially three types of measurements to be made: reflection coefficient, transmission coefficient, and wave-length. Most of the measurements were made with a Perkin-Elmer infra-red spectrometer, using a NaCl prism. For wave-length determinations, particularly the splitting of the transmission band of the transmission filter in the visible region, an ordinary student's spectroscope with a replica grating was used. The grating spacing was determined from the mercury spectrum. For measurements of transmission coefficient and band width of the transmission filters in the visible region the Perkin-Elmer instrument was used with a tungsten source. The instrument was calibrated for this region by means of a mercury arc, a helium arc, and, for the region around one to two microns, by the absorption in liquid benzene. (It was necessary to tilt the Littrow mirror in the instrument slightly in order to get the visible spectrum onto the exit slit.) The dispersion of the salt prism is quite good throughout most of the visible region, and the response of the bolometer (used as a receiver in this instrument) is satisfactory. Computed effective slit widths to give full-scale deflection of the recorder were in the neighborhood of 50A. For transmission measurements, the filter was introduced into the beam just before the entrance slit to the spectrometer proper. For reflection measurements the filter was interchanged with an aluminum mirror. The arrangement is shown in Fig. 1.

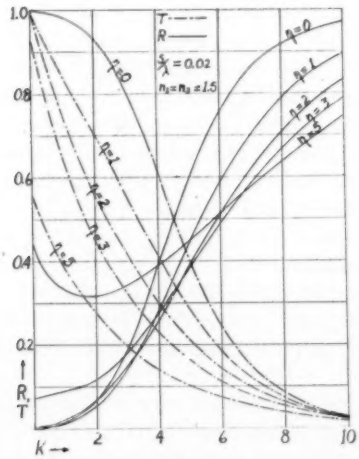

FIG. 2. Reflection and transmission coefficients of a metal film sandwiched between two dielectric layers whose indices of refraction are 1.5. The thickness ratio of the film is $s/\lambda=0.02$. R and T are given as functions of the extinction coefficient κ, with the index of refraction η of the metal film as a parameter which takes on the values 0, 1, 2, 3, 5.

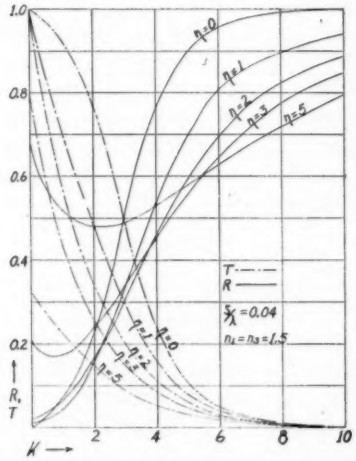

FIG. 3. Same as Fig. 2 except for the thickness ratio of the film—$s/\lambda=0.04$.

The equations developed for the transmission filter in Part I assumed that the regions I and V of Fig. 11 (Part I) were infinite. In practice, these are the substrate and cover glass, and the measurements are taken outside them. For this reason a correction must be applied. What was actually done was to find the transmission relative to a piece of clear glass of the same thickness as the completed filter. This is correct to first-order

terms, and is quite sufficient for the magnitude of the transmission coefficients being measured.

The transmission coefficients of the individual silver films were quite low (from 0.5 up to 5 percent). In these measurements an intermediate gray filter was used as a comparison. (The gray filter was made by depositing chromium on glass. The transmission coefficient was about 19 percent.)

DETERMINATION OF OPTICAL CONSTANTS—THE TRANSMISSION FILTER

In order to determine the applicability of the theory developed in Part I, it is in principle

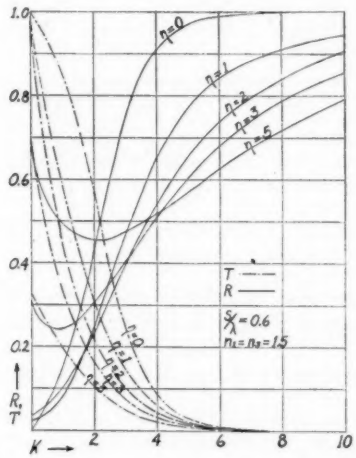

FIG. 4. Same as Fig. 2 except for the thickness ratio of the film—$s/\lambda = 0.06$.

necessary only to substitute into the filter equations values for the parameters for a particular filter, and to compare the resulting transmission or reflection coefficient with that obtained experimentally. The parameters in point are η, κ, and s (the index of refraction, extinction coefficient, and thickness of the metal films), and n_3 and Δ (the index of refraction and thickness of the dielectric layer). In practice, this is not feasible, since none of these parameters is known sufficiently well to obtain a close fit with the experimental data. Instead, our procedure will be to make measurements of transmission coefficients, wave-length, and shift in wave-length as a function of angle of incidence, and from these data calculate the parameters mentioned above.

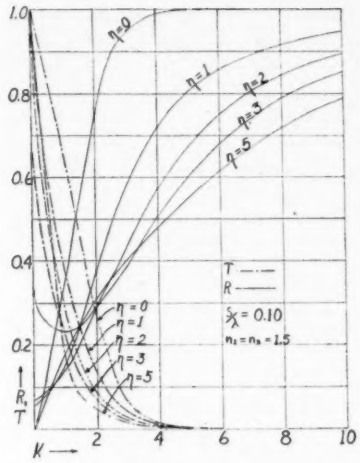

FIG. 5. Same as Fig. 2 except for the thickness ratio of the film—$s/\lambda = 0.10$.

If, then, we obtain values of the parameters that are in general agreement with other published data, or, as in the case of the two thicknesses involved, we obtain sensible values, we may say that the theory is an adequate description of the filters. In addition, this gives a new method of determining optical constants of thin films. At present we will be chiefly concerned with the transmission filter, which in all these measurements consists of two silver films separated by a layer of MgF_2.

Before proceeding with the method of analysis it is appropriate to list here the terminology that will be used.

T_1 = transmission of one of the silver films alone, at wave-length λ_0.

T_2 = transmission of the other silver film at wave-length λ_0.

T = average of T_1 and T_2.

$T_0 = TF_{max}$ = maximum transmission of filter, which occurs at wave-length λ_0.

W = band width of transmission band of filter as defined in Part I.

θ = angle of incidence of the radiation striking the filter.

$\lambda\theta_\perp$ = wave-length of the transmission band for which the electric vector E is perpendicular to the plane of incidence, and when the angle of incidence is θ.

$\lambda\theta_{11}$ = wave-length of band when E is parallel to plane of incidence, at angle of incidence θ.

$\lambda_{Av} = (\lambda\theta_{11} + \lambda\theta_\perp)/2$.

The above quantities are obtained directly from experiment. We shall also require a few other

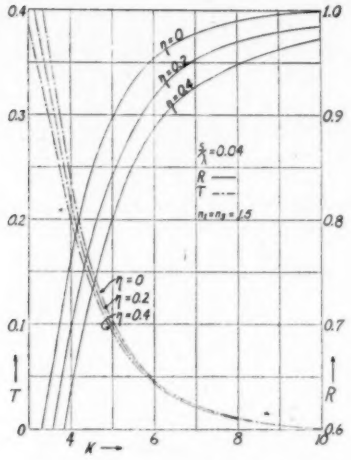

FIG. 6. Same as Fig. 2 except for the thickness ratio of the film—$s/\lambda=0.04$ and the fact that R and T as functions of κ are given over only a limited range. The parameter η takes the values 0, 0.2, 0.4.

terms which may either be computed directly from the experimental quantities or may be determined graphically.

R^L = reflection coefficient of single silver film as seen from region III of dielectric constant n_3 toward region I of dielectric constant n_1 (Fig. 5, Part I). From Eq. (51) of Part I,

$$R^L=1-(T/T_0^L).$$

y_0^L = phase shift in the reflected amplitude at $\theta=0$, as defined in Part I.

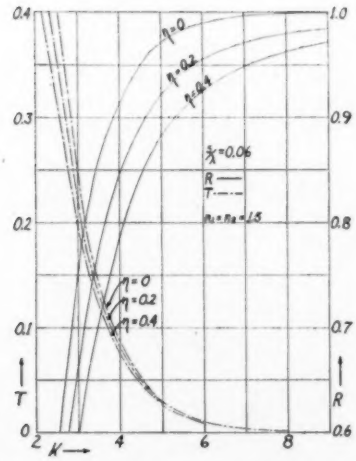

FIG. 7. Same as Fig. 6 except for the thickness ratio of the film—$s/\lambda=0.06$.

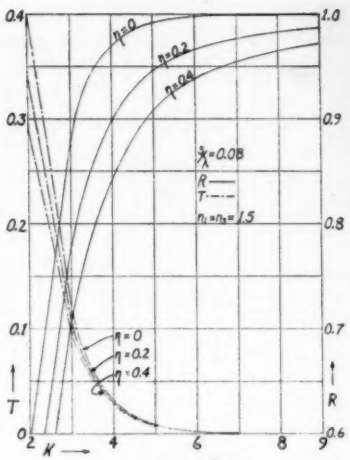

FIG. 8. Same as Fig. 6 except for the thickness ratio of the film—$s/\lambda=0.08$.

$y_{0\parallel}^L$ = phase shift in the reflected amplitude at angle of incidence θ, when E is parallel to the plane of incidence.

$y_{0\perp}^L$ = phase shift in reflected amplitude at θ, when E is perpendicular to plane of incidence.

An outline may now be given of the method of finding η, κ, s, n_3, and Δ from the available data.

1. Determination of the Index of Refraction n_2

In the transmission filter equation, given at the beginning of this paper, maximum transmission

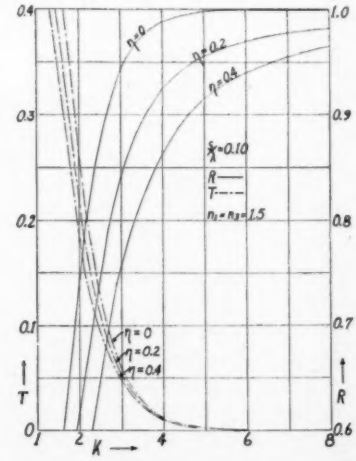

FIG. 9. Same as Fig. 6 except for the thickness ratio of the film—$s/\lambda=0.10$.

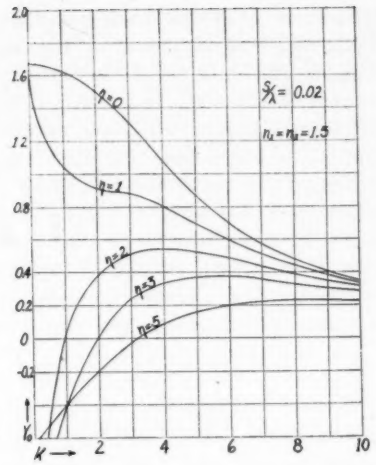

FIG. 10. The phase shift angle, at reflection y_0, of a metal film sandwiched between two dielectric layers whose indices of refraction are 1.5. The thickness ratio of the film is $s/\lambda = 0.02$. y_0 is given as a function of κ, with the parameter η taking the values 0, 1, 2, 3, 5.

is obtained when the argument of the sine in the denominator is $m\pi$, where m is an integer. This gives

$$(2\pi\Delta n_3/\lambda_0) - y_0{}^L = [2\pi\Delta(n_3{}^2 - \sin^2\theta)^{\frac{1}{2}}/\lambda_{\theta_{11}}] - y_{\theta_{11}}{}^L$$
$$= [2\pi\Delta(n_3{}^2 - \sin^2\theta)^{\frac{1}{2}}/\lambda_{\theta_\perp}] - y_{\theta_\perp}{}^L = m\pi.$$

Since λ_0, $\lambda_{\theta_{11}}$, and $\lambda_{\theta_\perp}$ are, in general, not the same,

$$y_0{}^L \neq y_{\theta_{11}}{}^L \neq y_{\theta_\perp}{}^L.$$

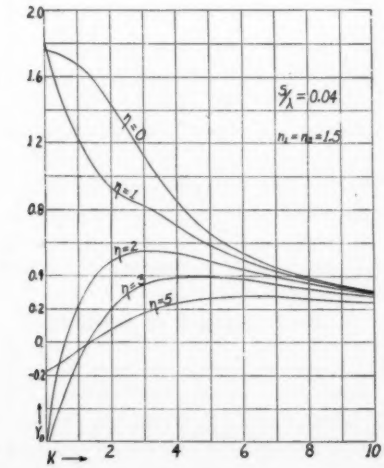

FIG. 11. Same as Fig. 10 except for the thickness ratio of the film—$s/\lambda = 0.04$.

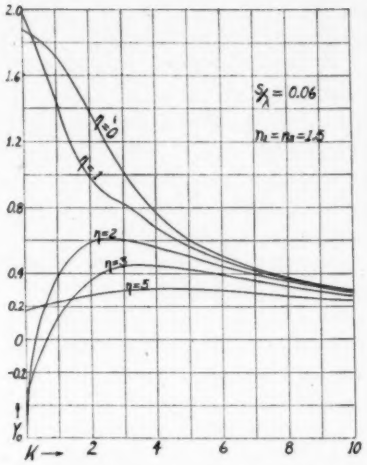

FIG. 12. Same as Fig. 10 except for the thickness ratio of the film—$s/\lambda = 0.06$.

It can be shown, however, that

$$(y_{\theta_{11}}{}^L + y_{\theta_\perp}{}^L)/2 = y_0{}^L$$

in the range of values in which we are working, and consequently we may write

$$2\pi\Delta n_3/\lambda_0 = 2\pi\Delta(n_3{}^2 - \sin^2\theta)^{\frac{1}{2}}/\lambda_{Av}.$$

This, then, may be solved for n_3, giving

$$n_3 = \sin\theta/(1 - \lambda_{Av}{}^2/\lambda_0{}^2)^{\frac{1}{2}}.$$

This is not a precision method of finding the

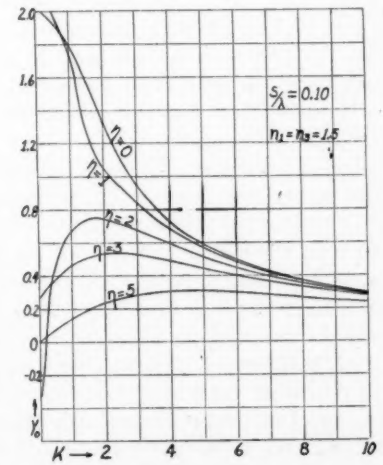

FIG. 13. Same as Fig. 10 except for the thickness ratio of the film—$s/\lambda = 0.10$.

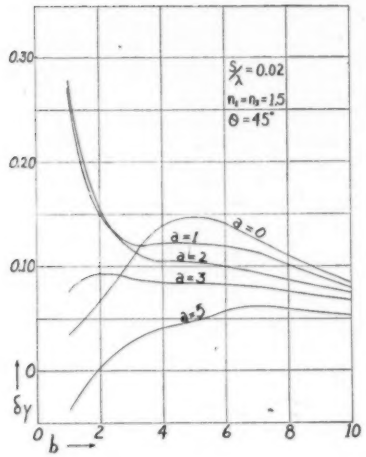

FIG. 14. The difference δy between the phase shift angles at reflection at oblique incidence. $\theta = 45°$, $s/\lambda = 0.02$ δy is given as a function of b with a as a parameter taking on the values 0, 1, 2, 3, 5.

value of n_3, but the results are sufficiently accurate that their influence on further calculations is small.

2. Determination of n and κ as Functions of s/λ

Having determined the value of n_3 and knowing the value of n_1, curves may be plotted using Eqs. (28) and (29) of Part I, showing R^L and T as functions of κ, using η and s/λ as parameters. Such curves are shown in Figs. 2–5. In these curves the value of the extinction coefficient κ ranges from zero to ten, the index of refraction η takes on the values 0, 1, 2, 3, and 5, and the thickness ratio s/λ takes the values 0.02, 0.04, 0.06, and 0.10. For the curves shown here, $n_1 = n_3 = 1.5$ and, hence, the direction from which R is taken is irrelevant. This set of curves is presented in the hope that it will be of general interest in the field of thin metallic films. For the case of silver, the curves of Figs. 6–9 are given. They are a magnified section of the previous set, applicable to the type of silver films to be found in practical transmission filters. The range of extinction coefficient κ is much the same, the index of refraction η takes on the values 0, 0.2, and 0.4, and the thickness ratio s/λ takes the values 0.04, 0.06, 0.08, and 0.10. R and T are plotted only over the range of values found to exist in the filters. For this second set of curves, $n_1 = n_3 = 1.5$, as before, for it was found that over the small range of variation of the index of refraction of the dielectric layer no significant difference is observed in the values of reflection and of transmission coefficients occurring in practical filters. From these curves, by use of the experimental values of R and T, η and κ may be determined and plotted as functions of s/λ for each filter. To determine η and κ uniquely for a given filter, it is then necessary to know the thickness of the film. Because the determination of the thickness of either the metal or the

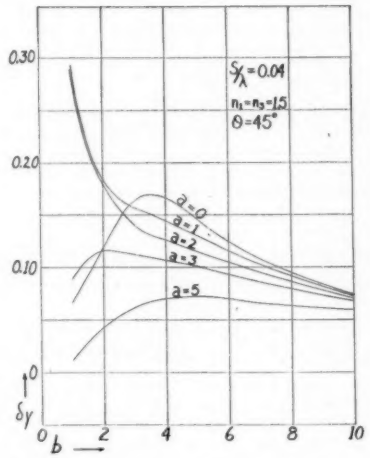

FIG. 15. Same as Fig. 14 except for the thickness ratio of the film—$s/\lambda = 0.04$.

dielectric layers from the geometry of the evaporating system involves certain assumptions relating the properties of the film to those of the bulk material, we have chosen to obtain the thickness directly from the properties of the filter. This is done by means of Eq. (54), Part I and requires the determination of the phase angle y_0 and the difference in phase angles for the two polarized components for oblique incidence.

3. Determination of y_0 and δy

Using Eq. (31) of Part I, curves may be plotted of the phase angle y as a function of κ, with s/λ and η as parameters. For $\theta = 0$, the two polarizations are identical, and the set of curves for y_0 results. These curves are shown in Figs. 10–13, using the same values of parameters as in the

curves of Figs. 2–5. For any value of angle of incidence other than zero there are two values of this phase angle, $y_{\theta_{\parallel}}$ and $y_{\theta_{\perp}}$, corresponding to the two polarizations. The difference between these two values of phase angle at a particular angle of incidence is the δy of Eq. (54). δy is plotted in Figs. 14–17 for the same values of parameters as used above** and for an angle of incidence $\theta = 45°$. From these curves, and from the values of η, κ, and s/λ determined from the measurements of R and T, it is now possible to find y_0 and δy as functions of s/λ. Recalling Eq. (54)

$$\delta\lambda/\lambda_{hw} = \delta y/(m\pi - y_0).$$

if the ratio $\delta y/(m\pi - y_0)$ is plotted as a function of s/λ, s/λ may be determined from the point on

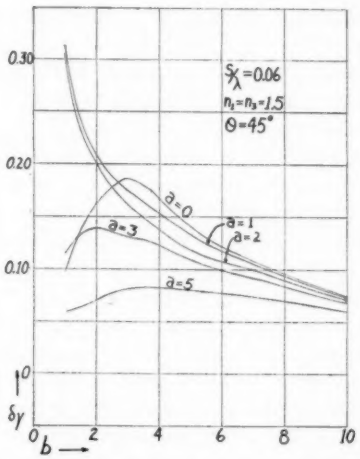

FIG. 16. Same as Fig. 14 except for the thickness ratio of the film—$s/\lambda = 0.06$.

this curve which corresponds to the experimentally measured value of $\delta\lambda/\lambda_{hw}$. From the value of s thus obtained the values of η and κ may be fixed.

Also, with y_0 known, the band width W and the dielectric thickness Δ may be found. This completes the solution of the problem.

As a check on consistency, measurements were also taken on the observed shift and splitting of the band at an angle of incidence of 30°, and the value of film thickness s was taken to be the average of these two determinations.

By way of illustration the procedure just outlined will now be carried through for a particular filter, which for purposes of labeling, will be called No. 21. It is a fairly typical example. Figure 18 is a reproduction of the spectrograph record from which the average transmission T of the silver films, the maximum transmission of the filter, T_0, and the band width W are determined. The upper curve in the figure is the transmission of the glass alone, to which the other transmissions are referred. The two nearly identical lines near the bottom of the figure are the transmission records of the silver films. The peaked curve is, of course, the filter record. The wave-length scale has been marked in. The ratio of any of the ordinates of the three lower curves to the corresponding ordinate of the upper curve is the transmission coefficient for that particular element at that wave-length. The band width is found by obtaining the two positions of half-maximum intensity on either side of the peak of the filter curve. The data obtained from this figure are

$$T = 0.048, \qquad W = 224\text{A},$$
$$T_0 = 0.386, \qquad R_{\text{calc}} = 0.923.$$

The value of wave-length used will be taken from the data obtained by the grating spectroscope.

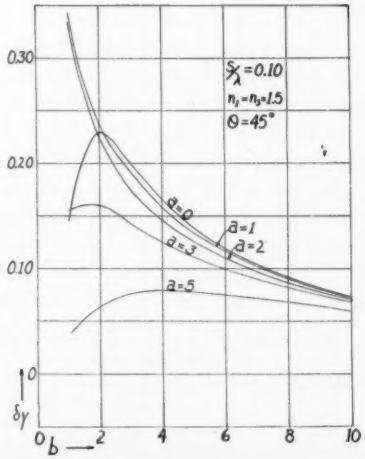

FIG. 17. Same as Fig. 14 except for the thickness ratio of the film—$s/\lambda = 0.10$.

** Actually, the parameters a and b have been used here rather than η and κ. A negligible error is introduced in the values for δy if η is taken to be equal to a and κ equal to b provided either a or b is larger than 3. The values for a and b in terms of η and κ are given in Eqs. (23) and (24), Part I.

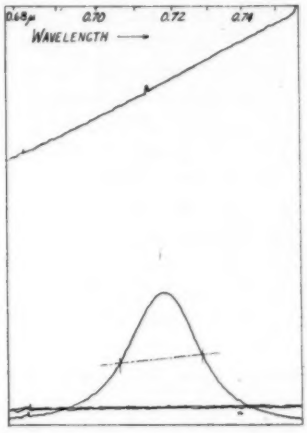

FIG. 18. Spectrograph record of transmission filter No. 21. The upper curve gives the variation in intensity of the tungsten source as a function of wave-length, with a clear glass plate in place of the filter. The two nearly identical curves at the lower part of the figure give the variation in intensity of light transmitted through each of the silver films of the filter, taken separately. The center curve gives the variation in intensity of light transmitted through the filter. The transmission coefficient for any of the three lower curves is obtained by taking the ratio of any of their ordinates to the corresponding ordinate on the upper curve.

These data are given in Table I. Included in this table are the quantities directly calculable from this data. The calculated value of n_3 is somewhat high, but for the present this will be neglected, and the value assumed to be 1.5 for the remainder of the calculations.

From the values of T and R, the curves of Figs. 6–9 yield η and κ as functions of s/λ; using these values of η and κ, the curves of Figs. 10–17 are employed to find y_0 and δy. These values, together with the values of δy determined for curves in which $\theta = 30°$ are tabulated in Table II, and are plotted in Fig. 19. On the curves for $[(\delta y/\pi - y_0)]_{30°}$ and $[(\delta y/\pi - y_0)]_{45°}$ of Fig. 18 the experimental values $(\delta\lambda/\lambda_M)_{30°}$ and $(\delta\lambda/\lambda_M)_{45°}$ which were obtained in Table II, are marked with crosses. The corresponding abscissae are the thicknesses obtained for the film (measured in wave-lengths). The average value of these gives $s_M/\lambda_0 = 0.042$. The corresponding values of η and κ are found to be $\eta = 0.13$ and $\kappa = 5.7$. Similarly, the value of y_0 is found to be 0.55. From this the dielectric thickness Δ and the band width W are found to be $\Delta = 1850$A and $W = 221$A. (The average value of n_3 as determined above was used in finding the dielectric thickness.)

TABLE I. Data taken from grating spectroscope for filter No. 21.

For $m=1$,			$\lambda_0 = 7162$A				
θ	$\lambda_{\parallel}$	$\lambda_{\perp}$	λ_M	$(\lambda_M - \lambda_0)$	$\delta\lambda$	$\delta\lambda/\lambda_M$	η_3
30°	6899	6741	6820	342	158	0.0232	1.64
45°	6588	6233	6410	752	355	0.0554	1.59

In Tables II, III, IV, and V, the experimental data and calculated results are given for nine filters. Filters numbered 21, 24, 25, 32, 33, 34, and 35 are all measured for first order only ($m = 1$). This is also true of filter No. 27; the dielectric layer of No. 27 is wedge shaped, however, and the filter characteristics are measured at seven places along the filter. (This filter was constructed on a $1\frac{1}{2}'' \times 6''$ glass plate.) Filter No. 36 has a somewhat thicker dielectric, and measurements are made for the orders $m = 1$, 2, and 3.

The data for η and κ of Table V are plotted in Fig. 20 as a function of wave-length. In a search for any effect due to thickness, the data were divided into three groups. Points marked with a cross ($\times$) are for thicknesses in the range 200 to 400A. Points marked with a circle are for the range 400 to 500A, and points marked with a plus ($+$) are for the range 500 to 600A. There is a slight tendency for the points of the first two groupings to appear higher than the others in both curves. The variation in the points of the first group is rather large, however, and not much significance can be attached to these points, except to remark that the same tendency is exhibited for the thinner films of Murmann's data.[4] The points marked by squares ($\square$) are taken from Murmann's data for his thickest film (294A).[5] The values obtained by him were

TABLE II. Values for the parameters of filter No. 21 as deduced from the curves of Figs. 2 through 17.

s/λ	η	κ	y_0	$\delta y_{30°}$	$\delta y_{45°}$	$\delta y_{30°}/(\pi - y_0)$	$\delta y_{45°}/(\pi - y_0)$
0.02	0.2	8.8	0.41	—	0.098	—	0.0359
0.04	0.14	5.9	0.54	0.059	0.126	0.0227	0.0484
0.06	0.084	4.45	0.69	0.072	0.157	0.0294	0.0640
0.08	0.063	3.65	0.81	0.083	0.178	0.0356	0.0764
0.10	0.053	3.12	0.92	—	0.193	—	0.0870

[4] H. Murmann, Zeits. f. Physik **101**, 643 (1936).

[5] These films were prepared by F. Goos (Zeits. f. Physik **100**, 95 (1936)) by sputtering in a hydrogen atmosphere at a pressure of 0.1-mm Hg. The deposits were made on quartz. The thickness was determined by weighing the film with a quartz torsion microbalance, and assuming bulk density.

TABLE III. Experimental values of reflection and transmission coefficients and band widths obtained for a series of transmission filters.

Filter	m	T_0	T_1	T_2	T	R_{calc}	W_{obs}
21	1	0.386	—	—	0.048	0.923	224A
24	1	0.250	0.030	0.030	0.030	0.940	130
25	1	0.541	0.175	0.185	0.180	0.745	440
27A	1	0.262	0.043	0.039	0.041	0.920	200
27B	1	0.177	0.021	0.018	0.020	0.951	140
27C	1	0.096	0.015	0.011	0.013	0.960	140
27D	1	0.077	0.012	0.008	0.010	0.964	140
27E	1	0.107	0.012	0.008	0.010	0.968	100
27F	1	0.146	0.013	0.009	0.011	0.971	140
27G	1	0.250	0.024	0.016	0.020	0.960	175
32	1	0.152	0.0153	0.0076	0.0114	0.971	90
33	1	0.110	0.0092	0.0096	0.0094	0.972	70
34	1	0.288	0.0196	0.0296	0.0246	0.954	160
35	1	0.493	0.107	0.075	0.091	0.870	288
36	1	0.069	0.0070	0.0060	0.0065	0.975	210
36	2	0.309	0.037	0.030	0.033	0.941	81
36	3	0.358	0.104	0.086	0.095	0.841	108

TABLE IV. Experimental values of wave-length of transmission band for angles of incidence 0°, 30°, and 45°.

			$\theta=30°$				$\theta=45°$			
Filter	m	λ_0	$\lambda_{\parallel}$	$\lambda_{\perp}$	λ_{Av}	$\delta\lambda$	$\lambda_{\parallel}$	$\lambda_{\perp}$	λ_{Av}	$\delta\lambda$
21	1	7162	6899	6741	6820	158	6588	6233	6410	355
24	1	6557	6328	6167	6247	161	6079	5676	5877	403
25	1	5648	5532	5338	5435	194	5309	4997	5153	312
27A	1	5027	4928	4750	4829	178	4713	4327	4520	386
27B	1	5485	5342	5179	5260	163	5096	4713	4904	353
27C	1	6014	5826	5661	5743	165	5534	5151	5342	353
27D	1	6513	6294	6120	6207	174	5952	5552	5752	400
27E	1	6983	6719	6539	6629	180	6364	5971	6164	393
27F	1	7302	7029	6849	6939	180	6642	6276	6459	366
27G	1	7498	7193	7038	7115	155	6847	6498	6667	349
32	1	7446	7174	7002	7088	172	6863	6497	6680	366
33	1	7043	6764	6591	6677	173	6475	6096	6285	379
34	1	7920	7552	7369	7460	183	7199	6832	7015	367
35	1	6556	6334	6177	6255	157	6092	5684	5888	408
36	1	13900	—	—	—	—	—	—	—	—
36	2	6969	6605	6514	6560	91	6215	6011	6113	204
36	3	4710	4486	4414	4450	72	4220	4089	4154	131

slightly higher than values given for bulk silver. The agreement between our data and those of Murmann is excellent for the values of κ. The values of η obtained by us are considerably lower than his values but not sufficiently different to make a marked difference in the properties plotted for transmission filters.

The accuracy of the determinations of η and κ is best described by the variations shown in the points on the curves of Fig. 20. A rough guess would be that the determination of κ is good to ± 10 percent for the thicker films. The values of η are perhaps good to ± 20 percent for the thicker films. These guesses are based on the consistency of the data. For the other quantities determined (s, n_3, and Δ) the accuracy is the same order of magnitude. The greatest uncertainty in the original measurements lies in the determination of the transmission of the single silver film, and the quantities η, κ, and s are all dependent on this measurement.

The value of Δ is dependent chiefly on the accuracy with which n_3 is known. The observed values of n_3 are much higher than are to be expected. The index of refraction of bulk magnesium fluoride is given as 1.39. In its use as a nonreflecting coating on glass it appears to have an index of refraction of around 1.3. The nonreflecting layers on glass are produced by high vacuum evaporation as is the layer used in the filters. This large discrepancy in the index of refraction is very interesting, for there can be no doubt of its existence. In this connection two things must be said. First, the existence of these large values of the index of refraction depends on the average of the two phase angles $y_{\theta_{\parallel}}$ and $y_{\theta_{\perp}}$ being y_0. Using the calculations upon which the δy curves are based, this can be shown to be so within a fraction of a percent over the range of values used here. Secondly, this large value of n_3 is observed as well in one commercial filter which has been measured, consequently it does not seem to be any result of the evaporation techniques used here. It might be expected that this abnormal value of n_3 is due in some way to the use of canada balsam in cementing on the cover glass, for this is the way all filters made here, as

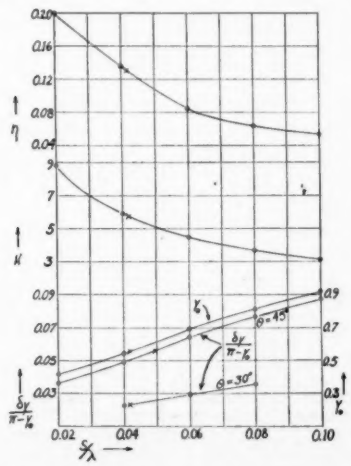

FIG. 19. Analysis of data for filter No. 21. η, κ, y_0, $[\delta y/(\pi - y_0)]_{30°}$ and $[\delta y/(\pi - y_0)]_{45°}$ are given as functions of s/λ.

TABLE V. Values of the parameters η, κ, s, n_3, and Δ as determined for the silver films of a group of transmission filters.

Filter	m	y_0	$s_{320°}$	$s_{413°}$	s_{Av}	η	κ	n_{3Av}	Δ	W_{calc}	W_{obs}	$n_{320°}$	$n_{413°}$
21	1	0.55	284A	316A	300A	0.14	5.7	1.61	1850A	221A	224A	1.64	1.59
24	1	0.64	370	465	420	0.10	4.70	1.61	1620	153	130	1.64	1.59
25	1	0.75	300	180	240	0.20	4.35	1.78	1200	700	440	1.84	1.73
27A	1	0.83	424	456	440	0.08	3.5	1.68	1100	182	200	1.84	1.62
27B	1	0.72	460	514	485	0.07	4.0	1.66	1270	114	140	1.76	1.58
27C	1	0.67	490	550	520	0.08	4.4	1.61	1470	103	140	1.68	1.54
27D	1	0.65	560	610	585	0.08	4.4	1.58	1640	96	140	1.65	1.51
27E	1	0.61	570	590	580	0.08	4.7	1.55	1810	90	100	1.59	1.51
27F	1	0.57	515	550	530	0.07	5.1	1.59	1880	84	140	1.61	1.57
27G	1	0.51	370	400	385	0.11	5.9	1.56	2010	117	175	1.58	1.55
32	1	0.55	510	510	510	0.075	5.35	1.61	1910	85	90	1.63	1.60
33	1	0.59	540	580	560	0.070	4.90	1.57	1820	78	70	1.57	1.57
34	1	0.54	430	420	425	0.106	5.55	1.52	2160	143	160	1.49	1.52
35	1	0.71	220	320	270	0.10	4.50	1.63	1560	375	288	1.67	1.61
36	1	0.35	—	—	—	0.21	8.60	—	4140	127	210	—	—
36	2	0.74	510	580	540	0.064	4.05	1.49	4130	77	81	1.48	1.47
36	3	1.24	575	510	—	0.04	2.2	—	4120	98	108	1.52	1.50

well as most commercial filters, are prepared. This is not the case, however, for a number of filters were measured before the cover glass was cemented in place, and in each case the value of n_3 obtained was in the neighborhood of 1.5 or larger.

There is some dependence of n_3 measured in this way on the angle of incidence. It will be noticed that in Table VI the value given for n_3 at $\theta = 45°$ is nearly always larger than the value measured at $\theta = 30°$. It is proposed that this effect is in some way due to the presence of the silver, and may be caused by the penetration of the second silver layer into the magnesium fluoride during evaporation. It is an effect which requires more study.

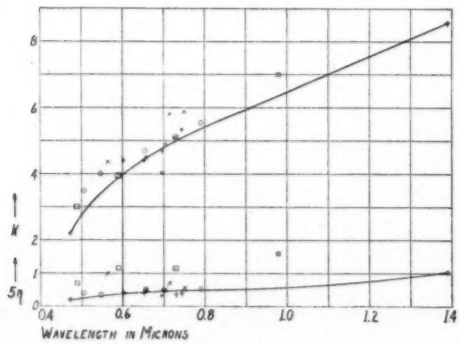

FIG. 20. Optical constants of silver films as determined by measurements on transmission filters. Points marked with a cross (×) are for thicknesses s between 200 and 400A. Points marked with a circle are for s between 400 and 500A. Points marked with a plus (+) are for s between 500 and 600A. Points marked with a square are taken from Murmann's data for his calculated thickness of 294A. Note that values of 5η rather than η are plotted.

The general results of the measurements of the transmission filters are very satisfactory. The over-all consistency of the data is good, values of the optical constants of silver are in agreement with those found by other workers, and values of the other quantities determined (thickness of silver, thickness and index of refraction of dielectric) are at least reasonable. An attempt was made to construct a filter with aluminum used as the metallic layers. The results obtained thus far have not been satisfactory. The filters show some color when viewed against a white background, but measurements of their properties in an attempt to deduce the optical constants of aluminum would require better photometric measurements than those used for the silver filters. It does appear, however, that the methods outlined here might be pursued to some extent in the study of the optical constants of thin metallic films.

THE REFLECTION FILTER

The production of reflection filters for the infra-red involves a somewhat more difficult technique than the production of transmission filters for the visible region. There are three reasons for this. First, the dielectric layer must be considerably thicker, and hence tends to become more rough on its outer surface. Second, the extremely high melting point of rhodium (*ca.* 2000°C) makes it a difficult material to evaporate. A third difficulty is the measurement of

the resistance of the semitransparent layer of rhodium. This was done experimentally by placing adjacent to the filter one or more 1″×3″ microscope slides, which had previously had aluminum contact layers evaporated on each end. These contact layers were held in clamps which were then connected to an ohmmeter, and the resistance was measured during the evaporation process. The evaporation was stopped when the ohmmeter recorded the desired resistance. Because of the non-uniformity of the "radiation pattern" around the filament, it was not certain that the resistance of the film on the filter was the same as that of the measured test strip. It would have been more desirable, although technically much more difficult, to have measured the resistance of the film on the filter directly.

The resistance of films produced in this way was not constant with time, although the change was normally only a few percent. Most of this change occurred during the first hour after production of the film. The resistance increased with time, probably indicating a slow oxidation process. The same change was observed with films of chromium. Palladium films were remarkably constant, although unsatisfactory for use on the filters. Since, however, the properties of the filter are not very sensitive to small variations in the resistance of the metallic layer, it was possible to produce satisfactory filters. The theoretical reflection coefficient at the fundamental frequency of the filter remains below 1 percent as the resistance of the film is changed from 308Ω/□ to 460 Ω/□.

Figures 21 and 22 show the properties of a typical filter, using aluminum as the mirror, MgF_2 as the dielectric, and rhodium as the semitransparent metal layer. The resistance of the rhodium layer is about 400 Ω/□. The solid curve shown in Fig. 21 is the theoretical curve for a filter in which $n=1.6$, and $f=1$. The experimental points obtained for a filter are shown on the same figure. The frequency ν_0 for the experimental filter was 1240 cm^{-1} ($\lambda_0=8.1\mu$). The minimum reflection coefficient was measured to be 0.016. The maximum reflection coefficient falls at slightly less than $2\nu_0$, because of the change in the index of refraction of magnesium fluoride. The maximum reflection coefficient is observed to be about 0.94 at the second overtone. (This is

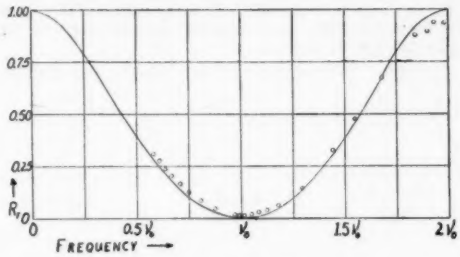

FIG. 21. Reflection coefficient of typical reflection filter in the neighborhood of the fundamental frequency. $\lambda_0=8.1\mu$. Resistance of semiconducting layer is approximately 400 Ω/□. The solid curve is the theoretical reflection coefficient for a filter in which $n=1.6$, and the resistance of the semiconducting layer is 377 Ω/□.

probably due to a fine layer of dust on the filter, which it was deemed unwise to remove. Earlier measurements made with the same filter gave substantially 100 percent reflection at the even overtones.) The measured value of the minimum reflection coefficient at $\lambda=2.8\mu$ is 0.002. The best explanation for the higher value of the minimum reflection coefficient at the fundamental is that the MgF_2 is beginning to absorb in this region.

The points on Fig. 21 were determined statically because of the difficulty in working around the absorption bands of water vapor in this region. The curve of Fig. 22 is a spectrogram of the same filter for the higher overtones. The minima shown are the third, fifth, seventh, ninth, and eleventh overtones. The seemingly more or less constant width is due to the changing dispersion in the NaCl prism. The upper curve in this figure was

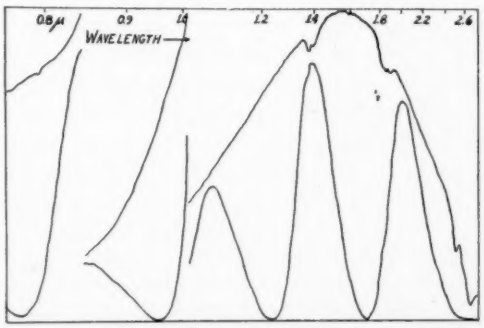

FIG. 22. Spectrograph record for filter of Fig. 21. The minima shown are for the third, fifth, seventh, ninth, and eleventh overtones. The upper curve is the reflection from an aluminum mirror in place of the filter. Reflection coefficient of filter is the ratio of ordinate on lower curve to corresponding ordinate on upper curve.

TABLE VI. The product of wave-length at minimum reflection coefficient by overtone number for the filter shown in Figs. 21 and 22.

m	λ_{min}	$m\lambda_{min}$
1	8.1	8.1
3	2.8	8.4
5	1.69	8.45
7	1.23	8.60
9	0.956	8.60
11	0.775	8.53

obtained with an aluminum mirror in place of the filter, and the source was a tungsten lamp. The absorptions occurring at 1.38μ, 1.88μ, and 2.66μ are due to water vapor. At the left end of the figure, the two breaks in the curve are where the spectrograph slits were widened to obtain more energy. The reflection coefficient of the filter is obtained in any case by taking the ratio of a given ordinate for the filter to the corresponding ordinate for the aluminum mirror.

One inference to be drawn from this curve is that the optical constants η and κ must be equal up to the shortest wave-lengths shown on this curve (0.76μ). The minimum reflection coefficient is less than 0.005 for all overtones up to the eleventh, where it is about 0.023. The product of wave-length at minimum reflection coefficient by overtone number should be constant and equal the wave-length of the fundamental if the index of refraction of the dielectric layer were constant. These products are shown in Table VI. The overtone number is indicated by m.

The success of the experimental filter for which $\lambda_0 = 8.1\mu$, together with the fact that the observed reflection coefficient so closely agrees with the predicted coefficient, indicates strongly that there should exist no intrinsic difficulty in producing a filter for the far infra-red region (*ca.* 100μ or longer). It appears that the major problem will be the technical one of finding a suitable dielectric layer which is both sufficiently smooth and sufficiently transparent. Further work along these lines will be continued.

We wish to thank Mrs. Lai-Wing Lee for her help in calculating many of the curves that have been presented. We wish also to acknowledge with gratitude the assistance furnished by a grant from the Research Fund of the Horace H. Rackham School of Graduate Studies.

Note added in proof. The following corrections to Part I should be made:

Equations (41), (42), and (43) should read:

$$R_{||}{}^{R} = [(n_1^2/p) - (n_3^2/q) - f]^2 / [(n_1^2/p) + (n_3^2/q) + f]^2 \quad (41)$$

$$T_{||}{}^{R} = [4n_1^2 n_3^2/pq] / [(n_1^2/p) + (n_3^2/q) + f]^2 \quad (42)$$

$$A_{||}{}^{R} = [4n_1^2 f/p] / [(n_1^2/p) + (n_3^2/q) + f]^2. \quad (43)$$

No other equations are affected by these alterations and the context remains unchanged.

JOURNAL OF THE OPTICAL SOCIETY OF AMERICA VOLUME 38, NUMBER 6 JUNE, 1948

Projection Screens for Home Television Receivers

R. R. LAW
RCA Laboratories Division, Princeton, New Jersey

AND

I. G. MALOFF
RCA Victor Division, Camden, New Jersey

(Received December 22, 1947)

One of the major problems of television development has been that of obtaining adequate brightness in the reproduced picture, particularly in the case of the projection receiver where large pictures are desired. Directional projection screens which concentrate the available light into the desired viewing field are an important aid in overcoming this difficulty. Although various directional screens have been proposed, the primary question always has been: How could a high quality screen be made at a cost that would permit its use in home projection receivers? This paper presents a study of the factors governing the design of projection screens for home television receivers and describes an improved laminated-plastic screen which provides a brightness gain of 7.5 without perceptible "hot-spot." If the viewing field is defined as that zone in which the brightness exceeds half the maximum value, it provides a vertical field of ±10 degrees and a horizontal field of ±25 degrees. In combination with large aperture, reflective optics it gives a 15- by 20-inch picture having highlights with a brightness of more than 75 footlamberts. This compares favorably with the highlight brightness obtained with direct-viewing kinescopes and more than satisfies the recommendations for good motion picture theater practice.

INTRODUCTION

ONE of the major problems in television development has been that of obtaining adequate brightness in the reproduced picture. This problem has been particularly difficult in the case of the projection receiver where large pictures are desired. In the first place, the brightness of the picture is reduced in proportion to the optical enlargement of the image, since no additional light is produced in the process. In the second place, the efficiency of projection optical systems is relatively low. The best light-utilization efficiency so far obtained in television projection systems is of the order of 30 percent.

A non-directional or diffusing projection screen diffuses the light of the picture in all directions so that the picture is seen with approximately the same brightness from whatever angle it is viewed. However, viewing from extreme angles is not desirable because of the accompanying distortion of perspective. Furthermore, the geometry of receiver surroundings imposes other limitations to the angles within which viewers are likely to congregate. Thus, the light sent to wider angles is largely wasted.

It is apparent, therefore, that the brightness of the picture viewed at a practical angle may be increased if that light which would otherwise be sent out at extreme angles and wasted is concentrated within useful viewing angles. A screen which accomplishes this is called a directional screen. It is the purpose of this paper to discuss some of the optical properties and design problems of this type of screen.

OPTICAL PRINCIPLES

Screen brightness may be conveniently measured in footlamberts. A perfectly diffusing surface is said to have a brightness of one footlambert when it is reflecting or emitting one lumen per square foot. This is the brightness of a perfectly diffusing, perfectly transmitting, or perfectly reflecting surface illuminated by a unit candle at a distance of one foot. To say that the brightness of a surface as viewed from a particular observation point is N footlamberts signifies that its brightness is the same as that of a perfectly diffusing surface emitting or reflecting N lumens per square foot.

For analysis, consider an ideal directional screen in which the optical elements are perfectly transmitting or perfectly reflecting and so oriented as to give a uniform brightness over a stipulated field. In order to have a standard of comparison, let B_0 be the brightness in candlepower per unit area of an ideal, perfectly diffusing

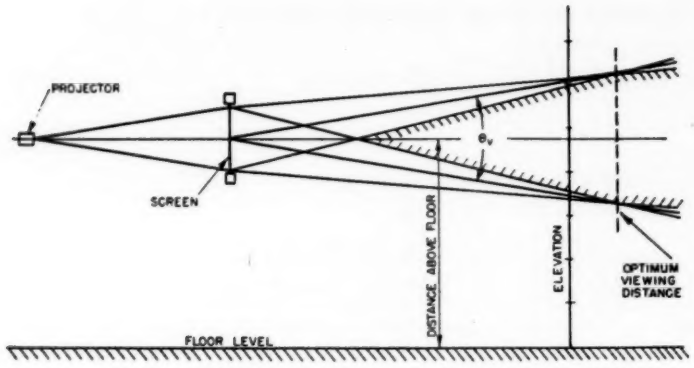

FIG. 1. Viewing field of idea directional screen.

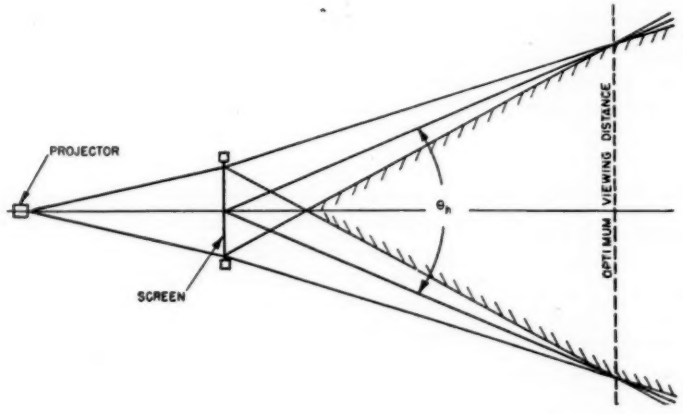

screen. The light flux emanating from unit area of this screen will be πB_0 lumens. (It should be kept in mind that while a point source of one candlepower generates 4π lumens of light flux, a perfectly diffusing surface having a luminous intensity of one candlepower emits π lumens of luminous flux on one side.) In the case of a directional screen, the individual lens elements serve to direct this same light flux into a specified viewing field θ_v degrees in vertical extent and θ_h degrees in horizontal extent, as shown in Fig. 1. The performance of a directional screen may be conveniently expressed in terms of the brightness gain and the viewing field. The gain may be computed in the following manner.

The light flux per unit area contained in an elementary cone of small solid angle is

$$dF = B d\Omega, \tag{1}$$

where B is the brightness in the direction of the axis of the cone. If the flux per unit angle is uniform over the field of view,

$$F = B \int_0^{\Omega} d\Omega = B\Omega. \tag{2}$$

But the total available light flux is πB_0, whereupon the brightness gain caused by the directivity is

$$\text{Brightness gain} = B/B_0 = \pi/\Omega, \tag{3}$$

where Ω, the solid angle, is the area subtended by the viewing angle on a sphere of unit radius. That is, brightness gain is the ratio of the brightness of the screen in question to the brightness of a perfectly diffusing, perfectly transmitting, or perfectly reflecting screen receiving the same illumination.

It may be impractical to provide a rectilinear field as shown in Fig. 1. For example, a simple

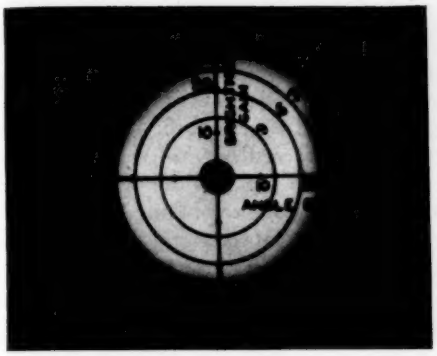

Directivity Pattern

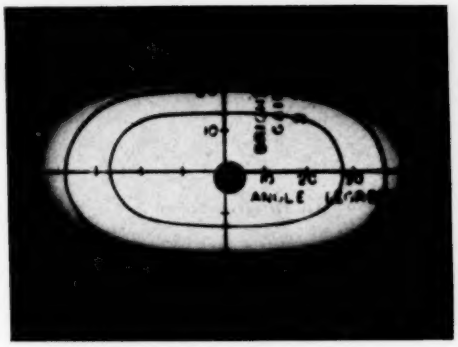

Directivity Pattern

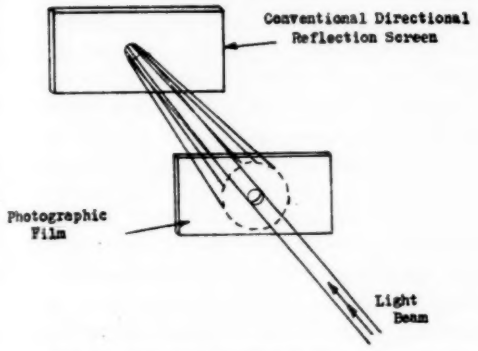

FIG. 2. Directivity pattern of conventional directional screen.

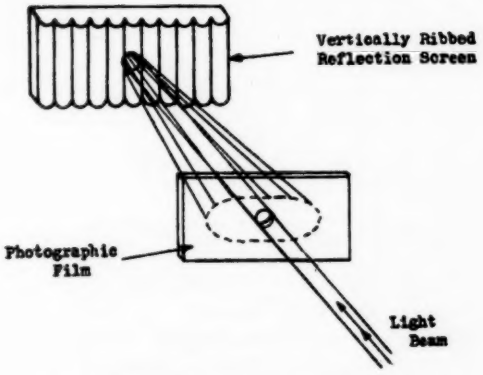

FIG. 3. Directivity pattern of vertically ribbed, directional screen.

reflection-type screen may have the axially symmetric directional properties indicated in Fig. 2. If the surface is provided with vertical ribs to give additional horizontal dispersion, the directional pattern shown in Fig. 3 is obtained. The brightness gain of an ideal screen with a viewing field of this shape may be readily computed in terms of the horizontal and vertical spread. The results of this computation are shown in Fig. 4. In the practical case, these values must be corrected for the losses in transmission or reflection.

DIRECTIONAL SCREEN DESIGN

An excellent analysis of the general problem of directional screen design has been given by Möller.[1] As he points out, the reflection, the transmission, and the beaded screens possess basically different characteristics. These characteristics are illustrated in Fig. 5. Figure 5b also shows how the field lens serves to bring the divergent rays to a common point on the axis in the case of the transmission screen. This lens is ordinarily of the "Fresnel" or lighthouse type.

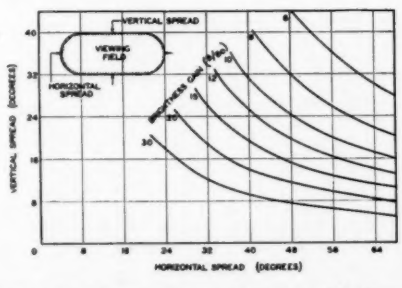

FIG. 4. Brightness gain as a function of horizontal and vertical spread.

[1] R. Möller, *Der Linsenraster Schirm*, Fernseh A. G. 1, No. 3, pp. 72–81 (April 1939).

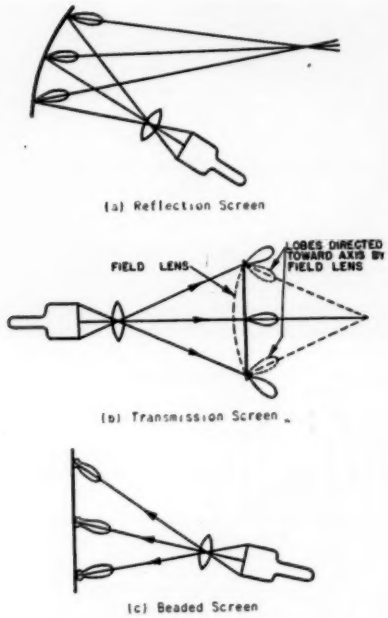

FIG. 5. Basic types of directional screens.

The beaded screen is obviously not suitable for use in home projection receivers inasmuch as it tends to return the light flux to the projector. As Möller suggests, the reflection-type screen may be adapted to the home projection receiver as shown in Fig. 6. In view of the difficulties of keystone correction and the inherent defects of the oblique optical system, this combination has not been as widely used as the transmission-type screen arrangement of Fig. 7, developed by Maloff and Epstein.[2]

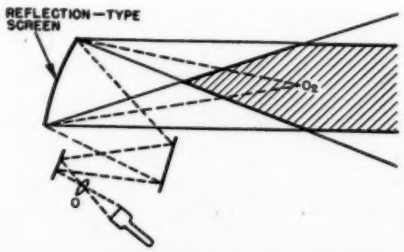

FIG. 6. Home projection receiver employing reflection-type screen.

[2] I. G. Maloff and D. W. Epstein, "Reflective optics in projection television," Electronics **17**, pp. 98–105 (December, 1944).

For television viewing in the home, it is considered that the ideal screen should provide uniform brightness over an angular field of ±10 degrees in the vertical direction and ±30 degrees in the horizontal direction, the brightness falling immediately to zero outside this region. This abrupt transition prompts the viewer to remain in the region of good reception. As may be seen from Fig. 4, an ideal screen with this directional characteristic should give a ninefold brightness gain as compared to a non-directional screen. When this value is corrected for the losses in transmission or reflection, the brightness gain becomes about seven.

Ground-glass screens, beaded screens, impregnated fabric screens, and other screens with axially symmetric directive patterns are not satisfactory. If such a screen is to cover a ±30-degree horizontal field, its brightness gain cannot exceed three.

Möller obtained the desired directive pattern by employing a large number of minute, accurately oriented lens elements. In order that the structure of the screen shall not limit the resolution, there should be several lens elements in the screen for each picture element. For modern television, this means a screen with millions of elements instead of the few thousand-element screen employed by Möller. The primary question always had been: How could such a screen be made at a cost that would permit its use in home projection receivers?

In an effort to solve this problem, a program of research on directional screens for television was begun by RCA. A number of methods for molding transparent plastic screens with lens elements were investigated. Before this work was inter-

TABLE I. Comparison of highlight brightness.

Method of reproduction (various systems)	Highlight brightness (footlamberts)
Television picture on new directional viewing screen (15- by 20-inch picture)	75
Television picture on 10BP4 direct viewing kinescope (7- by 9-inch picture)	60
SMPE recommendations motion picture theater practice (10- by 14-foot picture)	7–14

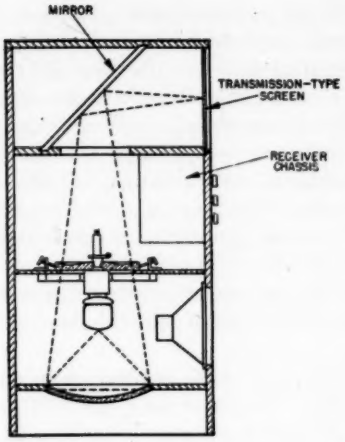

FIG. 7. Home projection receiver employing transmission-type screen.

rupted by the war, a home projection receiver using such a screen was made and demonstrated. In the course of these experiments, various combinations of "Fresnel" and crossed-cylinder lenses were studied. Crossed-cylinder lenses served to provide the desired vertical and horizontal dispersion as shown in Fig. 8, but whenever cylindrical lenses were combined with the "Fresnel," the geometric beat or "moirè" effect interfered with the projected picture. It was found that a thin layer of frosted gelatin placed between the two elements reduced the moirè to an unnoticeable amount. Furthermore, this same thin layer of frosted gelatin in combination with the wide-aperture optical system served to provide the required vertical dispersion. The desired additional horizontal dispersion could then be obtained by one set of vertically disposed cylinder lenses just as was done in the case of the reflection-type screens described in connection with Figs. 3 and 4.

The directional viewing screen resulting from these developments consisted of a field lens, a frosted gelatin sheet, and a multiple-element, vertical-cylinder lens. This screen left something to be desired. The two plastic elements tended to buckle away from each other due to wrinkling of the gelatin. There was also loss in light and contrast because of reflection and scattering at the internal surfaces.

As soon as the war ended, work on this project

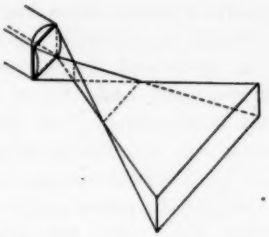

FIG. 8. Directivity pattern provided by crossed-cylinder lenses.

was resumed; this resulted in a substantially improved screen. In its present form the layer of gelatin has been replaced by a sheet of polyvinyl chloride. This Vinylite sheet contains an amount of silica opacifier which is just sufficient to give the desired vertical dispersion and render the moirè unobjectionable. Inasmuch as this sheet is only 0.010-inch thick, there is negligible transverse light scattering. When properly plasticized and stabilized, this sheet may be bonded directly

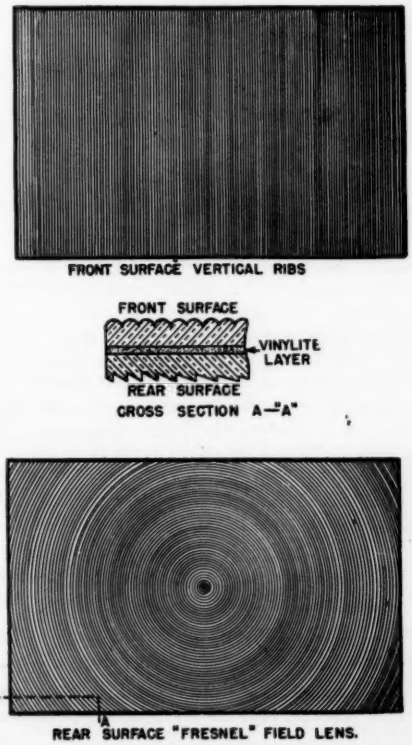

FIG. 9. Constructional details of new screen.

to the lens-element sheets. Thus, the two sheets of Plexiglas with the Vinylite sheet between them may be embossed and laminated in a heated press in a single operation.

The details of this screen are illustrated in Fig. 9. The field lens is of the "Fresnel" of lighthouse type. It has 50 spiral corrugations per inch and a focal length of approximately 50 inches. The vertical rib element has 100 cylinder lenses per inch. The radius of curvature of the individual cylinder lenses is approximately 0.010 inch. This screen should be mounted with the cylinder lenses toward the viewer.

PERFORMANCE DATA

The screen here described provides a brightness gain of seven without perceptible "hot spot." If the viewing field is defined as that zone in which the brightness is at least half the maximum value, it has a vertical viewing field of approximately ±10 degrees and a horizontal viewing field of approximately ±25 degrees.

In addition to its desirable directivity pattern, this screen has the added advantage that it appears dark relative to the room lighting if the lamps are so located that there are no specular reflections. As compared to conventional screens, there can be more room-light without harming the brightness and contrast of the picture. Furthermore, the inner and outer surfaces of the new screen are made of the most stable transparent plastic available. This plastic is unaffected by moisture, sunlight, fingermarks, or furniture polish and, if soiled, it may be readily cleaned.

In combination with modern projection tubes such as the 5TP4 and large-aperture reflective optics,[2] this screen gives a 15- by 20-inch picture having highlights with a brightness of more than 75 footlamberts. As may be seen from Table I, this exceeds the highlight brightness obtained with conventional direct-viewing kinescopes and more than satisfies the recommendations for good motion picture theater practice.

JOURNAL OF THE OPTICAL SOCIETY OF AMERICA VOLUME 38, NUMBER 6 JUNE, 1948

A Case of Unilateral Deuteranopia*

LOUISE L. SLOAN AND LORRAINE WOLLACH
Wilmer Ophthalmological Institute, Johns Hopkins University School of Medicine, Baltimore, Maryland

(Received November 24, 1947)

Studies are reported of a subject with deuteranopia of the right eye and mild deuteranomaly of the left. On the Nagel anomaloscope this subject, using the right eye, matched both spectral red and spectral green to yellow. The left eye did not differ from normal on this test. Selected pseudo-isochromatic charts and the Farnsworth-Munsell 100-hue test, however, revealed, in the left eye, definite color deficiency of the deutan type. Scores on the color threshold tester indicated a marked defect in the right eye, slight in the left.

Because of the relatively slight abnormality of the left eye it is possible to obtain reliable information as to the colors actually perceived by the deuteranopic right eye. Tests with the 100-hue series of Munsell papers and with a spectrometer showed that perception of red and green is entirely lacking. The Munsell papers were described as browns, grays, and blues. In the spectrum the range from 501 to 505 millimicrons was reported as white; longer wavelengths were reported as yellow, shorter ones, as blue. The only regions of the spectrum identical in appearance to the two eyes were those wave-lengths chosen by the deuteranomalous left eye as unitary blue (451–453) and unitary yellow (584).

THERE are rare exceptions to the general rule that congenital red-green color deficiency affects the two eyes equally. Instances have been reported[1] of subjects having normal color vision in one eye and partial or complete red-green deficiency in the other, and of subjects with defects in each eye differing significantly in degree.

* Paper presented at the winter meeting of the Optical Society of America, held in New York City, February 20–22, 1947.

[1] (a) W. Dieter, "Ueber die subjectiven Farbenempfindungen bei angeborenen Störungen des Farbensinnes," Zeits. f. Sinnesphysiol. **58**, Part II, 73 (1927); (b) W. Trendelenburg, "Ueber Vererbung bei einem Fall von anomalem Farbensinn des einen, und normalen Farbensinn des anderen Auges beim Mann," Klin. Monats. f. Augenh. **107**, 280 (1941).

Study of such individuals is of great importance for color theory. If one eye is normal or nearly so, the subject can, by comparing the color sensations of the two eyes, give valuable evidence as to the hues actually perceived by the more deficient eye.[2] Holmgren[3] and von Hippel[4] studied the same case of unilateral dichromasy, who was probably of the protanopic type. They differed somewhat in their conclusions as to the hues seen by the dichromatic eye. Holmgren stated that the color sensations appeared to be not unitary yellow and blue, but colors which would be described by the average normal as slightly greenish-yellow and a violet. Von Hippel, however, believed that the colors seen by the protanopic eye of this subject were unitary yellows and blues. He demonstrated that the indium, caesium, and sodium lines in the spectrum appeared identical in hue to the two eyes. These regions, i.e., 451 to 459 mμ and 589 to 590 mμ, are seen as violet and as slightly reddish-yellow by the average normal eye.[5] The apparent discrepancy can be reconciled, however, if it is assumed that the normal eye of this subject differs from the average normal in the wave-length regions corresponding to unitary blue and to unitary yellow. With the exception of the data on this one case, the literature provides little evidence of a quantitative nature as to the colors perceived by the protanope. Quantitative data are completely lacking for the deuteranope, since no case of unilateral deuteranopia has been reported heretofore, although Holmgren[6] in 1881 offered a prize of 400 crowns in the hope of obtaining such a subject for study.

PRESENT INVESTIGATION

During routine tests in which a group of high school students were examined binocularly with the Rabkin polychromatic plates[7] and monocularly (dominant eye) with a portable anomaloscope,[8] one subject, D. D., was found who failed the Rabkin plates but gave normal responses when the left eye was tested with the anomaloscope. It was discovered on further testing that the responses of the right eye in the anomaloscope test were characteristic of dichromasy (complete red-green color deficiency), while monocular tests with the Rabkin plates revealed essentially similar defects in each eye. D. D. has normal visual acuity in each eye and shows no evidence of ocular pathology. A brother, whom we have not been able to examine, believes that he has some degree of color deficiency. D. D. himself was unaware of any defect in his color perception until examined by us.

The results of more extensive study of the color perceptions of the right and left eyes of D. D. were as follows.

STANDARD TESTS OF COLOR PERCEPTION

1. Nagel Anomaloscope

Left eye.—The proportions of spectral red and green required to match spectral yellow were within normal limits and the range in matching proportions was not abnormally wide.

Right eye.—By suitable variation of the intensity of the yellow light, both red and green could be matched perfectly to yellow. The amounts of yellow required in each case are those characteristic of the deuteranope.

2. Pseudo-Isochromatic Plates

The charts employed were a selected group[9] of 41 plates from the American Optical Company, Ishihara, Dvorine, and Rabkin tests. The two eyes were tested separately. The results are shown in Table I, where it may be seen that with few exceptions the responses for the right and left eyes are identical. The only significant difference in the two eyes revealed by this type of test

[2] D. B. Judd, "The color perceptions of protanopic and deuteranopic observers," J. Opt. Soc. Am. **34**, 351 (1944).

[3] F. Holmgren, "Ueber die subjectiven Farbenempfindungen der Farbenblinden," Zentralbl. f. d. Med. Wiss. **18**, 898 and 913 (1880).

[4] (a) A. von Hippel, "Ein Fall von einseitiger congenitaler Roth-Grünblindheit bei normalem Farbensinn des anderen Auges," Arch. f. Ophth. **26**, Part II, 176 (1880); (b) A. von Hippel, "Ueber einseitige Farbenblindheit," Arch. f. Ophth. **27**, Part III, 47 (1881).

[5] D. B. Judd, "Hues of the spectrum colors," Letter Circular LC-454, Nat. Bur. Stand., November 6, 1935.

[6] F. Holmgren, "Flere Fall of ensidig Fargblindhed," Upsala Lakaref, Forh. **16**, 222 (1881).

[7] E. B. Rabkin, *Polychromatic Plates for Testing Color Vision* (State Publishing House of the USSR, 1939), second edition.

[8] L. L. Sloan, "The Eastman color-temperature meter used as an anomaloscope," J. Opt. Soc. Am. **34**, 618 (1944).

[9] L. L. Sloan, "An improved screening test for red-green color deficiency composed of available pseudo-isochromatic plates," J. Opt. Soc. Am. **34**, 618 (1944).

TABLE I. Results of test with selected pseudo-isochromatic plates (from Rabkin, American Optical Company, and Dvorine tests).

Normal	Typical responses of: Color deficient *P*	*PA*	*D*	*DA*	Responses of subject D. D. Right eye	Left eye
12	—	—	12	12	—	12
ct	*c*	*c*	*t*	*t*	*t*	*t*
30	160	160	16	16	—	10
96	9	9	6	6	6	6
tc	*t*	*t*	*c*	*c*	*c*	*bc*
Rows 9–16	3, 5, 7	9–16	1, 2, 4, 6, 8	9–16	1, 2, 4, 6, 8	9–16
9			5*		5	5
t			*c*		*c*	*c*
13			6		6	6
ct			—		—	—
ts			—		8	6
9			6		—	6
25			—		*bc*	6
t			*c*		*t*, *c*?	*t*, *c*?
ct			*ts* or *tls*		*ts*	*tls*
74			21		21	21
42			—		—	42
86			—		—	—
5			2		2	3
6			5		5	5
75			—		—	—
29			70		70	70
57			35		35	35
3			—		0	5
15			17		17	17
27			—		—	—
27			—		—	2—
47			—		—	—
56			—		—	—
89			—		—	—
39			—		—	4
3			—		—	—
92			—		—	—
62			—		—	—
95			—		—	—
26			—		—	2—
74			—		—	—
56			—		—	—
33			—		—	36

Explanation of Abbreviations

t = triangle
c = circle
s = square

P = protanope
PA = protanomalous
D = deuteranope
DA = deuteranomalous

* This plate and those that follow do not differentiate type or degree of red-green color deficiency.

is the failure on Rabkin's Plate 18 with the right eye only.[10, **]

[10] L. H. Hardy, G. Rand, and M. C. Rittler, "Tests for the detection and analysis of color-blindness. III. The Rabkin test," J. Opt. Soc. Am. **35**, 481 (1945).

** According to Rabkin, Plate 18 is an excellent test for the differentiation of anomalous trichromats and dichromats. This is confirmed by Hardy, Rand, and Rittler, reference 10, who found that 31 of 36 subjects failing this plate were classed as dichromats by other tests.

3. Color Threshold Test[11]

This is a test of the lantern type in which eight different lights (two reds, two greens, two yellows, a blue, and a white) are shown at each of eight different intensities. The scores of subjects with normal color vision range from 60 to a perfect score of 64. The scores of deuteranomalous and protanomalous subjects range from 64 to about 35; those of deuteranopic and protanopic subjects are usually 35 or less. With the left eye, D. D.'s score was 50, with the right, 35.

4. Farnsworth-Munsell 100-Hue Test[12]

The material for this test consists of 85 color chips from the Munsell 100-hue series. These are of equal value and chroma (5/5) and differ in hue by very small steps. Three forms of test were made with this material.

A. In the standard hue discrimination test devised by Farnsworth, the color chips are presented in four separate groups, each of which the subject attempts to arrange in order according to hue. The results are charted in the form of a profile which indicates the regions of the hue circle in which the discrimination is poor. Poor discrimination occurs in two opposite regions whose locations are characteristic of the type of color deficiency.

The profiles for the right and left eyes of D. D. (Figs. 1 and 2) do not reveal any significant difference in the two eyes. Both are characteristic of the deutan[13, ***] type of defect.

B. In the second test with this material, the hues to be arranged were divided into two instead of four groups; one containing reds, yellows and greens, the other blue-greens, blues, purples, and red-purples. The colors presented in the first group were the odd numbered ones from 39 to 81; those in the second group, the odd numbered

[11] L. L. Sloan, "A quantitative test for measuring degree of red-green color deficiency," Am. J. Ophth. **27**, 941 (1944).

[12] D. Farnsworth, "The Farnsworth-Munsell 100-hue and dichotomous tests for color vision," J. Opt. Soc. Am. **33**, 568 (1943).

[13] Anon, "Chromaticity classification of types of vision," I-S. C. C. News Letter No. 56, 7–8 (1944).

*** This and the corresponding term, protan, suggested by Farnsworth (reference 13), are used to distinguish the two types of red-green color deficiency, without further classification as to degree of defect. Deutans may be either deuteranomalous or deuteranopic; protans, either protanomalous or protanopic.

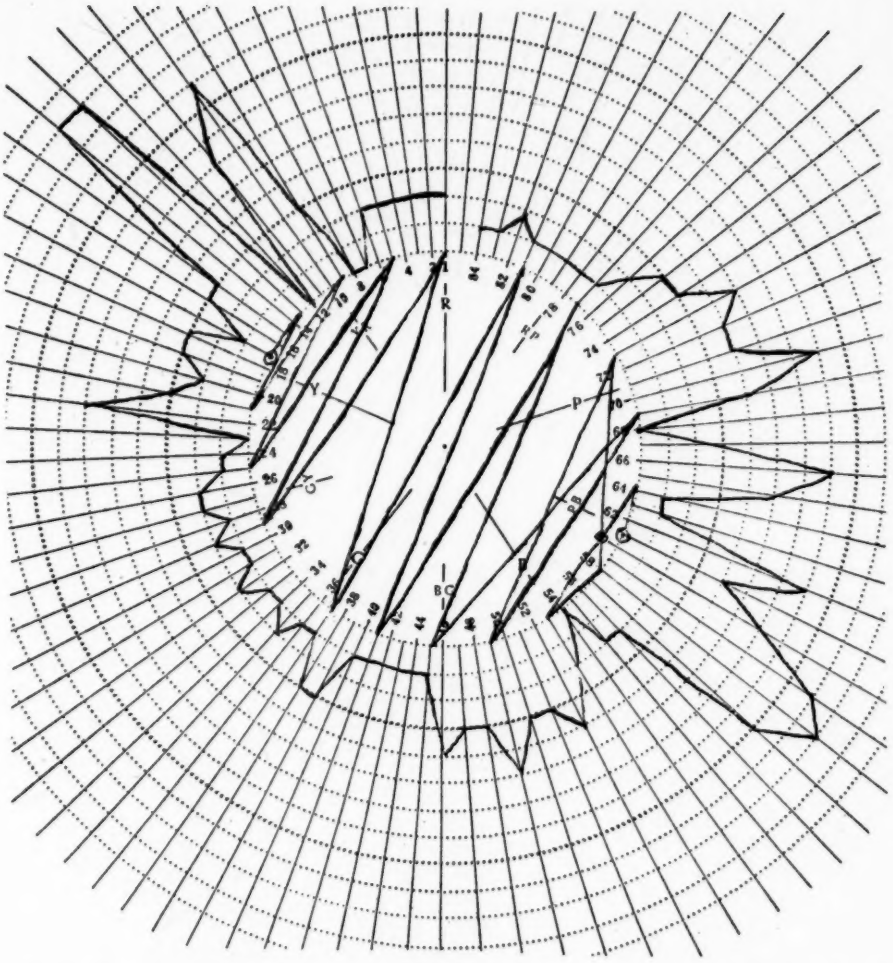

FIG. 1. Farnsworth-Munsell 100-hue test. Profile of the right eye. The connecting straight lines in the center of the graph show the order of arrangement of 21 hues selected from the complete series. See text.

colors, 83, 85, 1, 3, etc. to 37. With the left eye these were arranged in approximately correct order with only a few transpositions. With the right eye the errors were much greater. The order of arrangement is indicated in Fig. 3 by the connecting straight lines on the graph. It may be seen that reddish-yellows are placed next to greenish-yellows, and reddish-blues next to greenish-blues. These gross confusions of red and green are not revealed in the standard test, because the hues confused do not occur in the same group.

C. A third test was made by using only twenty-one hues (Nos. 1, 5, 9, etc.). The subject was instructed to start with No. 17 (yellow) and arrange the colors in regular order in a straight line or in a circle.† The results were as follows. *Left eye:* The colors were arranged in correct order, at first in a line, then in a circle when the subject noticed that the two ends of the line were alike. *Right eye:* The hues were arranged in the follow-

† This test is similar in principle to the Farnsworth dichotomous test (reference 12), which was not available to us at the time.

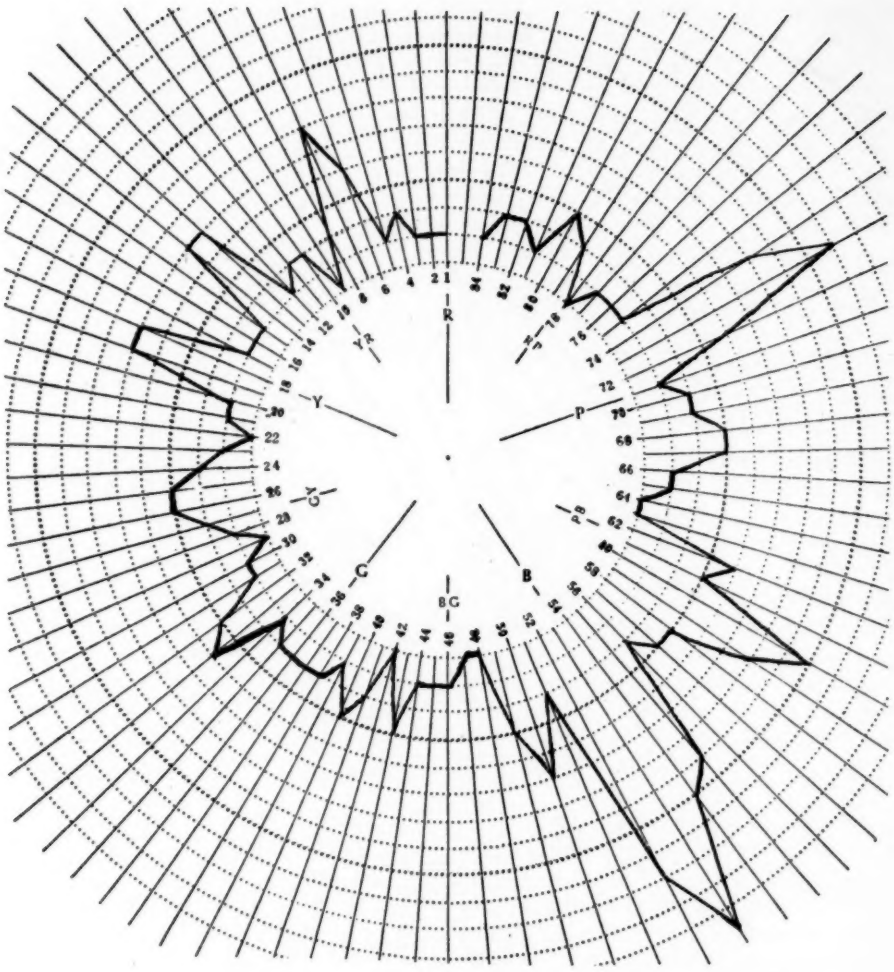

FIG. 2. Farnsworth-Munsell 100-hue test. Profile of the left eye.

ing order: 17, 13, 21, 9, 25, 5, 29, 1, 37, 81, 41, 77, 45, 69, 49, 73, 57, 53, 65, 61. The order of arrangement is shown diagrammatically in Fig. 1. The results are typical of those found in deuteranopia. The subject reported that the colors appeared to the right eye as a series varying from light brown to gray to blue.

DISCUSSION OF RESULTS

From the entire group of tests of color vision it may be concluded that the right eye is deuteranopic; the left eye, deuteranomalous. It is probable, moreover, that the defect in color perception of the left eye is of a very mild degree. It has been shown[14] that the small proportion of color deficient subjects who give normal responses on anomaloscope tests have, as a rule, a relatively slight defect. It is possible that, in some or all of the previously reported unilateral color defects, a slight abnormality in the supposedly normal eye might have been demonstrable if a greater number of tests differing in type had been em-

[14] L. L. Sloan, "Selection of color vision tests for the Army Air Forces," Arch. Ophth. 36, 263 (1946).

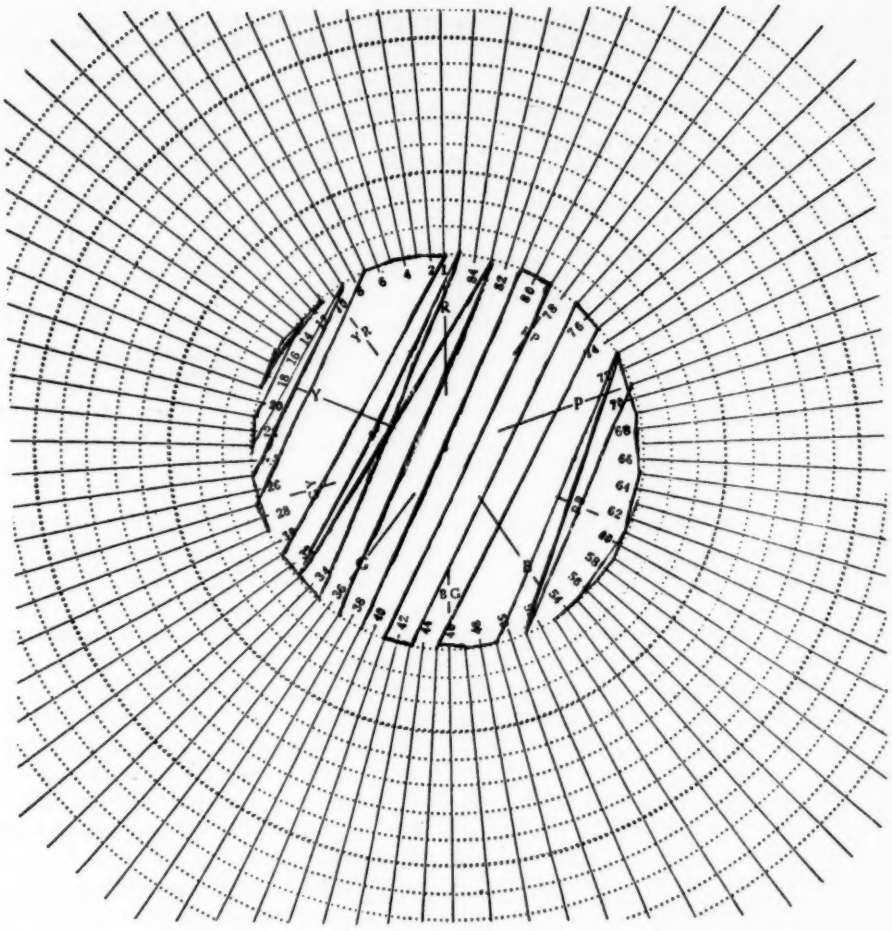

FIG. 3. Right eye. Order of arrangement of Farnsworth-Munsell colors when odd numbered hues were presented in two groups. See text.

ployed. An example is the case of unilateral deuteranomaly reported by von Kries[15] in 1919 and re-examined about 20 years later by Trendelenburg.[1(b)] The later studies showed that the color perception of the supposedly normal left eye was actually slightly deficient.

Colors Perceived by the Deuteranopic Eye

Our subject, though deuteranopic in the right eye only, is perhaps not an ideal case for investigation of the color perceptions of the deuteranope because of the anomalous color perception of the left eye. However, since this is of slight degree, it seems valid to assume that the color names used by him have essentially the same connotation that they have for the normal.

Comparisons were made of the color perceptions of the right and left eyes using papers of the Munsell 100-hue series illuminated by artificial daylight (Macbeth daylight lamp), and monochromatic stimuli provided by a Bausch and Lomb spectrometer.

The Munsell papers were two-inch squares viewed from a distance of about 40 cm. Only alternate hues of the complete series were used,

[15] J. von Kries, "Ueber einen Fall von einseitiger angeborener Deuteranomalie (Grünschwäche)," Zeits. f. Sinnesphysiol., **50**, Part II, 137 (1919).

TABLE II. Comparison of color perceptions of left and right eyes.

Munsell colors of 5 value, 5 chroma			Monochromatic stimuli	
Munsell hue notation	Dominant wave-length*	Color names given by subject	Wave-length	Color names given by subject
5 *PB*	475.9	pinkish-blue, left; blue, right	445	violet, left; blue, right
3 *PB*	478.1	blue, left and right; good match	450	blue, left and right; left, darker
			451–453	blue, left and right; good match
1 *PB*	480.1	blue, left and right; almost match	455	greenish-blue, left; blue, right
9 *B*	481.7	greenish-blue, left; blue, right		
7 *Y*	574.5	greenish-brown, left; brown, right	583	greenish-yellow, left; yellow, right
5 *Y*	575.6	brown, left and right; good match	584	yellow, left and right; good match
3 *Y*	577.7	reddish-brown, left; brown, right	585	orange-yellow, left; yellow, right
3 *BG*	494.4	blue-green left; bluish-gray, right	500	blue-green, left; bluish-white, right
1 *BG*	497.8	blue-green left; gray, right	501–505	blue-green, left; white, right
9 *G*	502.3	blue-green, left; gray with brown in it, right	506	blue-green, left; yellowish-white, right
5 *RP*	499.7*c*	purple, left; brownish-gray, right		
3 *RP*	504.9*c*	purple, left; gray, right		
1 *RP*	517.3*c*	purple, left; bluish-gray, right		

* Data from W. C. Granville, D. Nickerson, and C. E. Foss, "Tristimulus specifications for intermediate and special colors of the Munsell system," J. Opt. Soc. Am. **33**, 376 (1943).

since it had been found previously with the Farnsworth-Munsell test that the left eye could not distinguish smaller hue differences. The subject first selected several Munsell purple-blues which looked about the same to the left and right eyes. After a more careful inspection, using the left eye, 5 *PB* was reported as a slightly pinkish-blue; 9 *B* as slightly greenish; 3 *PB* and 1 *PB* as blue. When viewed in succession by the two eyes, 3 *PB* was judged a perfect match; 1 *PB* not quite as good. By a similar procedure 5 *Y* was selected by the left eye as unitary yellow and as the hue which was identical in appearance to the left and right eyes. The same procedure was used to select the hues seen as gray by the right eye. An approximate selection of several papers was first made. When these were placed side by side for better comparison and those appearing slightly yellowish or slightly bluish were rejected, 1 *BG* and 3 *RP* were finally chosen as the best grays. It should be noted that this method of determining the achromatic neutral point differs from the usual procedure in which the subject selects the color which matches a standard neutral. The dominant wave-lengths corresponding to the selected unitary and invariant colors, and to the neutral points are given in Table II.

A similar procedure was used to determine for monochromatic stimuli the wave-lengths corresponding to unitary blue and yellow for the left eye, the wave-lengths of the invariant hues for left and right eyes, and the wave-length of the neutral point for the right eye. The field of the spectrometer subtended a visual angle of about 4°. In these experiments, likewise, the unitary blue selected by the left eye was also the color which appeared identical to the right and left eyes. The wave-length selected as unitary yellow, though the closest approach to an invariant color for the two eyes, was reported as appearing slightly darker to the left than to the right eye. The results are summarized in Table II for comparison with those obtained with Munsell papers.

The two sets of data are in complete agreement in showing that the color perceptions of the dichromatic right eye include only blues, yellow, and the white-black series. The center of the spectral neutral region for D. D. is 503 mμ; the corresponding neutral point determined with Munsell papers is 498 mμ. The neutral points of 25 deuteranopes reported by Hecht and Shlaer[16] range from 491 mμ to 525 mμ with an average value of 504.3 mμ. Although the data for D. D.

[16] S. Hecht and S. Shlaer, "The color vision of dichromats. I. Wavelength discrimination, brightness distribution and color mixture," J. Gen. Physiol. **20**, 57 (1936).

are not strictly comparable because no standard neutral matching field was employed, they do not show a significant difference from previous findings. The dominant wave-lengths of the Munsell papers selected by D. D. as unitary blue and yellow are 478.1 mμ and 575.6 mμ. These also are in agreement with previously reported[5] values which range from 467 to 485 mμ and from 568 to 583 mμ. However, the wave-lengths selected in the spectrum, 452 mμ and 584 mμ, differ significantly from those chosen from the colors of low purity, and would be seen by the average normal eye as reddish-blue and reddish-yellow.

A tentative explanation for the abnormally reddish hues selected as unitary blue and yellow in the spectrum can be given if we assume that D. D. has ocular pigmentation[17,18] which is denser and significantly redder than the average normal. Two possible effects of such pigmentation must be considered. There is first the direct effect of its selective absorption which, for stimuli of low purity, produces a shift in chromaticity toward reddish-yellow. A secondary effect, opposed to the first, is the more or less permanent adaptation of the eye to reddish-yellow light. Since these two effects tend to cancel one another, ocular pigmentation may be expected to produce relatively little change in the appearance of Munsell colors of 5 chroma. In the case of spectrally homogeneous stimuli, however, no change in chromaticity can result from the direct effect of selective absorption, and the secondary effect of adaptation to reddish-yellow light is, therefore, unopposed. The wave-lengths in the spectrum selected as unitary blue and yellow would consequently be redder than those selected by the normally pigmented eye. A similar, though transient, effect of chromatic adaptation can be demonstrated in a normal subject by comparing the spectral stimuli selected as unitary blue and yellow after adaptation to darkness and immediately after adaptation to a high intensity of Illuminant *A*. It will be found that a longer wave-length yellow (reddish-yellow) and a shorter wave-length blue (reddish-blue) are selected when the eye is adapted to reddish-yellow light.

[17] E. Ludvigh and E. F. McCarthy, "Absorption of visible light by the refractive media of the human eye," Arch. Ophth. 20, 37 (1938).

[18] G. Wald, "Human vision and the spectrum," Science 101, 653 (1945).

Summary and Conclusions

Studies are reported of a subject with deuteranopia of one eye, mild deuteranomaly of the other. The deuteranopia of the right eye was demonstrated on the Nagel anomaloscope. The results of other tests such as the color threshold test, Rabkin's Plate 18 and a modified Farnsworth dichotomous test are in agreement with the diagnosis of deuteranopia. The red-green color deficiency of the left eye was demonstrated by pseudo-isochromatic plates, the Farnsworth-Munsell 100-hue test and the color threshold test. The results of the first two tests indicate that the defect is of the deutan type. The score of 50 on the color threshold test shows it to be a relatively slight defect. This is indicated also by the fact that the Nagel anomaloscope match is within normal limits.

In the spectrum and in the Munsell 100-hue series, the subject reported that with the right eye he saw only blues and yellows. The fact that perception of red and green is entirely lacking in the right eye was confirmed by determination of the hues which are identical in appearance to the left and right eyes. The only invariant hues are a blue and a yellow which to the left eye show no trace of either red or green.

The spectral locations of unitary blue and yellow for the left eye differ significantly from those of the average normal eye. This further evidence of the atypical nature of the color perceptions of the left eye might perhaps be caused by an abnormal ocular pigmentation.

The authors wish to acknowledge their indebtedness to Dr. D. B. Judd for valuable advice during this study and in particular for suggestions as to the possible influence of ocular pigmentation on the color perceptions.

An Industrial Application of Geiger-Müller Counters to the Analysis of Phosphorus in Steels

FORD R. BRYAN
Chemical and Metallurgical Engineering Research, Ford Motor Company, Dearborn, Michigan

AND

GEORGE A. NAHSTOLL
Chemical Engineering Department, Ford Motor Company, Dearborn, Michigan

The phosphorus content of steels is determined by means of a Littrow quartz spectrograph equipped with Geiger-Müller photoelectron counter tubes. Emphasis is placed on operation and maintenance procedures for open hearth and foundry furnace control. Arc excitation, which is essential for sensitivity and resolution of the phosphorus line from a nearby copper line, introduces variables requiring close regulation. Temperature of the spectrograph must be maintained at nearly a constant value to prevent the shifting of spectral lines at the focal plane of the instrument. Each determination requires about one minute after the sample has been prepared and loaded, and accuracies are comparable to routine chemical results.

MELTING specifications for irons and steels almost invariably call for rigid maximum limits in regard to the element phosphorus. In adapting spectrographic methods to ferrous analysis, the difficulty of determining phosphorus quickly and accurately has been a serious limitation. It has been possible to determine phosphorus spectrographically in non-ferrous alloys[1–4] and in minerals[5] by using customary photographic methods, since the lack of an interfering iron spectrum and the relatively high percentages involved have facilitated such determinations. However, attempts to analyze phosphorus in steels have presented several difficulties. Only a few phosphorus lines provide sufficient sensitivity for the determination of the 0.005 percent phosphorus sometimes required, and most of these more sensitive lines are subject to interference from the typical steel spectrum. The usable lines remaining are in the wave-length range requiring ultraviolet-sensitized plates and elaborate processing procedures, factors which have retarded the development of a photographic method thus far. The wave-lengths of these sensitive phosphorus lines are also too low to be readily detected by glass-enveloped, multiplier photo-tubes, which lose sensitivity rapidly below 2500A.

As an alternative to photographic and multiplier photo-tube methods, the application of Geiger-Müller tubes in a manner suggested by Duffendack and Morris[6] was initiated. The construction and testing of suitable equipment were conducted at the University of Michigan and have been described by Hanau and Wolfe.[7] The additional tests and industrial application herein reported were carried out in the laboratories of the Ford Motor Company.

APPARATUS

The major items of equipment used are: (1) an arc excitation source, (2) a temperature-controlled quartz spectrograph, and (3) the Geiger counter attachment with its associated electrical circuits.

Arc excitation equipment is preferable to the

[1] W. E. Milligan and W. D. France, "Determination of phosphorus in phosphorus bronze," Ind. Eng. Chem. Anal. Ed. **13**, 24–7 (1941).
[2] M. Milbourn, "The spectrographic analysis of copper and copper-rich alloys by the arc method," J. Inst. Metals **69**, 441–63 (1943).
[3] N. N. Semenov, "Quantitative spectral analysis of bronze and pig iron in the ultraviolet region of the spectrum," Zavodskaya Lab. **11**, 215–18 (1945).
[4] L. E. Vvedenskii and A. K. Andon'eva, "Spectral analysis of tin bronzes in the ultraviolet," Bull. Acad. Sci. U.S.S.R., Sér. Phys. **9**, 633–4 (1945).
[5] D. P. Norman and W. W. A. Johnson, "Spectrographic limit of detection of phosphorus, titanium, and zirconium in the direct current arc," Ind. Eng. Chem. Anal. Ed. **17**, 233–35 (1945).
[6] O. S. Duffendack and W. E. Morris, "An investigation of the properties and applications of the Geiger-Müller photoelectron counter," J. Opt. Soc. Am. **32**, 8–24 (1942).
[7] R. Hanau and R. A. Wolfe, "An investigation of the use of Geiger-Müller photoelectron counters in the spectrographic analysis of phosphorus in steel," presented at the 32nd Annual Meeting of the Optical Society of America, Oct. 25, 1947.

spark because of the much greater phosphorus line intensities available. The a.c. arc excitation source[8] is powered by a synchronous motor generator and includes two 10 kva-transformers, each with its 2200-volt secondary winding in series with a 1300-ohm ballast resistor. The transformers can be used either in series or in parallel to provide 1.7 amperes at 4400 volts or 3.4 amperes at 2200 volts, respectively. Adjustment of the Copel ballast resistance provides intermediate current values. An auxiliary starting circuit is used.

In order to regulate the temperature of the spectrograph the Bausch & Lomb large Littrow instrument employed is enclosed completely in a wooden cabinet which is insulated with a lining of ½-inch felt and fitted with a small fan for circulation. A tubular inlet is provided for the entrance beam, and sliding panels allow access to points of adjustment. A 110-volt heating element controlled by means of a mercurial thermostat maintains a degree of heat well above room temperature. A sensitive bimetallic thermostat was discarded because of irregularities caused by vibration.

Two Geiger-Müller counter tubes of like construction are mounted on a carriage fitted to the spectrograph at the plate holder position so that each tube with its attached exit slit can be placed to receive the wave-length desired. These photon counter tubes[9] were constructed with quartz envelopes, nickel cathodes, and tungsten anodes. The transparency of the envelope thus matches that of the spectrograph optics and allows photons of the required wave-length to enter the tube. The cylindrical cathode is provided with an entrance opening which permits radiations to fall upon its inner photosensitive surface. Filling the tubes with hydrogen gas at about 10 centimeters pressure provides non-self-quenching photoelectron counters sensitive to a useful wave-length range of from 2600A to 1850A. Sensitivity limits are determined in this case by the photoelectric threshold of the nickel which establishes the longer wave-length limit

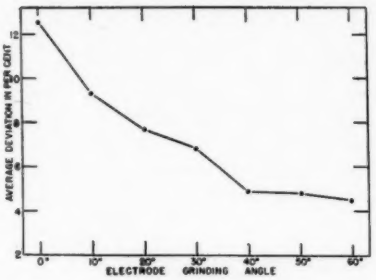

FIG. 1. The influence of grinding angle on the reproducibility of ratio readings. Average deviations were computed on the basis of ten exposures run at each of the seven angles chosen. The angles specified represent the amount of metal removed to form a conical end as measured from a plane perpendicular to the length of the electrode.

and by the quartz and air absorption which determines the shorter wave-length limit. The non-self-quenching properties tend to provide stable operating characteristics and relatively long life for these tubes. Operation voltage is about 800 volts, and a 150-volt Geiger region is typical.

Each counter tube is connected to Cyclotron Specialties quenching[10] and scaling[11] units, which together supply a regulated voltage to the tube, quench each pulse, and register one out of every eight counts upon a dial indicator. Provision is made for stabilized voltage at any value necessary for satisfactory tube operation. External quenching is required because of the non-self-

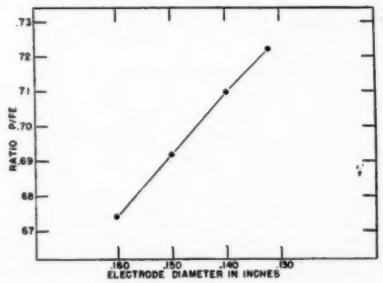

FIG. 2. The effect of small differences in electrode diameter on the ratio of phosphorus counts to iron counts. This range of diameters was found among a group of samples drawn into glass tubing of supposedly uniform bore. Variation of 0.005 inch in diameter results in an analytical error of about five percent of the amount of phosphorus present in the sample.

[8] O. S. Duffendack and K. B. Thomson, "Developments in the quantitative analysis of solutions by spectroscopic means," Proc. A.S.T.M. **36**, II, 301–9 (1936).

[9] O. S. Duffendack, H. Lifschutz, and M. Slawsky, "Production characteristics and reliability of Geiger-Müller counters," Phys. Rev. **52**, 1231 (1937).

[10] H. V. Neher and W. W. Harper, "A high speed Geiger counter circuit," Phys. Rev. **49**, 940 (1936).

[11] H. Lifschutz, "A complete Geiger-Müller counting system," Rev. Sci. Inst. **10**, 21 (1939).

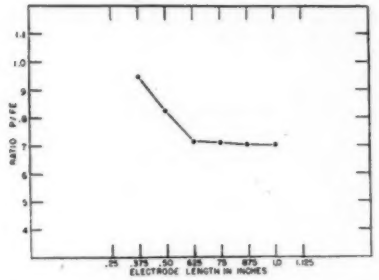

FIG. 3. The effect of changes in electrode length on the ratio of phosphorus counts to iron counts. The electrodes used were 0.156 inch in diameter, and the arc current was 1.7 amperes. A corresponding effect has been observed with pins of 0.25 inch diameter when using a 3.4-ampere arc. Excessively short pins can account for errors as large as 20 percent of the amount of phosphorus present.

quenching properties of the hydrogen-filled tube. The scale-of-eight electronic dividing circuit reduces the original number of pulses to a rate small enough to be registered accurately. Since counts from an arc source occur at random intervals and often at a rapid rate, it is necessary to consider the electrical resolution of the total recording circuit.[12] In the case of this particular equipment, the resolution is limited to 3600 equally spaced, scaled counts per minute by the register itself, beyond which a detrimental coincidence error becomes apparent. The register is a much greater restricting factor when counting random pulses and causes the coincidence error to become quite significant beyond about 500 scaled, random counts per minute.

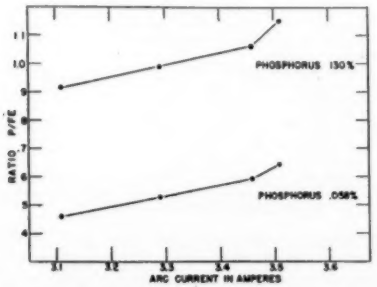

FIG. 4. The effect of variations in arc current on the ratio of phosphorus counts to iron counts. Electrodes of 0.25 inch diameter were used. A change of 0.03 ampere represents an analytical error of about five percent of the amount of phosphorus present.

[12] H. Lifschutz and O. S. Duffendack, "The counting losses in Geiger-Müller counter circuits and recorders," Phys. Rev. **54**, 714–725 (1938).

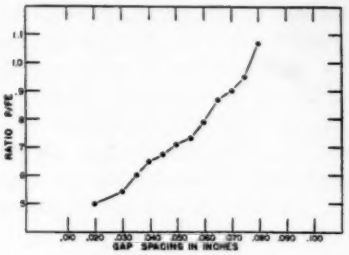

FIG. 5. The effect of small changes in gap spacing on the ratio of phosphorus counts to iron counts. The electrodes used were 0.25 inch in diameter and were arced at 3.4 amperes. Variation of 0.005 inch represents an analytical error of about five percent of the amount of phosphorus present.

OPERATION PROCEDURE

In order to obtain reproducible and accurate analyses with this equipment the operating conditions must be controlled with precision. Many of the factors requiring exactitude are associated with the characteristics of the arc source. The specific conditions utilized will now be presented, and the effects of variations in these conditions will be described.

Sample preparation.—Cast rods are prepared as self-electrodes by a grinding operation which produces a conical burning tip. An angle of 45 degrees is specified, representing the amount of metal removed as measured from a plane perpendicular to the length of the electrode.

Electrode angles of from 0 to 15 degrees result in high and non-reproducible ratios of phosphorus to iron, while angles ranging from 20 to 60 degrees give lower and more consistent ratios. It appears that the larger angles provide more consistent optical alignment and, consequently, less variation in quartz absorption.[7] The effect of grinding angle on the reproducibility of ratio readings is shown in Fig. 1. Precision in determining ratios is definitely improved by the use of larger grinding angles.

Electrodes ranging in diameter from 0.125 to 0.25 inch have been used; however, diameters should be within 0.005 inch of the diameter of the standards employed in constructing the working curve. Figure 2 illustrates the effect of small changes in electrode diameter on the ratio of phosphorus counts to iron counts. The amount of error does not appear to diminish with sizes up to 0.25 inch. A range of diameters from 0.130

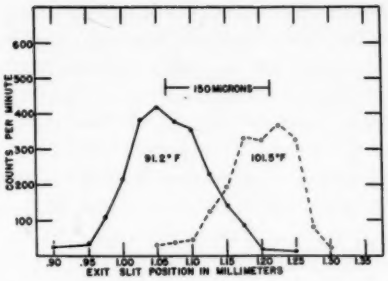

FIG. 6. The influence of temperature on the position of the phosphorus line (2136.2A). A temperature change of 10 degrees Fahrenheit results in a line shift of approximately 150 microns. Equilibrium temperatures were made possible by means of a fully enclosed spectrograph. Each of the two temperatures was maintained for several days before the corresponding series of readings was taken.

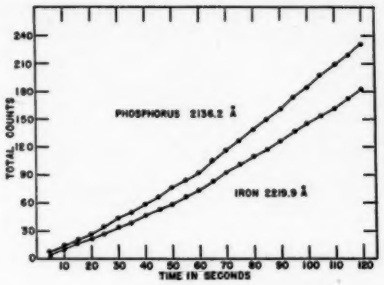

FIG. 7. A comparative record of phosphorus and iron counts accumulated during a continuous 2-minute exposure and read at 5-second intervals.

inch to 0.160 inch was found among a group of samples prepared by being drawn into glass tubing of supposedly uniform diameter, indicating that either precision-bore tubing or cast pins should be specified.

Reproducibility requires that electrodes be at least 0.625 inch in length. Trials disclose that phosphorus-to-iron ratios vary with pin length for pins of less than 0.625 inch, whereas longer pins may vary in length without affecting the ratio so greatly (see Fig. 3).

Source conditions.—Electrical source conditions are adjusted to provide 220 volts to the transformer primaries, and it is essential that the voltage be maintained to within plus or minus 3 volts. Currents from 1.7 to 3.4 amperes have been utilized with various electrode diameters. A low amperage should be used with small diameter electrodes in order to prevent burning irregularities and a higher current with large diameter electrodes in order to provide a sufficient number of counts for accurate calculations. In all cases, it is necessary to maintain the constancy of the current selected to within 0.05 ampere. The effect of small changes in arc current on the ratio of phosphorus counts to iron counts is depicted by Fig. 4. In this case, a variation of 0.03 ampere represents an analytical error of about 5 percent of the amount of phosphorus present.

The analytical gap is spaced at 0.060 inch, with variations of only 0.005 inch allowable. The choice of gap length does not appear to be critical; however, once chosen, this length must be rigidly maintained. Small changes in gap spacing affect the ratio of phosphorus counts to iron counts to the extent indicated in Fig. 5. A variation of 0.005 inch represents an analytical error of about 5 percent of the amount of phosphorus present.

Optical alignment.—Electrodes are aligned at a distance of 35 centimeters from the entrance slit of the spectrograph in order to provide a distance great enough for definite optical alignment without too much loss of sensitivity. No lens is employed, since constant slit illumination is more necessary than additional intensity. A spectrograph entrance slit 30 microns in width and 7 millimeters in height is used, with exit slits at the focal plane fixed at 200 microns width and 6.3 millimeters height. Normal focus and tilt adjustments for the tenth region (2100A to 2500A) of the spectrograph provide the wavelength range and dispersion required.

Lines used.—One exit slit counter tube assembly is located to receive the 2219.9A iron

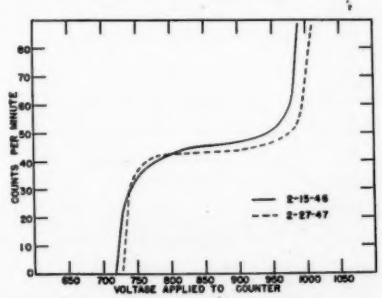

FIG. 8. Comparative plateaus obtained from a single counter tube before and after a year's operation. The tube does not appear to have deteriorated appreciably with use.

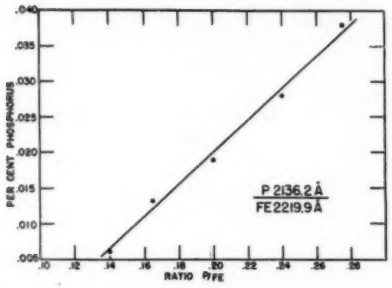

FIG. 9. A working curve for use in analyzing steels with low phosphorus content.

line and the other to receive the 2136.2A phosphorus line.[7] The exit slit is centered over the iron line by noting the position of the edges of the line during a scanning operation. Either audible or visual counting indication serves to determine the position of rapidly increasing and decreasing counts characteristic of the line edges. The exit slit is centered over the phosphorus line by noting the sharp increase in number of counts due to the edge of a strong copper line at 2135.97A. Returning the slit to within five divisions (50 microns) of the edge of the copper line places the slit directly over the phosphorus line to be measured. Locating the iron and phosphorus lines in this fashion takes no more than ten minutes. A rapid method of realignment is imperative since, in spite of our attempts at rigid temperature control, it is necessary to readjust slit positions once each eight-hour shift in order to insure proper alignment. The phosphorus line can be located without utilizing a copper line by employing electrodes with high phosphorus but no interfering copper; however, two pairs of electrodes are then required. A ratio method of setting tubes has also been proposed[7] but has not been adopted because of the added time involved.

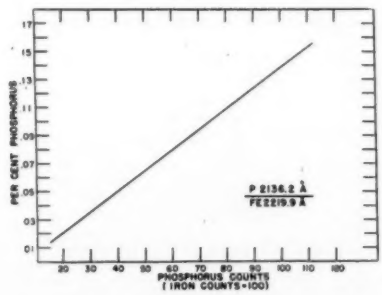

FIG. 10. A typical working curve wherein the percent of phosphorus in steel is plotted directly against phosphorus counts. In using such a curve a constant number of iron reference counts is required rather than a constant exposure time from sample to sample.

Temperature regulation.—In order to prevent spectral line shift caused by changes in prism temperature, an attempt is made to regulate the air within the spectrograph cabinet to within ±1°F at an arbitrary setting between 95° and 100°F. The temperature of the prism itself varies less since its time constant is much greater than that of the air. Assuming that exit slits are set perfectly, proper resolution of the phosphorus line from the copper line requires that line shift be held to a maximum of 40 microns.

The fully enclosed spectrograph has made possible the accurate measurement of line position at temperatures maintained at equilibrium for several days. These measurements indicate that the shift in line position is approximately 15 microns per degree Fahrenheit. Figure 6 shows the relative positions of the phosphorus line at two equilibrium temperatures.

Exposure time.—Exposure times are determined chiefly by three factors: (1) variation of line intensity with time, (2) the relationship of counting error to the total number of counts, and (3) the necessity for rapid analysis.

An exposure time sufficient to register 100 scaled iron counts has been adopted for low alloy steels. This number of iron counts is obtained in about one minute, and from 10 to 150 scaled phosphorus counts may be obtained during the same time interval. The plotting of the variation of line intensity ratio against time indicates that

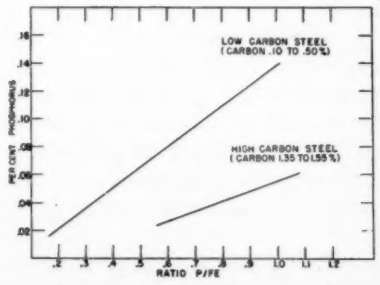

FIG. 11. A comparison of working curves for two alloys differing primarily in carbon content.

an exposure totaling 100 scaled iron counts will utilize fairly constant intensities and result in a reliable ratio (see Fig. 7).

Errors in counting random pulses have a definite mathematical relationship[13] to the total number of pulses counted. In general, the probable error in percent can be said to vary as the reciprocal of the square root of the total number of counts.

$$\text{Percent probable error} = 0.67n^{-\frac{1}{2}}(100),$$

where n represents total counts. Thus, in order to expect probable counting errors of less than 5 percent, it is necessary to totalize a minimum of about 200 unscaled counts or 25 registered counts. Because of both cosmic and optical backgrounds, which may aggregate some 40 unscaled counts per minute, the minimum total number of counts measured must be increased to compensate for this added error caused by background. Probable error is found to increase as the ratio of line counts to background counts decreases, according to the formula:

$$\text{Probable error} = 0.67[(N_1+N_2)^{\frac{1}{2}}/(N_1-N_2)],$$

where N_1 is the number of counts due to line radiation plus background, and N_2 the number due to background. Considering the 40 unscaled counts arising from background radiation, it becomes necessary to revise our minimum total number of counts to approximately 31 scaled or 250 unscaled when probable errors within five percent are desired.

Necessity for rapid analyses dictates the use of exposure times near the minimum required for acceptable accuracy. An exposure time of 100 scaled counts from the iron line was adopted as a compromise after considering the effects of the three factors just described. It may be found feasible in the case of very low percentages of phosphorus to extend the exposure time in order to gain accuracy.

Electrical operation of counters.—Electrical operation of the counters is readily accomplished by means of standard adjustments supplied with the commercial scaling units. The voltage-count relationship of the tube used to measure phosphorus is shown in Fig. 8. The similarity of the curves taken a year apart indicates that this type of tube is relatively stable. A small bottle of thorium nitrate is placed immediately in front of the exit slit to provide a constant source of radiation for determining the voltage-count relationship, and the midpoint of the plateau of the resulting curve is selected as the proper operating potential. Once adjusted, voltage and stabilizing controls may be advantageously locked in position, thus eliminating frequent manipulation.

Calculations.—Calculations required of the operator for each determination have been simplified for production use. During the experimental period calculations for each analysis were as follows:

Percent of phosphorus is a function of $(P_2-P_1)/([Fe]_2-[Fe]_1)$, where P_1 and $[Fe]_1$ are pre-exposure phosphorus and iron readings, respectively; and P_2 and $[Fe]_2$ are post-exposure phosphorus and iron readings, respectively. For production use, the counting circuits were modified to enable the operator to reset the registers

TABLE I. Phosphorus analysis of production samples.

Sample type	Pin diameter	Routine chemical analysis	Geiger tube analysis
4E	1/4	0.019	0.020/.019/.018/.020
LC No. 3	1/4	0.013	0.012/.012/.009/.011
LC No. 1	1/4	0.007	0.008/.009/.008/.008
LC No. 2	1/4	0.010	0.009/.010/.008/.009
LC No. 1	1/4	0.011	0.015/.014/.012/.014
LC No. 2	1/4	0.009	0.008/.012/.011/.012
Cupola AA Iron	3/16	0.17	0.169/.162/.175/.163
Cupola AA Iron	3/16	0.17	0.168/.165/.176/.168
Cupola AA Iron	3/16	0.165	0.164/.161/.157/.167
Cupola AA Iron	3/16	0.17	0.178/.165/.168/.171
Cupola B Iron	3/16	0.20	0.185/.183/.180/.190
Cupola B Iron	3/16	0.19	0.195/.187/.204/.190
Cupola AA Iron	3/16	0.17	0.190/.185/.181/.187
Cupola B Iron	3/16	0.19	0.197/.205/.203/.195
Cupola AA Iron	3/16	0.19	0.184/.185/.180/.185
SAE 1111	1/8	0.092	0.103/.099/.085/.083
SAE 1111	1/8	0.145	0.133/.137/.139/.134
Rim Steel	1/8	0.005	0.007/.006/.005/.009
SAE 1111	1/8	0.108	0.101/.104/.114/.109
Rim Steel	1/8	0.006	0.013/.011/.014/.010
SAE 1111	1/8	0.088	0.105/.108/.106/.107
Crankshaft	1/8	0.046	0.053/.047/.054/.053
Crankshaft	1/8	0.055	0.059/.062/.055/.051
Crankshaft	1/8	0.040	0.046/.053/.037/.036
Crankshaft	1/8	0.055	0.055/.055/.056/.049
Crankshaft	1/8	0.028	0.027/.025/.023/.023
Crankshaft	1/8	0.038	0.036/.044/.041/.034

[13] H. V. Neher, "Discussion of probabilities and errors in Geiger counter work," pp. 298–304 in Strong, J., "Procedures in Experimental Physics." New York: Prentice-Hall, Inc., 1938. Pp. x+642.

TABLE II. Deviations of Geiger counter results obtained in analyzing several typical steels. The columns headed "Deviation from mean" were derived by averaging deviations from the mean of each of four separate determinations made upon each sample; thus deviations, rather than analyses, were averaged.

Type of sample	Number of determinations	Concentration range	Maximum deviation from mean	Average deviation from mean	Maximum deviation from routine chemical analysis	Average deviation from routine chemical analysis
Open hearth steels	98	0.005–0.021 percent	0.004	0.001	0.006	0.002
Pistons	28	0.045–0.067 percent	0.003	0.001	0.008	0.003
Crankshafts	92	0.028–0.066 percent	0.007	0.002	0.015	0.004
Cupolas	92	0.10 –0.20 percent	0.013	0.004	0.020	0.008
Electric furnace steels	36	0.08 –0.145 percent	0.015	0.004	0.020	0.008

to zero before each determination and to control the exposure to provide a constant number of reference counts, resulting in percentage of phosphorus being a function of (P_2/k). By using the same value for k in making determinations as that used in setting up the working curve, the percentage of phosphorus becomes a function of P_2 alone. Interpolation of scaled counts is not required unless the total number of phosphorus counts is small, perhaps less than 20; and even in these cases the high probable error caused by random background counts may largely nullify the added exactness from interpolation.

Working curves.—Typical examples of working curves for use in analyzing steels are shown in Figs. 9 and 10. Either phosphorus counts or the ratio of phosphorus counts to iron counts may be plotted against percent of phosphorus to produce a working curve. A flattening of the curve at the upper end may indicate a lack of electrical resolution, while a flattening of the lower portion of the curve may denote a counting rate closely approaching that of cosmic- and stray-radiation background.

Separate working curves are required for steels differing appreciably in alloy type. Carbon, in particular, has been found to influence the ratio of counting rates. A comparison of working curves for two alloy types varying primarily in carbon content is shown in Fig. 11. A single working curve can be utilized to analyze steels of low alloy content with carbon from 0.10 to 0.50 percent. A distinctly separate curve is required, however, for a steel containing 1.35 to 1.55 percent carbon. In the case of carbon it is thought that the metallurgical form in which it exists affects the excitation characteristics. The small variations of constituents found within the specifications range of a particular alloy have not appeared to necessitate additional working curves.

Thus far, the only known factor causing a definite displacement of a working curve after it has been established has been the shift of spectral line positions caused by temperature change. The proximity of the copper line (2135.97A), which is 0.23A from the phosphorus line, has made it exceedingly difficult to control temperature to the degree necessary to prevent interference from even low percentages of copper. A few hours of operation without temperature control can result in copper interference causing erroneous ratio values when as little as 0.01 percent copper is present.

Since spectrographic standards with certified phosphorus analyses are not available, it is necessary to pour and to analyze chemically the required standard electrodes for each alloy type.

The Geiger counters, themselves, aided tremendously in tracing the effects of the operating variables described above. Data which would have required hours by photographic means was gathered in a matter of minutes. The suitability of direct reading receivers for the purpose of gathering spectrographic data cannot be overemphasized.

RESULTS

Analytical results appear to be sufficiently reliable to compete with routine chemical methods. Over a wide variety of samples, ranging from low alloy open hearth steels with a nominal 0.01 percent phosphorus to foundry irons containing 0.20 percent phosphorus, the deviations are within a tolerable range. Table I illustrates the comparison between Geiger counter and routine chemical analyses of several typical alloy types.

It will be noted that three different electrode diameters were encountered as a result of the sampling methods used at the various furnaces. A series of four determinations was run on each sample in order to ascertain reproducibility, which is more significant than deviation from the chemical result, since chemical analyses were strictly routine. Additional accuracy data as determined from a large number of samples is shown in Table II. On the basis of 346 determinations on typical production metals, average deviations from the mean of Geiger counter results range from 0.001 to 0.004 percent phosphorus. Average deviations from routine chemical analyses extend from 0.002 to 0.008 percent phosphorus. As may be expected, the greater deviations occur with samples having the higher phosphorus concentrations.

Experience indicates that exceptionally fine operation of the equipment can hold over-all errors to about five percent of the amount of phosphorus present. With ordinary production technique, however, errors of ten percent may be expected.

Permitting an average time of one minute for sample preparation and loading, the total analyzing time required becomes about two minutes per determination. This rate is consistent for any number of samples available at a given time. Once the instrument is in proper adjustment, one person can maintain the above rate. A second operator could possibly reduce the time required by 25 percent.

CONCLUSION

Although the apparatus and methods described were applied specifically to the determination of phosphorus in steels, it is hoped that this work will be of broader value by stimulating further efforts in the application of Geiger-Müller counters to the problems of spectroscopy. For example, it is conceivable that Geiger counters might offer the necessary approach for the successful determination of other elements which have thus far been difficult to analyze spectrographically. Furthermore, counter tubes may extend the range of direct reading instruments into the lower wave-length regions where the use of multiplier photo-tubes has not been feasible. Geiger counters should also prove extremely valuable as sensitive and instantaneous indicators for the study of what is now generally conceded to be the foremost cause of error in spectrographic analysis, namely, excitation problems.

The Quantitative Spectrographic Analysis of the Rare Earth Elements*

I. Determination of Samarium in Neodymium

II. Determination of Europium in Samarium

VELMER A. FASSEL AND HARLEY A. WILHELM
Institute for Atomic Research, Iowa State College, Ames, Iowa

(Received January 5, 1948)

Spectrographic methods applicable to the determination of small amounts of rare earth impurities in other rare earths are described. The specific examples discussed are the determination of samarium in neodymium and of europium in samarium. The procedures involve the high current d.c. arc excitation of rare earth oxide-graphite mixtures. Selected lines of the major rare earth constituent are used as internal standards. The experimental error of these methods is about 4 percent. Studies on the variation of the analytical intensity ratio during excitation and the effect of large changes in arc current, percent graphite, and weight of sample charge on the intensity ratio values are included.

I. INTRODUCTION

THE limited application of ordinary chemical procedures to the analysis of the rare earth elements has resulted in the development of a number of physical and physico-chemical methods. Of these, the spectrophotometric method[1,2] has possessed the greatest general utility. The lack of adequate sensitivity has, however, limited the use of this method for the determination of low concentrations of rare earth impurities. For example, the limits for determining samarium in purified neodymium and europium in purified samarium have been found to be approximately 1 and 4 percent, respectively.[3] The recent studies on large-scale rare earth fractionation[3] emphasized the need of developing a general method of analysis of adequate sensitivity to supplement the spectrophotometric procedures.

A literature survey on the scope and limitations of the various methods of rare earth analyses which have been proposed indicated that emission spectra offered the best possibilities of general adaptation to these analyses. In the present paper the spectrographic determination of low concentrations of rare earth impurities in other rare earths is discussed. The specific examples described are the determination of samarium in purified neodymium and the determination of europium in purified samarium. The spectrographic determination of major rare earth constituents in complex mixtures has also been investigated in this laboratory and the results from this study will be presented in a subsequent paper.

II. HISTORICAL

Selwood[4] has investigated the semiquantitative determination of a number of rare earth impurities in neodymium and yttrium. The studies by Bauer[5] on the use of the arc spectrum for the quantitative analysis of difficult to vaporize substances included an investigation of the determination of lanthanum oxide in synthetic mixtures of aluminum, calcium, and iron oxides. Hopkins *et al.*[6] evaporated rare earth nitrate solutions on graphite electrodes and excited these electrodes with a low voltage d.c. arc. Magnesium and zirconium were used as internal standards. The variations in their results were too large for a successful analytical method; the major error was

* Contribution No. 24 from the Institute for Atomic Research, Iowa State College, Ames, Iowa. Abstracted from a thesis presented by Velmer A. Fassel to the Graduate School of Iowa State College in partial fulfillment of the requirements for the degree of doctor of philosophy in chemistry. This document is based in part on work performed under Contract No. W-7405 eng-82 for the Atomic Energy Project.

[1] Prandtl and Scheiner, Zeits. anorg. allgem. Chemie **220**, 107 (1934).

[2] Rodden, J. Research Nat. Bur. Stand. **26**, 557 (1941); **28**, 265 (1943).

[3] Spedding, Fulmer, Butler, Gladrow, Gobush, Porter, owell, and Wright, J. Am. Chem. Soc. **69**, 2786 (1947).

[4] Selwood, Ind. Eng. Chem. Anal. Ed. **2**, 93 (1930).

[5] Bauer, Zeits. anorg. allgem. Chemie **221**, 209 (1935).

[6] Hopkins, McCarty, Scribner, and Lawrenz, Ind. Eng. Chem. Anal. Ed. **10**, 184 (1938).

attributed to the poor reproducibility of the d.c. arc discharge between electrodes prepared in this manner. Gatterer and Junkes[7] used essentially the same technique for determining europium in samarium. However, they increased the precision through multiple excitations (9 per sample) in order to favor a statistical reduction in the overall experimental error, and through the choice of another rare earth as internal standard in order to compensate more effectively for the excitation variables. While the accuracy of their method was satisfactory, the multiple electrode evaporations that were required were too time consuming for practical fractionation control. Lopez de Azcona[8] has developed a method for the determination of gadolinium in samarium based on diluting the samarium oxide with either sodium chloride or magnesium oxide spectroscopic buffer and using added molydenum or lanthanum oxide as internal standard. The observations from our moving plate studies, which are given in detail later, indicated that magnesium oxide, sodium chloride, or other materials more volatile than the rare earth oxides, lack one of the desirable qualifications of a spectroscopic buffer. This property is the ability to transport the material to be analysed into the discharge zone during the period the buffer is stabilizing the arc. The methods described in this paper employ a spectroscopic buffer that possesses this desirable property; they do not require the addition of an internal standard, and they involve a minimum of sample preparation.

III. APPARATUS

The complexity of the rare earth spectra made it imperative to employ a spectrograph of high dispersion. The instrument used was a Jaco-Wadsworth, 21-foot, stigmatic grating spectrograph[9] manufactured by the Jarrell-Ash Company of Boston, Massachusetts. The second-order spectra, which had a dispersion of 2.5 A/mm, was used exclusively.

The external optical system was designed to provide uniform illumination along the length of the slit and to achieve maximum illumination by insuring that the light entering the slit would fill, but not exceed, the aperture of the collimating mirror or grating. These conditions were fulfilled by employing a 10.0-cm focal length cylindrical quartz lens with its axis vertical placed 44 cm from the slit, and a 50-cm focal length cylindrical quartz lens with its axis horizontal placed directly in front of the slit. The latter lens was an integral part of the Jaco rotating sector assembly, the sector disk being located between the slit and the lens. The two cylindrical lenses were used, rather than a single spherical lens, in order that the light would fill the grating aperture horizontally without exceeding the aperture vertically. The light source was located 55 cm from the slit. A projection system[10] was used to aid in the precise alignment of the electrodes on the optical axis. The water-cooled excitation stand was patterned after the design of Scribner and Corliss.[11]

The power source for the high amperage d.c. arc used as excitation source was a General Electric 5-kw compound-wound generator powered by a General Electric 7-horsepower synchronous motor. The terminal voltage was adjusted by means of a shunt-field rheostat. A special resistance unit, designed for the adjustment of the arc current, consisted of ten resistance units made of $\frac{3}{16}\times 0.008$ inch Copel ribbon (resistance of 0.155 ohm/foot) wound on three slabs of $\frac{1}{4}''\times 16''\times 39''$ Transite. These slabs were mounted in an angle iron cage 39 inches wide, 19 inches deep, 30 inches high in the back, and 21 inches high in the front. The sides of the cage were covered with hardware cloth while the slanting top was made of plywood. A rotary resistor

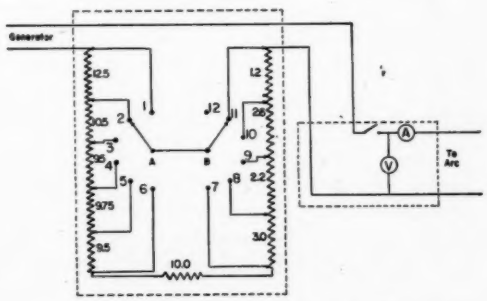

FIG. 1. Wiring diagram for resistance unit.

[7] Gatterer and Junkes, Spectrochim. Acta **1**, 31 (1939).
[8] Lopez de Azcona, Bol. inst. geol. y minero. Espana (**3**) **15**, 270 (1941).
[9] Jarrell, J. Opt. Soc. Am. **32**, 666 (1942).
[10] Smith and Fassel, Ind. Eng. Chem. Anal. Ed. **20**, in press (1948).
[11] Scribner and Corliss, J. Opt. Soc. Am. **33**, 515 (1943); J. Research Nat. Bur. Stand. **30**, 41 (1943).

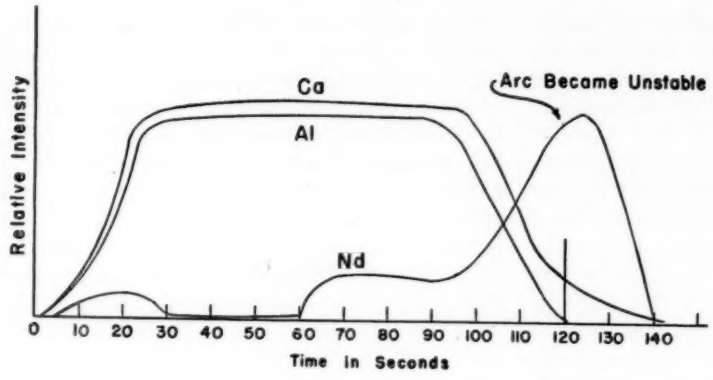

FIG. 2. Volatilization rates for Al_2O_3, CaO, and Nd_2O_3 mixtures.

selection switch was mounted on the slanting top. The large size of the unit provided for adequate spacing that permitted air circulation to prevent over-heating of the resistors. Copel ribbon was chosen as the resistance medium because of its low temperature coefficient of resistance. The values of the individual resistance units, and the wiring diagram for the whole unit are indicated on Fig. 1. Currents between graphite electrodes ranging from 2 to 18 amperes at 250 volts are readily obtained through the various resistor combinations.

The three-piece graphite electrode assembly described by Scribner and Mullin[12] was used. The anodes (lower electrodes) were machined from $\frac{1}{4}$-inch diameter National Carbon Company special spectroscopic graphite by means of a Jarrell-Ash Company electrode drilling machine and a motor-driven cutter constructed in the machine shop. The cathodes were $\frac{1}{8}$-inch diameter graphite pointed in an ordinary pencil sharpener. The electrode separation was adjusted to exactly 4 mm with the aid of the projection system and was maintained at this separation during arcing by means of the controls provided on the excitation stand.

The plates were processed in an ARL-Dietert developing machine,[13] and photometric measure-

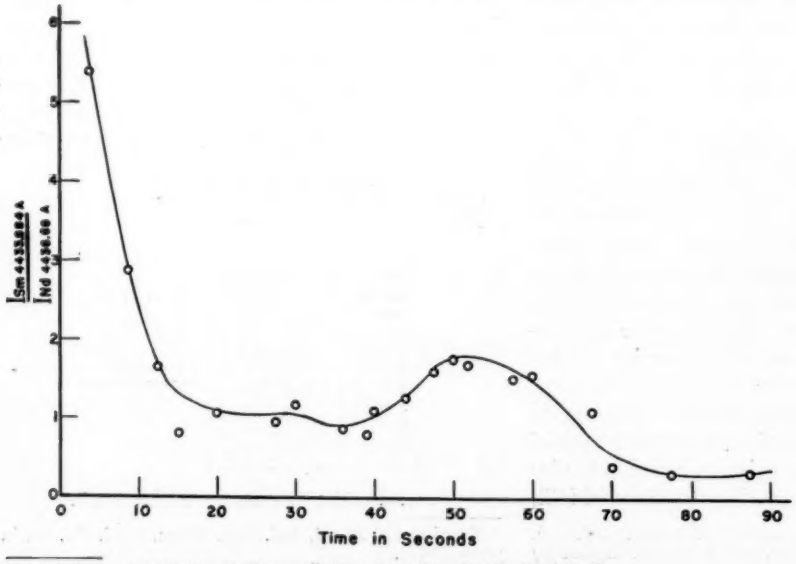

FIG. 3. Variation of intensity ratio with time: samarium in neodymium.

[12] Scribner and Mullin, J. Research Nat. Bur. Stand. **37**, 379 (1946).
[13] Schuch, J. Opt. Soc. Am. **32**, 116 (1942).

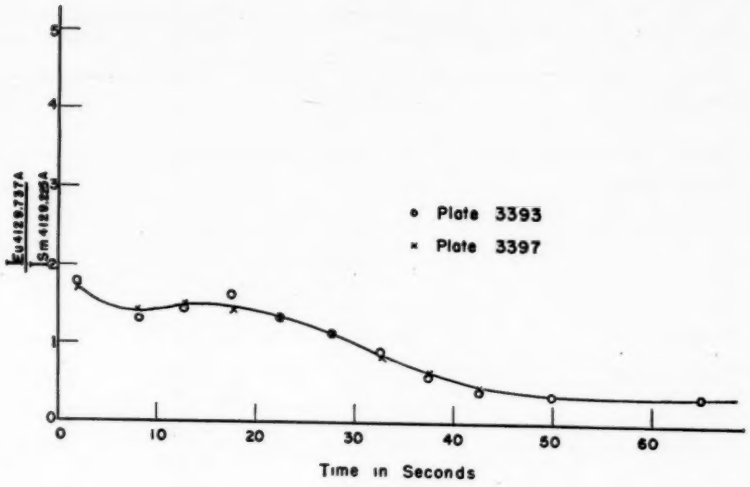

FIG. 4. Variation of intensity ratio with time: europium in samarium.

ments of the spectral lines were made with an ARL-Dietert Comparator-Densitometer.[14] An electronic voltage regulator[15] was used to assure constancy of illumination of the densitometer lamp.

Two types of emulsions were used in this investigation: Eastman Spectrum Analysis No. 1 and Eastman Type III-0. The calibration of the response of these emulsions was made by the two-step sector, preliminary curve method.[16] Sawyer and Vincent[17] have shown that the reciprocity and intermittancy effect for Spectrum Analysis No. 1 emulsion was negligible. Tests in this laboratory have shown that these effects are likewise negligible for Eastman III-0 emulsions. The developer used throughout this investigation was Eastman D-19. The temperature and time of development were uniformly maintained at 21°C and 4 minutes, respectively.

IV. METHOD OF EXCITATION

In order to develop methods of analysis of general application, it was necessary to give primary consideration to the chemical and physical forms in which rare earth mixtures were to be analysed. The logical choice of the chemical form of the sample was the ignited rare earth oxides since the samples from fractionation and other separation procedures are most readily converted to this form.

The refractory properties of the rare earth oxides confined the choice of feasible excitation sources to the a.c. spark or d.c. arc. Spark or similar a.c. discharge excitation has been effectively applied to the analysis of various inorganic substances by mixing the samples with graphite or other conducting materials and then forming into briquets suitable for excitation.[18–20] However, for analyses involving the less abundant members of the rare earth group, the desirability of reducing sample requirements to a minimum introduced a serious complication into the fabrication of pellets of suitable size and desirable mechanical properties. Emphasis was therefore directed toward d.c. arc excitation, even though the usual poor reproducibility of this discharge had to be overcome in order to develop successful analytical methods. Recent studies in a number of laboratories have shown that the defects of the d.c. arc could be overcome by the judicious choice of spectroscopic buffers, internal standards, and special types of electrodes. The experimental approach, therefore, was to determine the optimum conditions which would apply to rare earth oxide analyses.

[14] Dietert and Schuch, J. Opt. Soc. Am. **31**, 54 (1941).
[15] Dietert and Hasler, J. Opt. Soc. Am. **33**, 45 (1943).
[16] Churchill, Ind. Eng. Chem. Anal. Ed. **16**, 653 (1944).
[17] Sawyer and Vincent, J. Opt. Soc. Am. **33**, 247 (1943).
[18] Dietert, J. Opt. Soc. Am. **31**, 693 (1941).
[19] Churchill and Russell, Ind. Eng. Chem. Anal. Ed. **17**, 24 (1945).
[20] Helz and Scribner, J. Research Nat. Bur. Stand. **38**, 439 (1947).

TABLE I. Operating conditions for obtaining calibration data.

	Samarium in neodymium	Europium in samarium	
Line pair	Sm 4433.884A / Nd 4436.68A	Eu 4129.737A / Sm 4129.225A	Eu 4627.122A / Sm 4628.794A
Composition of sample charge	1:1 graphite-rare earth oxide	Same	Same
Weight of charge	15 mg	Same	Same
Type of electrode	Anode: ¼-in. diam. graphite, ¾ in. long with 2-mm deep cavity and wall thickness of ¼ mm	Same	Same
	Cathode: ¼-in. diam. graphite, 1 in. long and pointed	Same	Same
Excitation source	250 volts d.c. 17 amperes	Same	Same
Analytical gap	4 mm	Same	Same
Emulsion	Eastman III-0	Same*	Same
Wave-length photographed	4000–4625A	4000–4625A	4300–4925A
Order	2nd	Same	Same
Filter	Corning No. 774	Same	Same
Slit	0.03 mm	Same	Same
Sector apertures	143°, 90.5°, 57° (step sector)	4° (variable aperture sector)	143°, 90.5°, 57° (step sector)
Duration of excitation	80±10 seconds	60±10 seconds	60±10 seconds
Development	4 min. at 21°C in *D*-19 (Eastman)	Same	Same
Concentration range	0.10–2.0% Sm_2O_3	0.1–2.0% Eu_2O_3	0.01–0.2% Eu_2O_3

* Eastman spectrum analysis No. 1 or No. 2 plates may also be used.

Direct current arcs of currents as high as 18 amperes did not provide electrode temperatures high enough to vaporize a sufficient amount of the rare earth oxide to maintain a stabilized arc. Following the suggestions of Bauer[5] and Lopez de Azcona,[8] a number of experiments were performed in which the rare earth oxides were mixed with other metallic oxides whose volatility at the electrode temperatures was greater than that of the rare earth oxides, in order that increased vapor concentration in the discharge zone would stabilize the arc. The selection of the oxides used was based on relative boiling points determined by the spectrographic moving-plate method of Richardson.[21] An incidental observation from these studies was that zirconium oxide exhibited a relatively higher boiling point than the rare earth oxides. This substantiated the conclusion of Hopkins *et al.*[6] that zirconium was not an ideal internal standard.

Oxides such as those of aluminum, calcium, strontium, magnesium, chromium, and nickel successfully stabilized the arc when mixed with an equal weight of rare earth oxides and arced at 17 amperes. However, moving-plate spectrograms of these excitations indicated that the major portion of the rare earths was actually volatilized just prior to and after the arc became unstable at the end of the arcing cycle. This fractional distillation effect could not be overcome through the use of shallow thin-walled electrodes. Figure 2 shows qualitatively the volatilization rates for aluminum, calcium, and neodymium oxide as interpreted from the line intensities on the moving-plate spectrograms. The behavior of magnesium oxide and sodium chloride buffers was essentially the same as for aluminum and calcium oxide. Even though Lopez de Azcona[8] has developed a successful method for determining

[21] Richardson, *Proceedings of the Fifth Summer Conference on Spectroscopy and Its Applications* (John Wiley and Sons, Inc., New York, 1938), pp. 64–70.

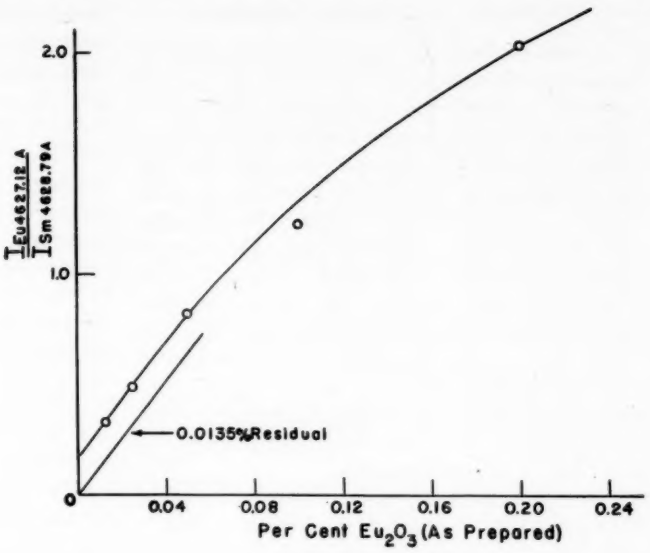

FIG. 5. Residual correction for Eu_2O_3 in Sm_2O_3 standards.

gadolinium in samarium by using magnesium oxide as a spectroscopic buffer, it was felt that greater reproducibility would be obtainable with a d.c. arc stabilized throughout the period when the rare earths were excited. This condition was obtained by the addition of 200-mesh powdered graphite[22] to the rare earth oxides. A systematic study of the experimental variables indicated that the optimum conditions were as follows: Composition of mixture, 1:1 graphite-rare earth oxides by weight; weight of charges, 15 mg; type of electrode, (anode) $\frac{1}{4}$-inch diameter graphite with 2-mm deep cavity and wall thickness of $\frac{1}{2}$ mm; excitation conditions, current of 17 amperes at 250 volts. The changes in arc current during an excitation using these experimental conditions were less than 0.5 ampere while voltage-drop fluctuations across the electrodes were of the order of 3 volts on a total voltage drop of 32 volts.

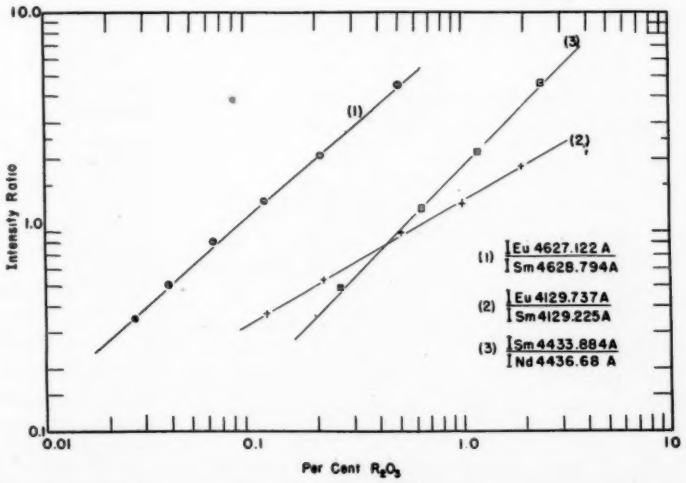

FIG. 6. Calibration curves for the determination of samarium in neodymium and europium in samarium.

[22] Churchill, Ind. Eng. Chem. Anal. Ed. 17, 66 (1945).

V. CHOICE OF INTERNAL STANDARD

In view of the unique similarity in the physical properties of the rare earths, the logical choice of internal standard was a rare earth oxide which was either present or could be introduced into a sample in a constant amount. Hopkins[6] has suggested the use of cerium since it could be most readily removed from a sample before reintroducing a definite amount. Lopez de Azcona[8] added lanthanum as internal standard in his method for determining gadolinium in samarium while Gatterer and Junkes[7] employed a line of the major constituent (samarium) in their procedure for determining europium in samarium. The latter technique is particularly convenient for the determination of minor constituents and was used for this investigation.

How well the choice of another rare earth as internal standard fulfilled the desired qualifications of maintaining a constancy of the analytical intensity ratio during the excitation period was determined by means of intermittent-type moving-plate spectrograms. The time intervals were generally 5 seconds, but were occasionally changed in order to obtain line intensities which could be measured on the densitometer. Figures 3 and 4 illustrate the curves obtained from selected line pairs for 0.9 percent of neodymium oxide in samarium oxide and for 0.5 percent europium oxide in samarium oxide.

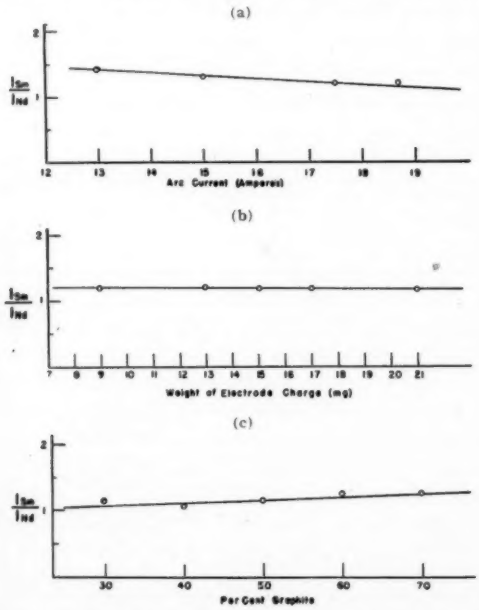

FIG. 7. Effect of large variations of (a) arc current, (b) weight of electrode charge, and (c) percent graphite on the intensity ratio.

The large change in the I_{Sm}/I_{Nd} ratio was also exhibited by other samarium—neodymium line pairs. Apparently the ratio N_{Sm}/N_{Nd}, where N_{Sm} and N_{Nd}, respectively, are the number of atoms/unit volume of samarium and neodymium in the discharge zone,[23] was undergoing rapid changes during the arcing cycle, presumably through different rates of vaporization of the samarium and neodymium. Such a dissimilarity in volatilization properties of near neighbors in the rare earth series was unexpected. If the vaporization had been purely a fractional distillation, a continuous decrease, without the observed increase between 40 and 70 seconds, should have been obtained. The observed increase could have originated either by an increase in the vaporization of the samarium or a decrease in the vaporization of the neodymium. A conceivable mechanism offered for these changes in volatility was that the reaction in the electrode charge may have involved an initial reduction of the rare earth oxides to metal and carbide formation followed by thermal decomposition of the latter to metal and carbon. A difference in the rates of any of these reactions may have occasioned the observed variations. The variation of the I_{Eu}/I_{Sm} ratio was quite different and approached the expected behavior. The possibility of improving the reproducibility of the integrated Sm/Nd ratio by using a pre-arc of about 20 seconds was considered. However, the observations that the intensity ratio *versus* time curves could be reproduced from exposure to exposure and that the mean deviation of the integrated ratio was 3 to 4 percent indicated that the pre-arc was unnecessary.

VI. QUANTITATIVE CALIBRATIONS

A. Preparation of Standards

The actual synthetic standard preparations were repeated several times. As more highly purified fractions became available through the

[23] Vincent and Sawyer, *Proceedings of the Sixth Summer Conference on Spectroscopy and Its Applications* (John Wiley and Sons, Inc., New York, 1939), p. 54.

large-scale, resin-column fractionations,[3] additional standards were prepared. In all cases, however, small residual impurity corrections were necessary. The standards were prepared by combining known volumes of standard solutions and then precipitating the rare earths by adding an excess of ammonium hydroxide. The precipitated hydroxides were filtered off and ignited to oxides at 900°C in an electric muffle furnace. The ignited oxides were mixed with an equal weight of 200-mesh, high purity graphite by grinding for several minutes in an agate mortar. In general, 100 mg of each standard was prepared. These ranged from 0.2 to 2 percent samarium oxide in neodymium oxide and from 0.0125 to 2 percent of europium oxide in samarium oxide. A watch glass with an off-center funnel hole was used in transferring the mixtures into the electrode cavity.

B. Selection of Line Pairs

Insofar as possible, line pairs were selected whose components possessed the desired equivalent excitation properties and intensities, and proximity of wave-lengths. For the determination of samarium in neodymium the most sensitive samarium line, whose use was not precluded by neodymium interference, was the singly ionized samarium line at 4433.884A. In order to select a neodymium line of suitable intensity it was necessary to employ weak unclassified lines. The line chosen was calculated by interpolation to be 4436.64A. This same line was reported by Bertram[24] as having a wave-length of 4436.835A, which, after applying the Rowland correction, gave a wave-length of 4436.68A. In order to attain the concentrational sensitivity desired with this line pair, an exposure intensity was required which necessitated background correction.

For the determination of europium in samarium, two lines were used; one for the determination of europium at moderately high concentration (0.1 to 2 percent), and another for the determination of europium at maximum sensitivity (0.01 to 0.3 percent). For the former, the neighboring 4129.737A europium line and the 4129.225A samarium line, both originating from the singly ionized atoms, were used. No background correction was necessary for this line pair. For the high sensitivity determinations the neutral atom europium line at 4627.122A and the unclassified samarium line at 4628.794A were selected. Background correction was necessary for this line pair.

TABLE II. Determination of accuracy by recovery experiments.

% Sm_2O_3 (first analysis)	% Sm_2O_3 added	Calculated total % Sm_2O_3	% Sm_2O_3 found	Error (% Sm_2O_3)	Percent error
0.27	0.20	0.47	0.48	0.01	2.1
	0.50	0.77	0.80	0.03	3.9
0.41	0.20	0.61	0.58	0.03	4.9
	0.50	0.91	0.92	0.01	1.1
0.18	0.20	0.38	0.40	0.02	5.3
	0.50	0.68	0.70	0.02	2.9
0.21	0.20	0.41	0.45	0.04	9.7
	0.50	0.71	0.76	0.05	7.0
0.00 (not detected)	0.50	0.50	0.48	0.02	4.2
0.52	0.50	1.02	1.07	0.05	4.9

% Eu_2O_3 (first analysis)	% Eu_2O_3 added	Calculated total % Eu_2O_3	% Eu_2O_3 found	Error (% Eu_2O_3)	Percent error
0.092	0.025	0.117	0.125	0.008	6.8
0.070	0.025	0.095	0.097	0.002	2.1
0.044	0.025	0.069	0.071	0.002	2.9
0.044	0.050	0.094	0.091	0.003	3.2
0.012	0.100	0.112	0.107	0.005	4.5
0.34	0.20	0.54	0.57	0.03	5.6
0.34	0.50	0.84	0.82	0.02	2.4
0.34	1.00	1.34	1.33	0.01	0.7
		Average percent error			4.1

C. Calibration Experiments

The experimental details used in obtaining the calibration data are tabulated in Table I.

The samples were arced to completion, i.e., until the whole sample was consumed. The "end-point" was readily detectable by the appearance of the unstable arc, a sudden drop in the arc current, and an increase in the voltage drop across the electrode. Duplicate exposures on two separate plates were made for each of the standards.

The photometric evaluations of the spectrograms were made in the usual manner,[16,25] i.e., the percent transmission data from the densitometer were converted to relative intensities by means of the emulsion calibration curves. Background corrections were made by converting the

[24] Bertram, Zeits. Wiss. Photog. **4**, 16 (1906).

[25] Pierce and Nachtrieb, Ind. Eng. Chem. Anal. Ed. **13**, 774 (1941).

average percent transmission of the background on each side of a line to relative intensity, and substracting this from the relative intensity of line plus background.

The corrections for residual impurity still present in the base for the standards were made by the graphical zero-intercept method.[26] This is illustrated for the europium in samarium calibrations in Fig. 5. Figure 6 illustrates the calibration curves obtained by plotting log intensity ratio *vs.* log concentration. The points on the curves are the average of the quadruplicate exposures.

D. Precision and Accuracy

An indication of the precision of these methods was obtained from the average deviation from the mean shown by the quadruplicate standard exposures, which were as follows: for samarium in neodymium, 3.6 percent; for europium in samarium (line pair Eu 4627.122A/Sm 4628.794A), 4.1 percent; for europium in samarium (line pair Eu 4129.737A/Sm 4129.225A), 3.5 percent. Additional data for determining the precision were accumulated by exposing a representative sample in duplicate on nine different plates exposed over a period of three weeks. The average deviation from the mean for single exposures was 5.8 percent; for duplicate exposures, 3.3 percent.

The non-existence of an independent method of analysis precluded the use of comparisons of analytical results as a means of checking the accuracy of the calibrations. An indication of the correctness of the calibrations was obtained by the so-called recovery experiments. These consisted of adding known amounts of samarium or europium to previously analysed samples followed by reanalysis of the impregnated portions. Table II summarizes the results from these experiments.

VII. EFFECT OF VARIABLES ON INTENSITY RATIOS

Since the internal standard technique was designed to reduce to a minimum the effects of accidental and random errors such as light source fluctuations, duration of stable arc, errors in weighing and transferring of the samples to the electrode, it was of interest to determine how effectively this was accomplished. Several of the variables, namely, arc current, weight of sample charge, and percent graphite added to the oxides, were individually changed through ranges considerably greater than ordinarily introduced by random or accidental errors. It was reasonable to expect that the secondary effects of changing the above variables would institute changes greater than those normally encountered in the effective excitation temperature, electrode temperature, duration of stable arc, rates of vaporization, and rates of chemical reaction in the sample charge. The effect of these changes would be expected to have greater influence on the integrated ratio for I_{Sm}/I_{Nd} than for I_{Eu}/I_{Sm} since the change of the former with time during normal excitations was shown to be much greater (Fig. 3). These experiments were therefore carried out with neodymium oxide containing approximately 0.5 percent samarium oxide. Figure 7 summarizes the results obtained. The virtual negligible effect of the large changes in the variables studied exemplified the successful application of the internal standard principle. Precise weighings during sample preparations were also shown to be unnecessary.

VI. DISCUSSION

The methods discussed should be readily adaptable to the analysis of any rare earth for small amounts of other rare earth impurities. As long as the total impurity content does not exceed four percent, the concentration of the major constituent may be considered constant enough for internal standard purposes without introducing significant errors. A minimum amount of sample preparation is required and for ordinary fractionation control the precision of individual determination is adequate. Under normal operating conditions, 4 man-hours provide adequate time for all operations necessary for single analysis of 15 samples or duplicate analysis of 10 samples. The sample requirements are reasonable; only 10 mg are required for a single analysis and approximately 17 mg for duplicate analysis.

Experiments are now in progress to adapt this method to the determination of other rare earth impurities in praseodymium, gadolinium, ytterbium, and yttrium.

[26] Cholak and Story, J. Opt. Soc. Am. **32**, 502 (1942).

JOURNAL OF THE OPTICAL SOCIETY OF AMERICA VOLUME 38, NUMBER 6 JUNE, 1948

The Normal Probability Curve as an Approximation to the Distribution Curve of the High Intensity Searchlight

FRANK BENFORD
General Electric Research Laboratory, Schenectady, New York

AND

JOHN E. BOCK
General Electric Illuminating Laboratory, Schenectady, New York

(Received December 23, 1947)

The light from high intensity electrodes comes principally from the luminous gas confined within the hemispherical crater of the anode. The distribution of intensity in the beam formed by the source with an accurate paraboloidal reflector has a marked resemblance to the normal probability curve. This resemblance has been investigated, using all available data of known reliability, and the agreement between curve and test is remarkable. From both theory and test, it is known that the beam formation is influenced by the ratio of the focal length of a mirror to its diameter, and the standard form of mirror has been found to give the best agreement with the probability curve. Also, there is a certain operating latitude allowable in current for given electrodes, and within these limits the intensity curve is relatively unchanged in form. Three sizes of searchlight, 24", 36", and 60" in diameter, have been investigated and all give the same distribution. From these facts, it seems that the probability curve is applicable throughout the range of standard high intensity practice, and with this in mind a test procedure is suggested that may lead to lower testing costs and increased accuracy. Several attempts at a theoretical derivation have failed, and the data are here presented solely as a complete collection of available field tests.

THE writers recently had occasion to review the literature of the high intensity arc with the purpose of finding a working theory that would permit an engineering computation of its beam formation. This computation was made graphically by one of the authors a number of years ago, but while the method was successful from a technical standpoint, it was tedious to carry out and required considerable preliminary data on the arc and the paraboloidal mirror. The method of computation presented here requires no data on the arc or mirror other than the knowledge that they are normal examples of high intensity searchlight practice as known for the last thirty years. The computation is based on photometric tests on points in the searchlight beam, and it will be shown that from only three points the complete beam can be accurately computed.

The high intensity positive carbon is characterized by having a relatively large core heavily impregnated with fluorides. The vapor of the fluorides become intensely luminous upon the passage of current and the development of these electrodes has been centered about the idea of generating, energizing and containing these gases so that they would form a stable source of light. The success of these efforts can be judged from the fact that the intrinsic brilliancy of one typical arc is five and one-half times as great as that of a corresponding plain carbon arc.

For each diameter of the positive electrode there are both lower and upper limits of current. If the current density is too low, the arc degenerates toward the plain carbon state; that is, the luminous gas is no longer the principal source of light. If, on the other hand, the density is too great, the arc becomes unstable and the crater is no longer able to properly contain the gas. These features are mentioned because data will be given to show that when the current is maintained within allowable practical limits, the same computation method applies over the normal range of currents for a given electrode.

SOURCE OF DATA

The data of this paper are drawn entirely from the files of the Illuminating Laboratory, General Electric Company, Schenectady, New York. The dates of test are given since data taken before 1920 are often unreliable. At that time, the supporting parts for the mirror were often not rigid enough to hold the mirror in its proper shape, and since the mirror must be used as a precision

TABLE I.

Date of test	No. of curves	Dia. of mirror	Dia. of positive	Arc currents	Max. candles	Beam radius	Beam lumen	Lumen factor
1944	4	24″	11.0 mm	77.5	$58 \cdot 10^6$	0° 58′	22,250	1.099
1944	4	24″	11.0 mm	100.0	$84 \cdot 10^6$	1° 3′	35,875	1.011
1945	2	36″	13.6 mm	150.0	$205 \cdot 10^6$	1° 2′	86,775	1.081
1945	6	36″	16.0 mm	150.0	$216 \cdot 10^6$	1° 2′	86,030	1.135
1945	1	36″	13.6 mm	190.0	$196 \cdot 10^6$	1° 6′	104,100	1.173
1945	2	36″	16.0 mm	190.0	$210 \cdot 10^6$	1° 15′	131,100	1.085
1926–28	2	60″	16.0 mm	150.0	$860 \cdot 10^6$	0° 41′	—	—
1916–28	2	60″	16.0 mm	225.0	$1000 \cdot 10^6$	0° 37′	—	—

article, the effects on the beam were disastrous. The tests that have been used were all on mirrors that were properly supported, and the mirrors themselves are known to have been of high optical quality.

The data in Table I are grouped according to the rated diameters of the mirrors, and there is a further subdivision where two different currents, or two sizes of positive electrodes, are used by the lamp.

THE NORMAL PROBABILITY DISTRIBUTION

The usual method of presenting searchlight beam data is to plot the intensity of the beam, in candles, against beam radius, in angular measure, and the plot is made on rectangular coordinates. The resultant curve bears a resemblance to the normal probability curve, whose equation may be written in the form

$$p = A \exp[-B\theta^2].$$

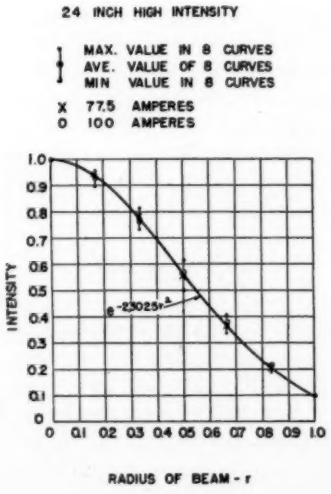

FIG. 1.

The remainder of this paper is taken up with a comparison of the beam distribution, as found by test and the values yielded by this equation when the constants A and B have been given appropriate values.

For the sake of easy comparison, all the candlepower curves have been reduced to unity at the center and, correspondingly, A has also been given a value of 1. It is customary to define the edge of a searchlight beam as the points where the intensity falls to 0.10 of the central maximum. Let us arbitrarily call this angular radius unity, then for $\theta = 1$ in the equation, B must have the value 2.303 to yield $p = 0.10$ at the beam boundary.

The test data were read off the plotted results of the tests after the ten percent point had been accurately located, and the radius of this edge point was then divided into six equal steps to obtain the data of the report. The test data given here are, therefore, not the original data, since the photometric readings were naturally at various fractions of the beam radius in the different tests.

TEST DATA

There are available four tests on a 24-inch searchlight operating at 77.5 amperes and four tests at 100 amperes, both using the same electrodes. In Fig. 1 the curve is a computed probability curve. The 77.5-ampere test points are plotted as crosses and the 100-ampere points as open circles. The averages of all eight tests are given as dots, and it is these that should be first compared with the probability curve. Reading on the relative intensity scale at the left, the disagreement at the $\frac{1}{6}$, $\frac{1}{3}$, $\frac{1}{2}$, $\frac{2}{3}$, and $\frac{5}{6}$ points are of the order of -1 percent, 0 percent, 0 percent, $+1$ percent, and $+1$ percent. The 77.5-ampere points

for the same fractions of the radius are approximately +1 percent, +2 percent, −1 percent, 0 percent, and +0 percent, while for 100 amperes we have −2 percent, −2 percent, +1 percent, +2 percent, and +2 percent.

Considering the normal errors encountered in the difficult photometric task of measuring a searchlight beam, these results are highly suggestive. For example, each group of four tests is in better agreement with the probability curve than with the other group. This might be taken as an indication that the addition of more data would improve the agreement, but this assumption can be checked only by actual tests.

The vertical lines drawn through the test points give the extreme range covered by data of the individual curves. In general, the separation between the curve and the average of the tests is a small fraction of the separation between the highest and the lowest reading from the test curves. This indicates that the agreement is as good as could be expected from the amount of scatter.

The data of the 36″ high intensity searchlight are given in Fig. 2. Eleven curves were available, eight at 150 amperes and three at currents from 185 to 195 amperes. In general, the agreement with the theoretical curve is as good as in Fig. 1 and there is no obvious departure from the relations found for the smaller searchlight.

There are only four test curves available for the 60″ searchlight, for while many tests were made, they were on electrodes that were in the developmental stage. In Fig. 3 the crosses give the results of tests at 150 amperes and the circles give the data of 200 and 250-ampere arcs. The data here are too few to permit speculation as to accuracy, or as to any meaning that may be attached to the observed deviations from the probability curve.

In 1927, an experiment was made with three 36″ diameter paraboloids of focal lengths 14.75″, 18.75″, and 25.16″. Of these, the paraboloid of normal focal length (14.75″) gave probability distribution approximately while the others were more at variance. The data here are too few to be dogmatic, but the evidence is that the distribution from the standard mirror is a better fit to the probability curve than is the distribution from the same diameter of mirror with longer focal

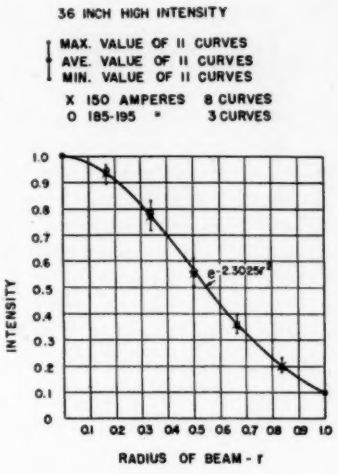
36 INCH HIGH INTENSITY
MAX. VALUE OF 11 CURVES
AVE. VALUE OF 11 CURVES
MIN. VALUE OF 11 CURVES
X 150 AMPERES 8 CURVES
O 185-195 " 3 CURVES
INTENSITY
RADIUS OF BEAM - r
e-2.3025r²

FIG. 2.

lengths. From this we can assume that the mirror must be of standard proportions, that is, having a focal length of 40 percent of the active diameter. Computations and photometric tests of beam formations show a marked variation when the focal length is changed for a given diameter of mirror, and it is thus necessary to make the qualification that the agreement with the probability curve occurs only for standard mirrors.

A summary of all available data has been made and is given in Fig. 4. The points given are averaged from 23 prints of beam distribution of

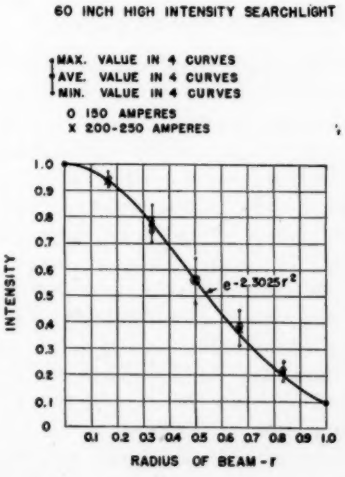

FIG. 3.

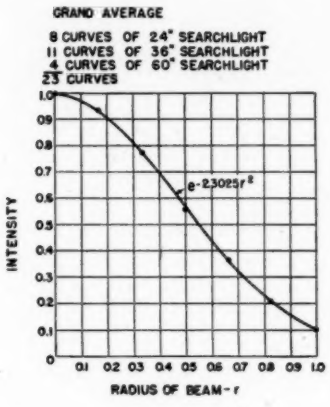

FIG. 4.

24″, 36″, and 60″ high intensity searchlights. The average separation of the points from the normal probability curve is about one-half of one percent, which is far smaller than the variations between, say, two successive beam tests, however carefully they might be made. Since a very considerable amount of photometric work went into the determination of the test points, they should be given a high rating in searchlight accuracy. Also, since the three sizes of searchlights investigated all yield almost identical curves and these curves are not appreciably altered by moderate changes in electrode current, it seems that the probability curve covers a rather wide range of high intensity searchlight performance.

LUMENS IN THE BEAM

The distribution of light in the high intensity beam is not symmetrical about the axis. The flame that emerges from the top of the crater gives the lower part of the beam an added intensity that is clearly visible. The usual test procedure is to take photometer readings on the horizontal axis of the beam and ignore the other diameters. The same procedure seems to be followed by all laboratories, and they can compare results on an even footing except in one case. The Illuminating Laboratory is equipped with an integrating hemisphere that is capable of receiving the entire beam and measuring its luminous content. This reading will not agree with the computed lumens based on a horizontal traverse. In the preceding tabulation, some factors are given for the conversion of computed beam lumens into actual beam lumens. When an electrode is operated at currents higher than the original rating, the flame becomes proportionally stronger and the factor becomes larger, which is the general trend observed in Table I.

Assuming a symmetrical beam, the beam lumens can be computed from a knowledge of the central intensity and the angular width. Let us first take the case of a beam having a central intensity of 1 candle and unit radius and let the intensity fall off according to the probability distribution to one-tenth at the boundary. The lumens are found from

$$F = 2\pi \int_0^1 \exp[-kr^2] r dr$$

$$= (\pi/k)[e^{-k} - 1],$$

but e^{-k} by definition equals 0.10, and k therefore equals 2.3025. These values give $F = 1.228$ lumens.

The radius θ of a searchlight beam is usually given in degrees and minutes, and the degree of arc is here used as the unit of radius. Also, let I_0 represent the central intensity of the beam in candles. The original equation for beam lumens then becomes, upon the substitution of numerical values

$$F = (I_0\theta^2/2674)f,$$

where f is the factor given in the last column of Table I. In the absence of the exterior flame light f would be equal to 1.

The lumens given in Table I are from the indoor test with the integrating hemisphere. To take a numerical example, in line 1, the beam radius θ is 0.966 degrees and I_0 is 58.10^6 candles. The computed beam flux is

$$F = (58.10^6 \cdot 0.966^2/2674) = 20{,}240 \text{ lumens},$$

and since the test showed 22,250 lumens, the factor is

$$f = (22{,}250/20{,}240) = 1.099.$$

This indicates that the inclusion of the flame light around the upper rim of the crater increases the measured beam lumens 9.9 percent above the computed lumens from a traverse of the beam along a horizontal line.

A TESTING PROCEDURE

Use may be made of the knowledge that the high intensity beam has a definite and constant form of distribution curve. A testing procedure such as the following will save considerable time and work.

Make the customary preliminary photometric exploration to find the center of the beam, using both horizontal and vertical traverses. Set the azimuth scale to read zero when this central point in the beam is on the photometer. Next select two points on opposite sides of the center and each at about $\frac{2}{3}$ or $\frac{3}{4}$ of the apparent beam radius, say at 0.75° radius. The entire photometric test is then made on these three points, left, center, and right, in succession. The tests are repeated a number of times and the order of points occasionally reversed so that any change in the transmission of the atmosphere will not seriously affect the relative values of the three points.

Take an average of the left and right readings and call this average I_s. Also call the center reading I_0. Next determine the ratio of I_s to I_0 and get

$$P = I_s/I_0.$$

Let the computed value of P be 0.30 which, from the curve, indicates that the selected radius of 0.75° is at 0.72 of the beam radius and the radius itself is

$$r = (0.75/0.72) = 1.042 \text{ degrees.}$$

Since only three points in the beam are photometered in place of the customary 9 to 13, more readings can be taken on each and the resultant beam data should have a materially increased accuracy over that found by methods used at present.

An Illuminant-Stable Color Vision Test, I

ELLIS FREEMAN
The University of Texas, Austin, Texas
(Received December 30, 1947)

The best practical test of color vision is the printed polychromatic, typified by the Ishihara. Its flaw is that, being calibrated to a standard illuminant which is required for actual testing, it becomes undependable with deviations from this standard. In practice the standard is rarely provided, because it requires special artificial installations which are rarely available or even appreciated as a necessity. Hence, improper illumination is the rule rather than the exception, and accounts for the passing of 50 percent of color defectives in the Navy, for example. The present report, the first of a projected series, discusses solely the *basic technical aspects* of a new polychromatic printed test for *red-green* deficiency which retains stability and diagnostic integrity under a range of illumination far wider than that encountered in testing under natural or artificial sources, from minus-blue to 14,000°K. With this, testing may be done in disregard of composition of illuminant. Thus a source of error is eliminated which has seriously impaired the utility of what is otherwise the most desirable type of practical test.

I. THE PROBLEM

THE most convenient means of testing color vision for general purposes is printed polychromatic plates, typified by those of Ishihara. These, however, are adjusted to, and require for administering, standard daylight, that is, Illuminant *C*, 6500°K, a color temperature rarely maintained in actual testing. Indeed, testing is generally performed by persons who are difficult to sensitize to an appreciation of the critical role of the illuminant, and who, were they so sensitized, would rarely have the equipment to maintain the prescribed color temperature. As a result, testing is conducted under illuminants ranging from very yellow tungsten lamps of the vacuum type at 2400°K to very white sky light from windows of 10,000°K. Moreover, even where the source itself may be *C*, the effective spectral distribution delivered to the test plates may be very materially altered by reflectors, shades, and walls. Hence, non-standard illumination is the rule rather than the exception and is "the largest contributing factor" to the passing of 50 percent of color defectives in from one to five physical examinations in the Navy, for example, despite the strong admonition in the *Manual of the Medical Department* to exercise "particular care."[1]

TABLE I. The specifications of the six inks of the Illuminant-Stable Color Vision Test for red-green deficiency.

Designation of ink	DWL	Percent purity	Percent luminous reflectance
a	575.3	73.3	42.4
b	579.4	73.7	42.0
c	582.2	73.7	42.0
d	584.1	73.0	41.9
e	586.2	73.3	41.1
f	590.0	73.8	41.5

Since the printed polychromatic test is the test of preference from every practical viewpoint, it seemed worth considering the possibility of purging it of its basic defect, namely, its instability under non-standard illuminants. The problem is reducible to the question: Can a group of inks be specified which, while altered by shifts in illumination, will, after each change, still maintain the relationships within the group, *inter se*, necessary for diagnostic integrity? That is to say, do the altered stimuli continue to be confusable by defectives and discriminable by others? Put in still another way: As the colors, under change of illumination from standard, leave a particular confusion zone of the *chromaticity diagram*, do they keep together and enter a new zone in common? Furthermore, since the confusion zones of *protanopes* and of *deuteranopes* are not coincidental, is it possible to have inks which lie only within the overlapping portions of the two classes of zones as illumination changes? Also, as the inks change in luminous reflectance from one illuminant to another, do they change together

[1] Lt. Dean Farnsworth, "A survey of methods in administering pseudo-isochromatic test plates for color vision," Color Vision Report No. 3, Medical Research Laboratory, U. S. Submarine Base, New London, Connecticut, November 6, 1943.

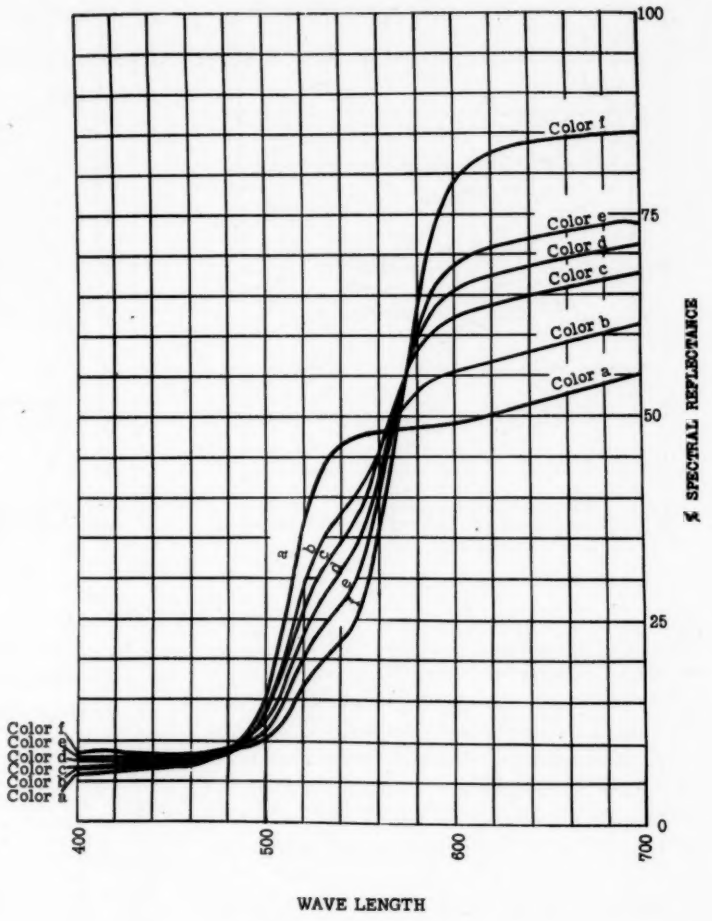

FIG. 1. Family of spectrophotometric curves showing percent spectral reflectance of the six inks.

and thus remain equally light *inter se?* As a final requirement, can these inks be so chosen as to avoid embarrassment from the anomalous luminosity curve of the *protanope?*

II. THEORETICAL CONDITIONS FOR SOLUTION

The above requirements may be generalized in the proposition:—given a fixed polychromatic reflecting surface, successively integrated with incident light of several widely altered spectral distributions, the stimulus delivered to the eye under one light is to be the *testing equivalent* of the stimulus delivered under another. This proposition implies a set of self-balancing factors which should maintain diagnostic equivalence and integrity despite changes in illumination of wide range. The presence of such a set of self-balancing factors could, by a legal analogy, be regarded as the maintenance of a "constructive," if not actual, standard illuminant.

The range of illumination for which it was desired to select inks capable of maintaining diagnostic integrity was 2848°K (Illuminant *A*) to 13,700°K (Illuminant *Z*).[2]

The location of the inks on the *chromaticity diagram* was determined by the configuration of the diagram itself, by the chromaticity locus of the above selected range of illumination, and by

[2] While the data in this paper are confined to the given range, it will be shown in a subsequent report that in practical performance the inks maintain diagnostic integrity at color temperatures far below that of Illuminant *A*.

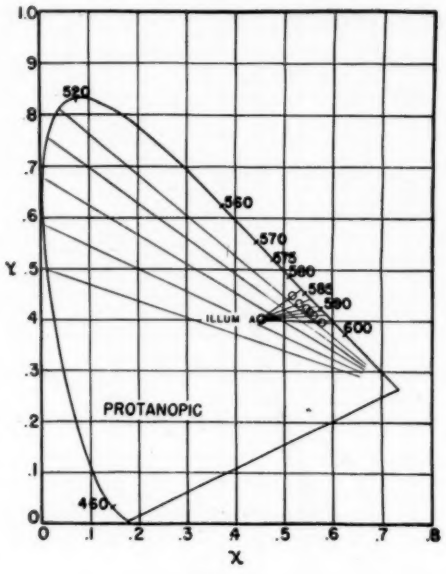

FIG. 2A.

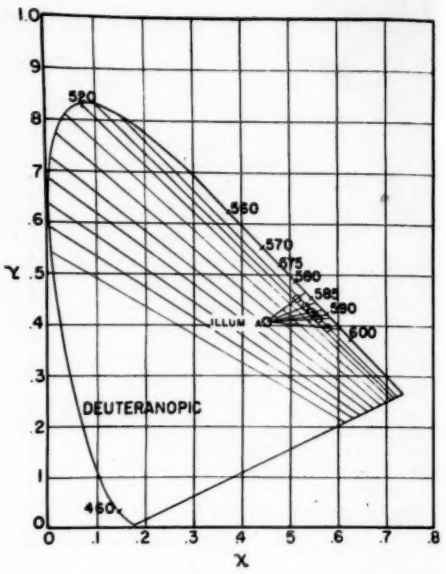

FIG. 2B.

the character of the confusion zones. A first approximation suggested that if a group of neighboring yellows in the spectral locus were used as the base of a triangle and sides constructed from the limiting points of this base to the position of Illuminant *C* as apex, the triangular area would contain the chromaticities most likely to behave as required. After numerous computations and readjustments, the following specifications as to principle were established and submitted to ink technologists as a target to shoot at: Six inks were to be prepared at intervals of 3 millimicron, in dominant wave-length (under *C*) 575, 578, 581, 584, 587, 590, respectively; and these were to be of (1) maximal purity consistent with both of the following, (2) equal purity, and (3) equal luminous reflectance.

III. RESULTS

The results accomplished in meeting these specifications are given in Table I. The family of curves in Fig. 1 and the corresponding values in Table II represent the spectrophotometric percent spectral reflectance of the six inks. These data may be regarded as a precise specification of the inks finally chosen.

The percent spectral reflectance was applied to the standard tristimulus values and spectral

TABLE II. Percent spectral reflectance of the six selected inks.

Lamda	*a*	*b*	*c*	*d*	*e*	*f*
400	6.0	6.5	6.5	7.5	7.5	8.5
10	6.0	6.5	7.0	8.0	8.0	9.0
20	6.0	6.5	7.0	8.0	8.0	8.5
30	6.0	6.5	7.0	8.0	8.0	8.5
40	6.0	7.0	7.5	8.0	8.0	8.5
50	6.0	7.0	7.5	8.0	8.0	8.5
60	7.0	7.0	8.0	8.0	8.0	8.5
70	7.0	7.5	8.0	8.5	8.0	8.5
80	8.0	8.5	9.0	9.0	9.0	9.0
90	10.0	10.0	10.0	10.0	9.5	9.5
500	15.0	14.0	13.0	12.5	11.0	10.0
10	25.0	22.5	19.0	17.5	16.0	13.0
20	36.0	29.5	26.0	23.0	21.0	17.0
30	45.0	35.0	32.0	28.0	24.5	20.0
40	47.0	38.5	35.0	31.0	27.5	23.0
50	47.0	42.0	40.0	36.0	32.0	28.0
60	48.0	46.0	45.0	44.0	40.0	36.0
70	48.0	50.0	52.0	52.0	50.0	50.0
80	49.0	53.0	58.0	60.0	61.0	64.0
90	49.0	54.5	60.5	64.0	67.0	74.0
600	49.0	55.5	62.0	65.5	69.0	79.0
10	50.0	56.0	63.0	67.0	70.0	82.0
20	50.0	56.5	63.5	67.5	71.0	83.0
30	51.0	57.0	64.0	68.0	71.5	83.5
40	52.0	58.0	65.0	68.5	72.0	84.0
50	52.0	58.5	65.0	69.0	72.5	85.0
60	53.0	59.0	66.0	69.5	73.0	85.0
70	53.0	59.5	66.5	70.0	73.5	85.0
80	54.0	60.0	67.0	70.5	74.0	85.0
90	54.0	60.5	67.5	71.0	74.0	85.0
700	55.0	61.0	68.0	71.5	74.0	85.0

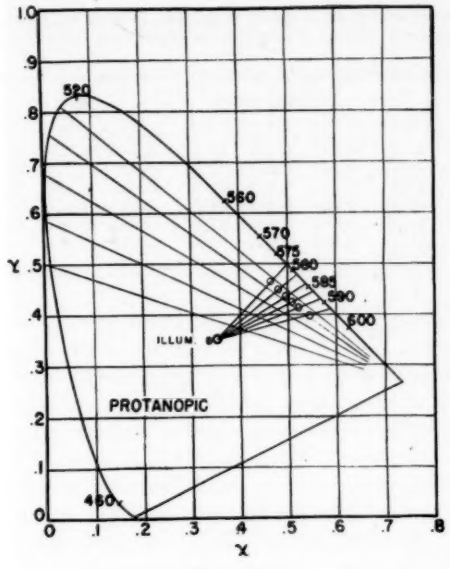

FIG. 3A.

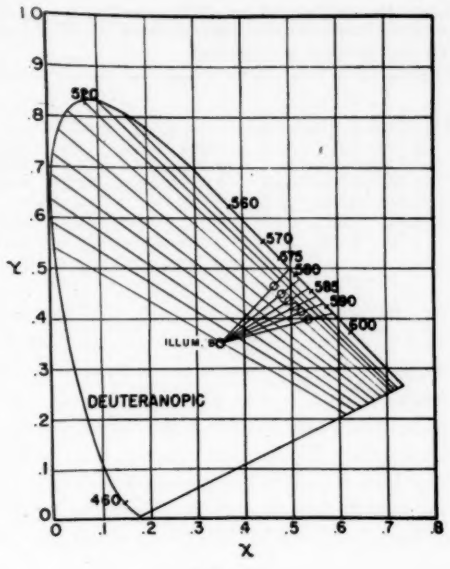

FIG. 3B.

distributions for illuminants[3] to make the integrations for computing corresponding trichromatic coefficients and percent luminous reflectance.

Table III gives the trichromatic coefficients x and y and percent luminous reflectance for each ink under Illuminants A, B, C, Macbeth 7500 K, and Z, respectively.

Corresponding to these trichromatic coeffi-

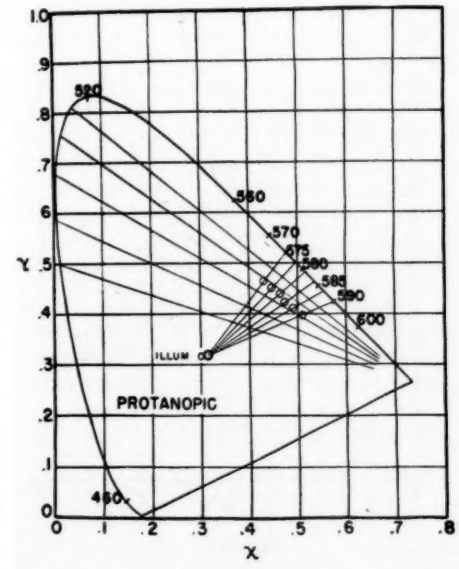

FIG. 4A.

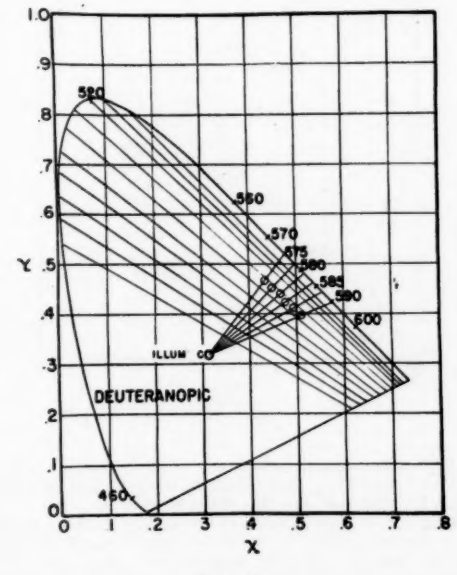

FIG. 4B.

[3] Color Measurement Laboratory, Massachusetts Institute of Technology, *Handbook of Colorimetry* (The Technology Press, Cambridge, Massachusetts, 1936); and J. Opt. Soc. Am. **34**, 636 (1944), Table IIIa, last column.

TABLE III. Trichromatic coefficients and percent luminous reflectance for each of the six inks under various illuminants. From these trichromatic coefficients Figs. 2A to 7, inclusive, have been plotted. From the corresponding luminous reflectances Fig. 8 has been plotted.

Ink	Ill. *A*			Ill. *B*			Ill. *C*			Macbeth 7500°K			Ill. *Z*		
	x	*y*	% L. R.	*x*	*y*	% L. R.	*x*	*y*	% L. R.	*x*	*y*	% L. R.	*x*	*y*	% L. R.
a	0.516	0.452	45.6	0.464	0.461	43.5	0.434	0.466	42.4	0.425	0.467	42.2	0.393	0.467	40.8
b	0.533	0.436	46.2	0.479	0.447	43.0	0.449	0.452	42.0	0.440	0.453	41.7	0.411	0.444	39.4
c	0.545	0.426	48.3	0.495	0.434	44.2	0.465	0.437	42.0	0.456	0.437	41.8	0.424	0.429	39.7
d	0.553	0.418	48.7	0.508	0.421	44.1	0.477	0.422	41.9	0.468	0.422	41.6	0.432	0.417	39.0
e	0.562	0.411	48.5	0.521	0.409	43.3	0.492	0.408	41.1	0.482	0.408	41.1	0.442	0.408	37.8
f	0.578	0.397	50.9	0.535	0.396	44.5	0.506	0.396	41.5	0.497	0.396	40.8	0.464	0.392	37.9

cients, the chromaticity of each ink has been plotted twice for each of the above five illuminants, once for the *protanope* and once for the *deuteranope* in each case. These plots, Figs. 2A to 6B inclusive,* show that, with the single exception of ink *a* under Illuminant *Z* in Fig. 6A,[4] all inks occupy such a position under each illuminant as to be simultaneously in a *protanopic* and a *deuteranopic* confusion zone,[5] as originally required.

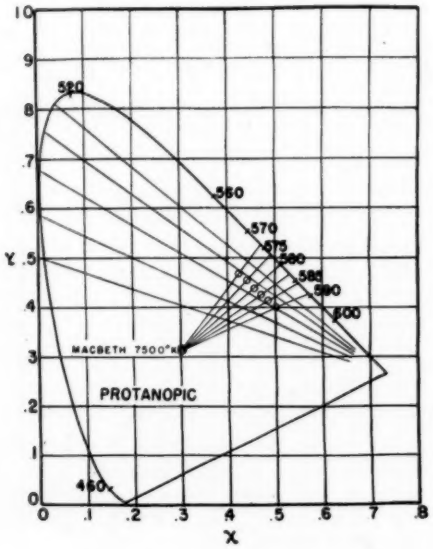

FIG. 5A.

Figure 7 is a plot of the trichromatic coefficients of Table III. For any selected color temperature of illumination the corresponding trichromatic coefficients of the inks may be read off, the *x* value from the lower portion and the *y* value from the upper. Thus the chromaticities of the inks and their positions in confusion zones may be quickly determined for any illuminants intermediate to those represented in Table III and Figs. 2A to 6B inclusive. These results suggest that, at least as far as chromaticity goes, specifications have been well met and that the six inks preserve their diagnostic integrity through a range of illumination from *A* to *Z*.

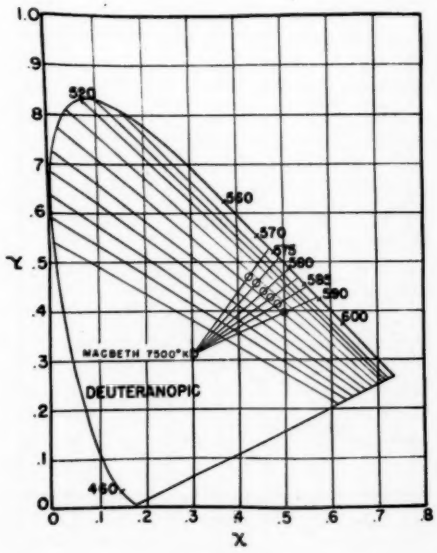

FIG. 5B.

* All confusion zones in Figs. 2A to 6B, inclusive, are Dr. Judd's adjustment of Pitt's zones to the I. C. I. coordinate system (J. Opt. Soc. Am. **33**, 305 (1943)).

[4] This ink lies just outside the boundary of the zone in which the other five lie. In a subsequent paper dealing with the design and validation of the test plates the expedient by which this minor difficulty has been resolved will be presented.

[5] F. H. G. Pitt, "Characteristics of dichromatic vision," Medical Research Council, Report of the Committee on the Physiology of Vision XIV; Special Report Series No. 200, London, 1935, pp. 47–49; also Deane B. Judd, "Facts of color-blindness," J. Opt. Soc. Am. **33**, 304–305 (1943).

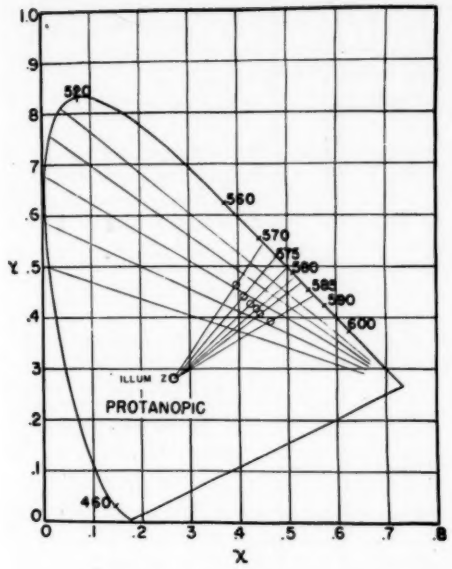

FIG. 6A.

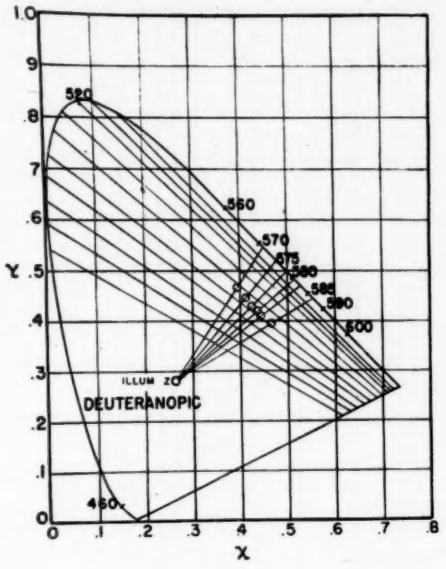

FIG. 6B.

Similarly, it appears from Table III and the family of curves in Fig. 8 that equality of brightness of inks *inter se* under each illuminant has been maintained, with the exception of *f* at the low extreme and *a* at the high extreme of color temperature.[6]

IV. CONCLUSION

In view of the foregoing, the evidence indicates that the six inks specified in Table I meet the requirements for the theoretical solution of the problem of designing a printed polychromatic red-green test which shall remain stable under illuminants ranging from *A* to *Z*. The final requirement that the inks shall conform to conditions imposed by the luminosity function of *protanopes* has also been satisfied. It is evident from the luminosity curves for *normals* and *deuteranopes*, on the one hand, and for *protanopes*, on the other, that the group of yellows selected will, *as a group*, appear lighter to the former and darker to the latter, but that *inter se* will not be otherwise affected. Since for *protanopes* (as for *deuteranopes*) luminosity relationships within the group of colors have been maintained, diagnostic integrity remains unaffected by the difference in absolute level.

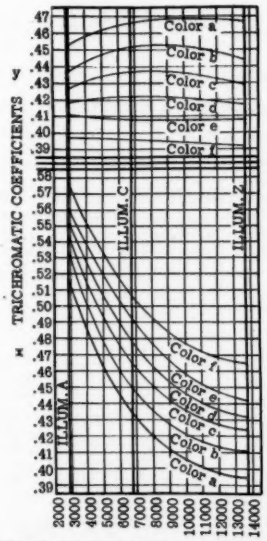

FIG. 7. Change of trichromatic coefficients of the six inks with change of illumination.

[6] The expedient by which these two minor difficulties have been resolved will also be discussed in the report that is to follow. It may suffice here to say that as long as it is possible to make groupings of pairs of approximately equal brightness (within 1 percent of each other), the deviants mentioned offer no obstacles.

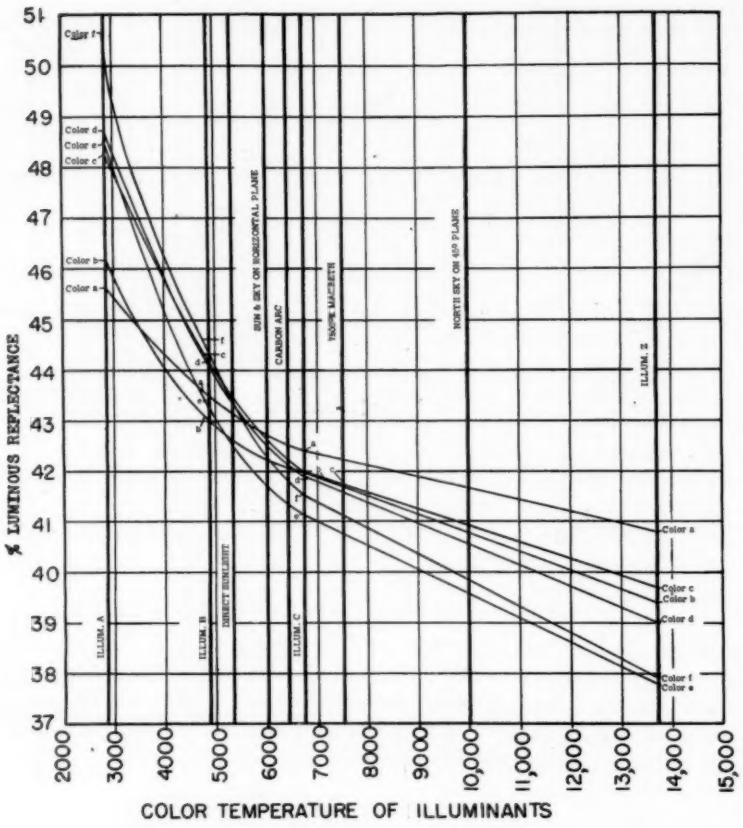

FIG. 8. Change of luminous reflectance of six inks with change of illumination.

A second report will present the practical design and accomplishment of the test in which these inks have been employed, together with the results of validation studies.[7]

[7] Preliminary work has also been done toward a polychromatic printed test for blue-deficiency which shall remain stable under wide fluctuations of illumination. The principle is identical, but with the blue test the specific problem lies in reducing the red component to the vanishing point instead of so reducing the blue component as in the present red-green test.

Great indebtedness is herewith acknowledged and thanks expressed to Mr. Walter Granville, Miss Dorothy Dolton, and the engineering staff of I.P.I. for their painstaking efforts in producing inks and swatches to meet rigorous and quite unconventional specifications, and to Mr. Carl C. Foss, Professor Arthur C. Hardy, and Dr. Deane B. Judd for their valuable suggestions and criticisms.

JOURNAL OF THE OPTICAL SOCIETY OF AMERICA VOLUME 38, NUMBER 6 JUNE, 1948

The Quantitative Spectrochemical Determination of Barium, Strontium, and Calcium*

WERNER HARTMANN AND BETTY E. PRESCOTT
Bell Telephone Laboratories, New York, New York

(Received January 2, 1948)

The procedure herein described was developed for the determination of barium, strontium, and calcium in mixtures of the carbonates of these metals in which they are present in the respective ratios of approximately 10:10:1. While the procedure is primarily designed for samples ranging in weight between 50 and 200 micrograms, it is also applicable to samples of greater weight by diluting solutions thereof to proper working concentration. Samples are dissolved in dilute hydrochloric-acetic acid; 500 micrograms of copper (as nitrate solution) is added to each, and the solutions diluted to 1.0-ml volume. Aliquots of these solutions and of a graduated series of standards, similarly prepared, are pipetted to water-proofed graphite electrodes, dried, and excited in the alternating current arc. The resulting spectra are recorded on the same plate, and the determinations are made by the usual internal-standard technique.

RECENT developments in the field of electronics have brought about the introduction of increasingly smaller vacuum tubes. This decrease in size of tubes is, naturally, accompanied by a corresponding decrease in size of their component parts—including the amount of emission coating material applied to the cathodes. The coating material usually consists of mixtures of barium and strontium carbonates, with or without the additional admixture of calcium carbonate. Cathodes currently being received in this laboratory consist chiefly of the triple carbonate type coating, with the request to determine quantitatively the barium, strontium, and calcium present in the coatings, the total weight of which ranges between 50 and 200 micrograms, with accuracy of ±10 percent or better. The following procedure was developed to meet these requirements.

A secondary application of the procedure, noted in the course of the experimental work, will probably be of more general interest than the primary application. This is the determination of barium, strontium, and calcium in mixed carbonate samples of any magnitude greater than 50 micrograms, by diluting solutions thereof to proper working concentration to lie within the range of available standards. The conventional wet methods of analysis for these three elements in presence of each other are lengthy and involved; this procedure will therefore result in a considerable saving of time.

* Presented at the meeting of the Optical Society of America, Cincinnati, Ohio, October 23–25, 1947.

PROCEDURE

A. Preparation of Standards

The composition of the samples for which the method was designed lay within the following ranges: barium carbonate 45–55 percent; strontium carbonate 40–50 percent; and calcium carbonate 5–10 percent, a Ba:Sr:Ca ratio of approximately 10:10:1. A graduated series of standards in this ratio was prepared, the lowest containing 10 micrograms each of barium and strontium plus 1 microgram of calcium per ml; the next, 20 and 2 micrograms, respectively; then 40 and 4, 80 and 8, 160 and 16, and the highest, 320 and 32.

These standards were prepared by diluting a master solution containing 1.44 gram of barium carbonate, 1.68 gram of strontium carbonate, and 0.25 gram of calcium carbonate per 100 ml (equivalent to 10 mg each of barium and strontium and 1 mg of calcium per ml) to the above concentrations, each of the standards cohtaining also 0.5 ml of 10 percent acetic acid, 0.1 ml of HCl, and 500 micrograms of copper per ml. It is, of course, prerequisite that each of the three carbonates be reasonably free of the other two elements. The use of copper as an internal standard was decided on after preliminary work without an internal standard yielded highly erratic results.

B. Preparation of Samples

Since no analyzed samples were available at the time the development of this method was

TABLE I. Composition (micrograms per ml).

Synth. solns. Ba	Sr	Ca	No. of det's	Results of spectro. analysis (average of indicated No. of det's) Ba	%Δ	Sr	%Δ	Ca	%Δ
20	20	2	16	19.5	±7.7	19.8	±5.1	2.0	±4.0
30	30	3	4	29.8	±1.0	32.0	±2.2	3.2	±0.6
40	40	4	4	40.3	±1.5	38.5	±3.4	3.9	±2.6
60	60	6	90	58.7	±4.8	63.0	±5.6	6.2	±5.6
80	80	8	12	78.3	±6.1	84.5	±5.7	8.7	±4.6
120	120	12	20	124.0	±4.7	122.9	±6.1	12.4	±5.6
180	180	18	7	190.0	±7.9	170.3	±6.2	17.2	±5.8

TABLE II. Composition (micrograms per ml).

Sample number	Chem. analysis Ba	Sr	Ca	No. of det's	Results of spectro. analysis (avg. of indicated No. of det's) Ba	%Δ	Sr	%Δ	Ca	%Δ	Total carbonates Taken	Found
1	50.5	38.6	3.9	12	49.8	±5.2	40.0	±5.0	3.8	±7.9	150	148.4
2	—	—	—	16	53.2	±6.0	37.8	±4.8	3.3	±5.2	150	148.3
3	51.5	37.8	4.2	12	49.2	±5.5	38.6	±4.9	3.9	±5.1	150	145.3

undertaken, it was necessary to use synthetic samples to ascertain the accuracy of the procedure. For this purpose, an additional series of "standards" was prepared, similar in all respects to the standards except in concentration of barium, strontium, and calcium. For these, the concentrations were: 30 micrograms each of barium and strontium plus 3 micrograms of calcium per ml; 60 and 6, 120 and 12; and 180 and 18. The greater part of the experimental work was based on these four solutions; later on, an additional one containing 80 and 8 was prepared to provide an extra point of reference.

During the course of the development of the method, two lots of triple carbonates were obtained on which a wet analysis had been run. These were therefore analyzed by the proposed method to provide an independent check. For this purpose, 1500 mg samples were taken, dissolved as in the case of the standards, and diluted to a concentration of 150 micrograms per ml, each ml also containing 0.5 ml of 10 percent acetic acid, 0.1 ml of HCl, and 500 micrograms of copper.

Inasmuch as the purpose of this paper is to present the procedure, together with the evidence supporting its validity, no results of the actual analysis of cathode coatings will be given, since their actual weight was not known and the results would have no evidential value. However, the preparation of the standards and of the synthetic samples was made to conform to the preparation of the cathode coatings for analysis, and this should therefore be described. The samples to be analyzed consisted of triple carbonates *in situ* on nickel cathodes, and it was necessary, first of all, to remove the coatings without attacking the base material. The cathodes were therefore immersed in approximately 1 ml of hot 10 percent acetic acid, which caused the coating to dissolve away from the base. The base was removed and rinsed with distilled water, the washings being added to the solution, which was then evaporated to dryness. The residue was redissolved in 0.5 ml of 10 percent acetic acid plus 0.1 ml of HCl. Five hundred micrograms of copper (0.1 ml of copper nitrate solution containing 5 mg of copper per ml) was added, after which the solution was adjusted to 1.0-ml volume. The necessity of using acetic acid and HCl in this portion of the work accounts for its use in the remainder, similarity of standards and samples being a desideratum.

C. Electrodes

Upper and lower electrodes used in this work consisted of purified graphite rod, $\frac{3}{16}$-inch diameter by $1\frac{1}{2}$ inches long, with flat ends, the solution-bearing surfaces of which were water-proofed with a few drops of a solution of halowax in carbon tetrachloride prior to use. (All electrodes are the National Carbon Company's "special highest purity" grade, and are satisfactory for this analysis without additional purification.)

For the lower range of standards (10:10:1 to 160:160:16), 0.05 ml of standard and sample solutions was pipetted to each of a pair of electrodes, to serve as upper and lower electrodes per exposure. For the higher range (40:40:4 to 320:320:32), 0.05 ml of solution was pipetted to one electrode, to serve as the lower *versus* a blank upper electrode. Before arcing, the electrodes were dried under an infra-red lamp.

D. Excitation and Photography

All exposures were made with the 2100-volt alternating current arc at 2.05 amperes. It was, however, found necessary to vary the time of exposure for the lower and the higher ranges of standards. For the 10:10:1 to 160:160:16 range, exposure time was 2 minutes, with the radial sector set to transmit approximately 30 percent of the emitted light. For the 40:40:4 to 320:320:32 range, in order to insure complete vaporization of the material, exposure time was 3 minutes, with the sector set to transmit approximately 20 percent of the light. Spectra were recorded on Eastman Process Panchromatic plates, which were developed, fixed, washed, and dried in accordance with standard photographic procedure.

E. Photometry

The wave-lengths of the lines used for photometry were:

Ba 5853.7 *vs.* Cu 5782.1,
Sr 4607.3 *vs.* Cu 5105.5,
Ca 4226.7 *vs.* Cu 5105.5.

The densities of these lines in the spectra of both standards and samples were measured, and concentration of element x was plotted *versus* $\log_{10}(D_x/D_{Cu})$, where D is the density of the lines designated by the subscripts. The amount of x in the sample was determined from this curve. Since spectrograms of appropriate standards were taken on each plate along with those of the samples being analyzed, each plate was in effect calibrated in terms of the standards. (This procedure is permissible when the densities of the lines lie between 0.2 and 2.0, as was the case throughout this work.)

Results of the analyses of the synthetic samples are shown in Table I, and those of the triple carbonate samples in Table II.

COMMENTS

The data in the tables show the accuracy as well as the precision of the procedure. The accuracy in all cases is well within the ±10 percent limit initially established as a prerequisite, and in many cases is ±5 percent or better. The precision is equally satisfactory. (In this paper, the term "accuracy" is used to denote the approximation of the observed results to the true values in the case of the synthetic solutions, and to the results of the chemical analysis in the case of the analyzed samples of triple carbonates. The term "precision," expressed by "%Δ," represents the deviation of all observed results from their average value.)

In Table II, the values listed under "chem. analysis" were obtained by calculation, *viz.*, percentage composition, as determined by the wet method, applied to the weight of sample taken (150 micrograms). The data in the column "total carbonates found" were obtained by converting the observed barium, strontium, and calcium quantities to their respective carbonate values and adding. The agreement between these and the amount of sample taken constitutes a valid check on the accuracy of the method.

CONCLUSION

Although this procedure was designed to include samples of triple carbonates to a minimum weight of 50 micrograms, the data herein presented apply only to a minimum of 75 micrograms. However, with the introduction of an additional lower standard, *viz.*, 5 micrograms each of barium and strontium plus 0.5 microgram of calcium per ml, and with the resulting lower point on the curve it is reasonably certain that the 50-microgram sample limit can be attained without difficulty. Furthermore, it is quite probable that the procedure can be applied to triple carbonates with Ba:Sr:Ca ratios other than 10:10:1, or to double carbonates ($BaCO_3-SrCO_3$) for the determination of the barium and strontium content, provided that in either case suitable standards are used.

The authors wish to thank Messrs. E. K. Jaycox and G. S. Mueller of these laboratories; the former for invaluable suggestions, comment, and criticism throughout the work, and the latter for purification of the barium and strontium carbonates which made the work possible.

Athermalization of Optical Systems*

DAVID S. GREY
Research Laboratory, Polaroid Corporation, Cambridge, Massachusetts

(Received January 2, 1948)

Equations are given for the condition that the focal surface of a lens system remain at a predetermined position for a range of ambient temperatures. Simple methods of satisfying these equations for lens systems composed predominantly or entirely of plastic components are described.

DURING the recent war plastic elements were first used as a practical substitute for optically ground and polished glass. The use of this medium presented various new problems of lens design and execution, one of the more interesting being the effect of a change in ambient temperature on the lens system.[1] The purpose of this paper is to present methods of eliminating the effects of changes in temperature on the position of the focal surface.

In general, it is not necessary to consider the effect of temperature changes on the back focus of lens systems composed of glass elements. This is not true, however, of lens systems made of synthetic resins or other media possessing large coefficients of thermal expansion. Typical linear polymers, such as polystyrene, polymethyl methacrylate, and polycyclohexyl methacrylate, have coefficients of expansion nearly ten times as great as those of optical glasses. The rates of change of index with temperature are also much greater in these polymers. The coefficients are listed numerically in Table I. From these quantities the effect of temperature changes on the position of the focal surface may be computed.

THIN-LENS TREATMENT**

The case of thin-lens systems will be treated first. For a lens of negligible thickness, the well-known law of paraxial image formation is:

$$(1/S)+(1/S')=(n-1)[(1/R_a)-(1/R_b)]. \quad (1)$$

This equation may be differentiated with respect to temperature. All the variables may be subject to thermal change.

$$(D_TS/S^2)+(D_TS'/(S')^2) = -[(1/R_a)-(1/R_b)]D_Tn + [(D_TR_a/R_a^2)-(D_TR_b/R_b^2)](n+1). \quad (2)$$

The operator D_T denotes the temperature derivative. (D_TR_a/R_a) and (D_TR_b/R_b) are both equal to the thermal coefficient of expansion E_T, so Eq. (2) may be more conveniently written:

$$(D_TS/S^2)+(D_TS'/(S')^2) = (1/f)[-(D_Tn/(n-1))+E_T]. \quad (3)$$

The quantity $[-(D_Tn/(n-1))+E_T]^{-1}$ appears in a functional manner equivalent to the Abbé ν value, or color derivative of index change. The thin-lens thermal equation may finally be reduced to the simple expression:

$$(D_TS/S^2)+(D_TS'/(S')^2)=-1/f\nu_T, \quad (4)$$

where ν_T, the "thermal nu value," is equal to the quantity $[(D_Tn/(n-1))-E_T]^{-1}$. This formally reduces the thin-lens formulas of achromatization to formulas of athermalization, for systems composed of any number of thin lenses separated or in contact. It is only necessary to replace the ordinary index of change of refractivity with color, ν, by ν_T. A general thin-lens formula for athermalization of focal point is

$$D_TS_N'=-\sum_{k=1}^{k=N}(h^2/f\nu_T)_k, \quad (5)$$

where D_TS_N' denotes the change of focal point with temperature, f the focal length of the kth lens element, ν_T its thermal nu value, h_k the paraxial incident height at the kth surface, the paraxial ray being chosen so that $h_N=S_N'$.

* The work reported in this paper was done under Contract OEMsr-70 for the National Defense Research Committee.

[1] The same problem was studied simultaneously in England at Combined Optical Industries, Ltd. See Br. Pat. 561,503.

** Equations similar to (1) through (6) were derived by J. W. Perry in connection with thermal effects on glass lens systems. J. W. Perry, Proc. Phys. Soc. (London) **55**, 257–285 (1943).

The sum is taken over all components of the lens system.

From Table I, the thermal nu values may be computed. For these materials they are:

polycyclohexyl methacrylate:
$$\nu_T = -30\times10^2,$$
polystyrene: $\nu_T = -33\times10^2,$
optical glass: $\nu_T = -1000\times10^2$ to $+833\times10^2.$

A simple lens of polycyclohexyl methacrylate would therefore change its focal length by 0.03 percent per degree centigrade. Since linear polymers tend to have nearly the same value of ν_T, it is not feasible, in general, to athermalize a system composed entirely of this type of optical medium. Methods of obtaining the optical constants necessary to athermalize are described below.

Athermalization with Glass Components

Optical glass, as shown above, has a thermal nu greatly different from that of the linear polymers; incorporation of one or more glass elements into a plastic lens system provides a range of variables permitting athermalization. Since the glass has the larger nu value, it should, in lenses of positive power, be used as a converging component. Crown glass should be used to facilitate solution of the achromatization equation. It is usually possible to arrange that this glass component be an outer element of the lens system, so that it incidentally provides a protection for the softer plastic surfaces.

Various expedients may be used to reduce the labor of fulfilling this extra condition of athermalization. If the components are not widely separated, it is for most purposes sufficient to set the power of the glass component equal to the power of the system. If the components are more widely separated, a correction to this condition may be computed with the aid of Eq. (5). Bending of the lens components and small changes of separation will not necessitate reathermalization.

A lens component may be compounded into glass and plastic elements, each material having the same index and Abbé nu value. This method is the easiest for the designer, but is not recommended generally because it is wasteful of elements.

TABLE I.

	Expansion coefficient per degree C	Index change per degree C
polycyclohexyl methacrylate	7.6×10^{-5}	-13.1×10^{-5}
polystyrene	7.1×10^{-5}	-13.6×10^{-5}
optical glass[a]	about 0.8×10^{-5}	-0.3×10^{-5} to $+1.3\times10^{-5}$

[a] G. W. Morey, *The Properties of Glass* (Reinhold Publishing Corporation, New York, 1938).

Athermalization with Cross-Linked Polymers

The Lorentz-Lorenz relation between index and density predicts that ν_T can be expressed in the form $1/\nu_T = -F(n)E_T$, where

$$F(n) = [[(n^2+2)(n+1)/2n]+1].$$

For polycyclohexyl methacrylate ($n=1.506$) the computed value of $F(n)$ is 4.55 and the measured value 4.4. For polystyrene ($n=1.591$) the computed and measured values, respectively, are 4.69 and 4.2. It has been found that the approximation $1/\nu_T = -4.5E_T$ is sufficiently accurate for investigating the possible usefulness of various synthetic resins in effecting athermalization.

Cross-linked polymers possess smaller thermal coefficients than linear polymers. Polyethylene dimethacrylate, for example, has a value of $E_T = 2.3\times10^{-5}$. The smaller expansion coefficient of polyethylene dimethacrylate indicates that it has a thermal nu value about three times as large as those of the linear polymers. The Abbé number of this material is also relatively large ($\nu=54.4$) so it readily permits the simultaneous solution of the athermalization and the achromatization equations. On the other hand, cross-linked polymers with relatively low Abbé numbers render simultaneous achromatization and athermalization more difficult.

Thus far in the discussion we have seen that athermalization imposes an additional condition to be fulfilled in the lens design and might lead either to increased complexity of the lens system or inferior corrections. An ideal situation (if the effect of lens thicknesses is still neglected) would be to have the ratio of the thermal nu value to the Abbé number a constant for all materials used in the lens system. Then reference to Eq. (5) shows that a lens system would be athermalized if and only if it is achromatized. Athermalization

would require no extra computation, and would lead to no compromise of lens performance or complexity.

Polymers formed of mixed cross-linked and linear resins can be used to provide materials having this property. The coefficient of expansion for a mixed polymer is intermediary between those of the components. It follows that one may polymerize ethylene dimethacrylate with cyclohexyl methacrylate in such a ratio that the Abbé number of the mixture is to the thermal nu of the mixture as the Abbé number of polystyrene (31.5) is to the thermal nu of polystyrene. If the lens elements have appreciable thicknesses, this mixing ratio should be altered slightly.

THICK LENSES

The complete equation of athermalization may be derived by differentiating with respect to temperature the Gaussian optics of a thick lens system. If both conjugates lie in media of index unity, the result of the procedure is the formula

$$D_T S_N' = -(D_T S_1/S_1^2) - \sum_{k=1}^{k=N} [[(\phi_a h_a^2 + \phi_b h_b^2)/\nu_T] + (h_a/S_a')^2 n^2 D_T(t/n) + (h_b/S_b')^2 D_T L]_k, \quad (6a)$$

where the symbols have the following meanings:

S_1 is the object distance.
$[n]_k$ is the refractive index of the kth lens.
$[t]_k$ is the thickness of the kth lens.
$[L]_k$ is the separation between the kth lens and the $(k+1)$th lens.
Subscript "a" refers to the surface of the kth lens on which light is first incident.
Subscript "b" refers to the second surface of the kth lens.
$[\phi_a]_k = [(n-1)/R_a]$.
$[\phi_b]_k = [(1-n)/R_b]_k$.
$[h_a]$ is the paraxial height at the surface a_k; the paraxial ray is so chosen that $h_N = S_N'$.

If the conjugates lie in media of indices n_0 and n_0', Eq. (6a) becomes

$$D_T S_N'/n_0' = (S_N'/(n_0')^2) D_T(n_0') - [(n_0 D_T S_1 - S_1 D_T n_0)/S_1^2] - \sum_{k=1}^{k=N} [[(\phi_a h_a^2 + \phi_b h_b^2)/\nu_T] + (h_a/S_a')^2 n^2 D_T(t/n) + (h_b/S_b')^2 D_T L]_k. \quad (6b)$$

For Eq. (6b) the paraxial ray is so chosen that $h_N = S_N'/n_0'$.

It is not expedient to make continuously computations according to Eq. (6b) in the process of a lens design. This equation serves as a ready means of estimating the errors due to athermalization by the thin-lens formula and the error of neglecting the thermal expansion of the lens housing. It permits approximate allowance for these errors by adjustment of the thin-lens formula. A thick lens may be treated as two thin lenses, each with a plane surface cemented to a plane parallel slab of thickness equal to the lens thickness. The resulting optical system may be approximated to a train of thin lenses, and the plane parallel slabs neglected. An upper limit of the error caused by this approximation may be computed. Each quantity

$$[(h_a/S_a')^2 n^2 D_T(t/n)]_k$$

will generally be less than or not greatly larger than $[tE_T]_k$. It is usually to be expected, then, that neglect of the plane parallel slabs as indicated above will lead to an error of athermalization of the magnitude $\bar{E}_T \sum t_k$, where $\bar{E}_T$ is the average coefficient of expansion of the lens materials and $\sum t_k$ is the total of lens thicknesses. Giving $\bar{E}_T$ and $\sum t_k$ the generous values, respectively, of 8×10^{-5} per degree centigrade and 50 mm, the upper limit of usual errors due to the approximation is estimated to be 4×10^{-3} mm per degree centigrade. This value of 4μ per degree centigrade is, for ordinary purposes, acceptable. A critical design or one containing large values of

$$(h_a/S_a')^2 n^2 D_T(t/n)$$

can be approximated more closely by inspection of Eq. (6b) without the labor of actual computation.

A particularly simple method of rendering a

system free of thermal change of focus to a high degree of precision is to athermalize by the method of copolymers and to use as the constituents of the copolymer materials which have nearly the same index of refraction and Abbé number. Athermalization can be approximately effected by mixing the constituent polymers in such a ratio that thermal and chromatic ν values are proportional for all lens materials and by making a final adjustment of the mixing ratio to remove the effects of mounting expansion and lens thicknesses. This final readjustment of thermal properties will not necessitate redesign of the lens system. Such a copolymer may be formed from ethylene dimethacrylate ($E_T=2.3\times10^{-5}$) and cyclohexyl methacrylate ($E_T=7.6\times10^{-5}$). The index and Abbé ν value of ethylene dimethacrylate are 1.5099 and 54.4 and of cyclohexyl methacrylate, 1.5066 and 56.2.

Contributions of a Mirror

Equation (6b) may be construed to include a front-surfaced mirror. If the jth surface is a front-surfaced mirror, the contribution of this element to the sum on the right-hand side of Eq. (6b) is

$$h_k^2[-(2/R)^2E_T+(1/S')^2D_TL]_k.$$

In the specific case of an optical system consisting only of a concave mirror, athermalization may be accomplished by spacing the mirror from the focal surface by means of a material having the same value of E_T as the mirror. Then the rate of change of S' is exactly compensated by the thermal expansion of the spacer because $D_TL=E_T$ and $(2/R)=-(1/S')$. For a Schmidt system with plastic components this expedient compensates the major part of the thermal effects, but there is a residual aberration caused by the thermal change in index of the aspheric surface.

It is worth while to note that this type of athermalization is not at all effective for a refractive system unless the spacer has a much higher value of E_T than the lens. Only about one part in 4.5 of the thermal effects in plastic lenses is caused by the change of radii; the remainder is due to the change of indices.

FIG. 1. Athermalized telescope. Army T-108 telescope for use as sight on anti-tank guns. Although this telescope is only 3-power, the eyepiece and objective are 3″ in diameter to achieve a 1″ diameter exit pupil and 6″ eye relief. The eye relief was necessitated by the carriage jump of the gun. This extraordinary allowance for freedom of head movement required that the focus of the objective remain accurately at the aiming reticle for all possible temperatures of use. Athermalization of the focus was effected by use of a single glass element in the otherwise all-plastic lens system.

EXPERIMENTAL VERIFICATION OF ATHERMALIZATION METHODS

Both types of athermalization have been tested in this laboratory. The lens used was a 15-inch focal length telescope objective 3 inches in diameter (Fig. 1). This objective was constructed in three forms:

(a) A Fraunhofer doublet containing a polycyclohexyl methacrylate "crown" element and a polystyrene "flint" element.

(b) A compounded crown of spectacle crown glass and polycyclohexyl methacrylate elements, and a flint element of polystyrene.

(c) A copolymer of about 50 percent polycyclohexyl methacrylate and 50 percent polyethylene dimethacrylate as the crown element, and polystyrene as the flint element.

The performance of the objectives was exactly as predicted within the limits with which the several ν_T could be determined. Objective (a) changed focus at the rate of about 3 percent per

100°C, and objectives (b) and (c) changed focus by less than 0.08 percent for a 100°C change of temperature. Experimental techniques were not sufficiently elaborate to determine whether the residual thermal changes in objectives (b) and (c) were caused by inadequate knowledge of thermal coefficients or by an effect analogous to the "secondary spectrum" of chromatic aberration. It is rather likely that the former is the case, for thermal residuals were measured by performance as mounted in an instrument containing an Amici mirror system between the objective and the focal plane. The thermal expansions of the housing and of the mirror system were included in the athermalization only by estimate. It is interesting to note that an athermalized plastic or glass-plastic system can be rendered less subject to thermal change of focus than an all-glass system, particularly when the expansion of the mounting is included in the athermalization equation.

The methods of athermalizing a lens system by use of a glass component and of athermalizing a Schmidt system by use of a spacer were used during the past war in instruments produced by the Polaroid Corporation.

Errata: Reflection and Transmission Interference Filters
Part I. Theory

L. N. HADLEY AND D. M. DENNISON
University of Michigan, Ann Arbor, Michigan

[J. Opt. Soc. Am. **37**, 451 (1947)]

Page 456, Eq. (31). For "$\tan y_\perp{}^R$" read "$\tan y_\perp{}^L$." An alternate correction would be to interchange p and q throughout this equation, since interchanging p and q is equivalent to interchanging the directions right and left.

Page 457, Eq. (32). Coefficient of the second term in the denominator. For $[1-(a^2-b^2)/pq]$ read $[1+(a^2-b^2)/pq]$.

Page 464, column 2, paragraph 2, line 10. For "···polarized with electric vector parallel to the plane···" read "···polarized with electric vector perpendicular to the plane···."

Page 464, Eq. (54). Right-hand member of the equation. For $\cong\lambda_{\bar{m}}\delta y^L/m\pi$ read $\cong\lambda_{\bar{m}}\delta y^L/(m\pi-y_{\bar{m}})$.

A Condensed Arc Source Unit for Spectrochemical Analysis

D. A. SINCLAIR
Munitions Supply Laboratories, Melbourne, Australia

(Received December 2, 1947)

A description is given of a source unit of the spark-ignited arc type. The unit has some original features providing wide versatility without elaborate equipment. Some critical requirements for the successful operation of this type of source unit are discussed, illustrations of various cycles are given, and a comparison made between the different types of arc-current pulses.

THE term "condensed arc" is here applied to that form of intermittent arc discharge of a condenser such as may be obtained using the Pfeilsticker[1] type of circuit further developed by Kingsbury and McClelland[2] and by Walsh,[3] or the multisource unit of Hasler and Dietert.[4] The name is suggested by simple analogy with "condensed spark" and seems to the writer to fill satisfactorily a need for a general and concise term to cover a type of discharge which is likely to come into wide usage.

In this paper is described a unit which has been developed in these laboratories over the past six years to bridge the gap between the sensitive but erratic d.c. arc and the more reproducible but less sensitive spark sources previously available. The need for such a source was felt particularly in zinc-base alloy analysis, to which work the first application was made. A very wide field of usefulness is apparent, however, not only in cases where high sensitivity combined with precision is demanded, but also in general analysis, where often a satisfactory compromise set of conditions for a particular application is not available in ordinary arc or spark sources. The unit may be simply and inexpensively constructed from standard equipment and provides d.c. and a.c. arcs, either condensed or uncondensed. Although developed from an independent design here, the circuit is basically similar to Pfeilsticker's and, as in the unit of Hasler and Dietert, a wide range of variables is provided in the discharge loop. Some original features extend its versatility beyond that of already published circuits, and observations made on details of operation will be of interest to other workers in this field.

CIRCUIT

The simplified circuit diagram is shown in Fig. 1. That section of the circuit drawn in heavy line may be regarded as the main discharge loop, into which high voltage pilot-ignition (or triggering) sparks are introduced and d.c. or a.c. charging currents are fed as indicated. The function of the "sustainer bridge" (C_2R_2) will be discussed later.

The igniting spark is very weak, carrying less than one-eighth of the current of the primary (G_2) spark discharge, which is itself low powered. By-pass condensers can therefore be quite small in capacity and voltage rating, and it was in fact found undesirable to use more than 0.005-μf capacity as a by-pass at C_3 (see discussion in next section). There seems to be no advantage in using higher powered sparks; on the contrary, it was found with one experimental circuit that, whereas a weak 0.0003-μf condenser spark succeeded in igniting an arc, a strong 0.005-μf spark failed and even extinguished an already established arc. Capacities smaller than 0.001 μf, however, lead to excessive loss from wiring capacity effects.

A high frequency auto-transformer at T_1 is simpler and much more efficient than a Tesla coil with separate primary and secondary coils, and allows a much smaller minimum inductance in the discharge loop. The 1:8 ratio gives an effective voltage step-up of about 1:4, since only about half the total voltage in the primary spark circuit is available across the single turn in the

[1] K. Pfeilsticker, Zeits. f. Elektrochemïe **43**, 719 (1937); *ibid.*, Spectrochem. Acta **1**, 424 (1940).
[2] G. W. I. Kingsbury and J. A. C. McClelland, "Polarographic and spectrographic analysis of high purity zinc and zinc alloys for die casting," H. M. Stationery Office (London) 49 (1945).
[3] A. Walsh, Metal Industry **68**, 243 (1946).
[4] M. F. Hasler and H. W. Dietert, J. Opt. Soc. Am. **33**, 218 (1943).

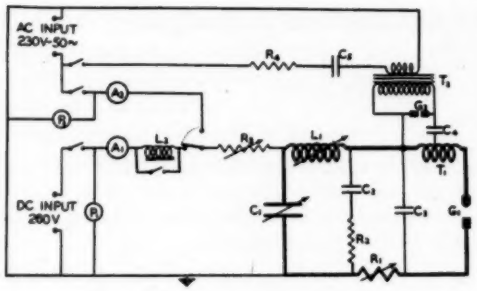

FIG. 1. Circuit for continuous and condensed arcs, d.c. or a.c.

C_1 0–124 μf, 400 v working, banks of 4, 8, 16, 32, 64 μf. (0.04 μf minimum fixed in parallel for residual by-pass.)
C_2 5 μf, 400 v working.
C_3 0.002 μf, mica, 2000-v peak.
C_4 0.0015 μf mica, 20,000-v peak.
C_5 4–6 μf, 400 v working (for phase advance to counteract lag in T_2).
L_1 0–168 millihenries, 14 B and S gauge enamel-covered copper wire, total resistance 6.3 ohms, tapped at 0, 0.1, 0.3, 0.9, 2.5, 7.5, 17, 34, 67, 168 mh.
L_2 0.75 henry, iron-cored choke, falling to $0.15H$ at 5 amp.
T_1 H.F. auto-transformer, 0.025 mh, 8 turns rubber-covered heavy-gauge wiring, coil 8 in. square ×2 in. long, primary one turn.
T_2 1:100 high voltage transformer, high impedance secondary, output about 3 ma.
R_1 0–50 ohms, tapped at 0, 0.5, 1, 2, 3, 4, 6, 9, 14, 20, 30, 50 ohms.
R_2 75 ohms (30 gauge Nichrome).
R_3 0–1200 ohms, coarse, medium, and fine controls.
R_4 0–300 ohms. (Some variation in R_4 and C_5 has been found necessary to allow for changes in leakage currents in the high voltage circuit with change in humidity.)
A_1 0–10 amperes d.c.
A_2 0–10 amperes a.c.
P_1, P_2 Pilot lights.
G_1 Analytical gap, up to 8 mm.
G_2 Spark gap, either fixed 2 mm or synchronous (see Fig. 2).

T_1 primary. Hasler and Dietert[4] in the multi-source unit use, in effect, a 1:1 auto-transformer of impedance equal to that of the whole discharge loop.

The electrodes in the spark circuit were originally zinc alloy (4 percent aluminium) rods 12 mm in diameter and spaced 2 mm apart. Zinc was chosen because of its ready sparking properties, being less subject to anomalous discharges than the more noble metals[5] and, although the metal is readily oxidized, the oxide does not form a resistant film. The fixed spark gap has now been replaced by a rotary synchronous gap with means of selecting sparks every half-cycle, on alternative half-cycles, or every fourth half-cycle. The first design eliminated unwanted sparks, but it was found that this system caused minor complications in the T_2 circuit. Sparking voltage was higher with 50 sparks per second than with 100 and lower with 25, and compensating alterations in the primary circuit were required. A later design (see Fig. 2) provides 100 sparks per second in all cases, but allows the unwanted spark currents to pass through on a loop excluding T_1, thus making the charging sequence in T_2 independent of the selected frequency of ignition.

There is still an apparent difference in the sparking voltages in that a regular discharge can be maintained across a much wider gap with the higher frequencies of ignition than with the lower. This is probably because a spark jumps more readily shortly after the extinction of a previous discharge, and this effect disappears as the period between discharges is lengthened.

Inductance L_1 and resistance R_1 can be located in various positions in the discharge loop, but the line from T_1 to the arc gap G_1 must be kept well insulated and free from capacity by-passes to earth, otherwise sufficient voltage build-up across the gap may be impossible. The arrangement shown, in which R_1 separates the arc gap from earth, was chosen for convenience of tapping by an oscilloscope, which requires one plate to be earthed.

Sources of power are a.c. 230-volt 50-cycle mains tapped directly through a filter (not shown), and an a.c.-d.c. motor generator of maximum output 260 volts.

REQUIREMENTS FOR IGNITION

Provision of a spark across the arc gap is not necessarily sufficient to ensure ignition of the arc even though adequate voltage may seem to be available. Conditions to be fulfilled are (a) that the gap resistance shall be reduced to a low level by the spark ionization and (b) that the arc current shall then maintain a supply of ions sufficient to keep the gap resistance low. As Kaiser[6] has demonstrated, the passage of a normal spark reduces the voltage across the gap to about 50 volts, and if the arc circuit is capable

[5] H. Kaiser, Proc. 7th Summer Conf. on Spectroscopy and Applications 77 (1940).

[6] H. Kaiser and A. Walroff, Ann. d. Physik **34**, 4, 257 (1938).

of impressing a voltage higher than this an arc discharge should ensue. It is possible, however, that the inductive delay in the arc circuit may be such that the ionization produced by the short-lived high frequency discharge will have decayed below the critical level before the arc current has reached a self-maintaining value (of the order of 1 ampere). Under such circumstances no appreciable arc discharge will occur.

The amount of inductance that can be tolerated in the arc-discharge loop will depend on the voltages available and the persistence of the ionization produced by the spark. Using 260-volts d.c. it was found that ignition began to be uncertain when the inductance was raised above 5 mh. As it was desired to experiment with higher inductances, some means of prolonging the ionization was sought. As already mentioned, higher powered sparks proved ineffective. A valve oscillator was considered, but a much simpler ignition aid was devised which prolonged the ionization long enough to enable over 100-mh inductance to be used. This is the sustainer bridge (C_2R_2 in Fig. 1) which provides, in parallel with the main discharge loop, a subsidiary non-inductive discharge loop, for the purpose of maintaining a low current arc long enough to fill the gap between the decay of the high frequency oscillations and the building up of the main discharge. The higher the inductance L_1 the greater the capacity C_2 required in the sustainer. One microfarad is adequate for values of L_1 up to 15 mh, but 5 μf is used for the higher inductances. The initial hook visible in the current traces of Fig. 3k and 1 and Fig. 4a, b, and c is due to the discharge of C_2.

Another complicating factor which may prevent ignition is encountered when the by-pass condenser C_3 is made too large. In this case the main discharge is forestalled by the short sharp discharge of this condenser and further discharge does not develop, probably because the ions are explosively dispersed in the same way as when a high powered spark extinguishes an established arc. A capacity even as low as 0.01 μf at C_3 has been found to be troublesome in this respect.

It is also observed that ignition becomes difficult when the cathode is hot molten metal, but that a molten anode is not similarly troublesome. The reason for this is not yet clear.

DISCHARGE AND RECHARGE SEQUENCES

Satisfactory ignition having been achieved, there will then follow a surge of arc current which may drain the reservoir condenser C_1 to below arc-maintaining voltage, or even past zero voltage, depending on the degree of inductive inertia and on the limitations imposed on the charging current. If the arc current falls below a certain critical value (about 1 ampere), the arc will be extinguished and the voltage required for re-ignition will rise rapidly to sparking potential, the rate of rise depending on the material and temperature of the electrode tips and on the velocity of air draughts across the gap, etc.

It is possible that the voltage across the gap may be reversed to an extent sufficient to restart the arc current in the opposite direction, but with this unit the discharges are not usually oscillatory because the circuit is either overdamped or of such low natural frequency that the pause at reversal is long enough to allow the re-ignition voltage to rise above that available. Over a certain range of settings, however, one or two reversals are often observed, as in Fig. 3 (i, j).

To ensure that the discharge is self-extinguishing, it is necessary to impose appropriate restraint on the charging current. This may be accomplished by resistance alone, but much more effectively by a combination of inductance and resistance. The inclusion of the L_2 choke

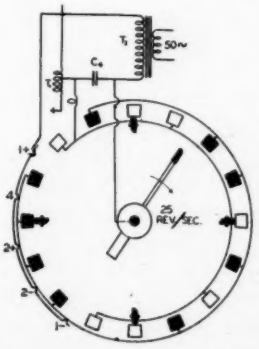

FIG. 2. Schematic details of synchronous gap G_2. The single rotary electrode sparks against 4 fixed electrodes at 90-degrees intervals. The ring of contactors mounted on Bakelite can be set in 5 different positions to make effective 1, 2, or 4 sparks per revolution with alternative polarities for 1 and 2.

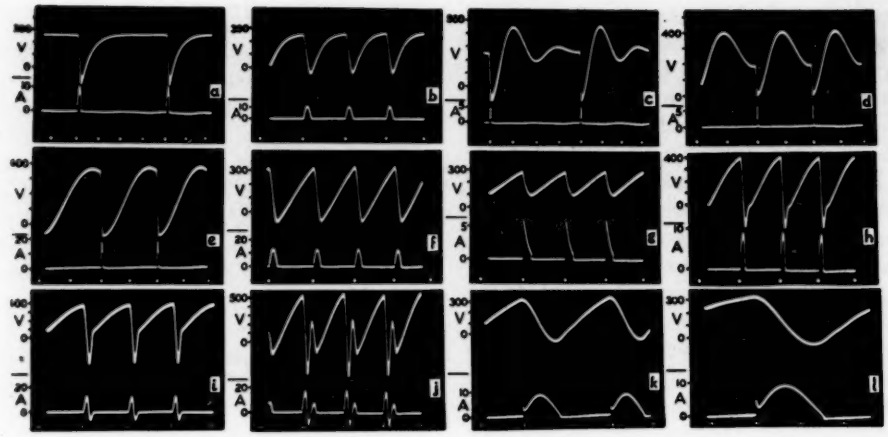

FIG. 3. Oscillograms from the d.c. condensed arc circuit. In each case the upper trace represents the voltage across C_1 and the lower the discharge current as indicated by the voltage across R_1. Time spots at the bottom are at 0.01—second intervals. In the table below are given the corresponding circuit constants, the units being C_1 microfarads, L_1 millihenries, R_1 ohms, A_1 amperes, DF number of discharges per second.

	a	*b*	*c*	*d*	*e*	*f*	*g*	*h*	*i*	*j*	*k*	*l*
C_1	32	32	8	8	24	32	32	8	16	16	84	124
L_1	7.5	7.5	7.5	2.5	2.5	7.5	0	17	7.5	7.5	67	168
R_1	0.5	6	0.5	1	6	6	30	2	0.5	0.5	2	2
A_1	0.3	1.0	0.07	0.08	0.5	1.4	0.6	0.7	0.4	1.2	2.2	1.6
L_2	out	out	in	in	in	in	in	in	in	in	in	in
C_2R_2	out	out	out	out	out	out	out	in	out	out	in	in
DF	25	100	25	50	50	100	100	100	100	100	50	25

not only prevents the rapid response of the charging circuit to a fall in potential of C_1, but it also enables C_1 to be charged to voltages higher than that of the d.c. supply, and makes possible a much wider range of discharges.

If the charging current is able to prevent the electrode potential from falling below the critical level, a continuous discharge will ensue, little affected by subsequent high frequency pulses superposed on it, though it may be a little unstable on account of the condenser in parallel with the arc gap. This instability is negligible if the by-pass C_3 is small and an adequate resistance is inserted between C_1 and the arc gap. When a continuous d.c. arc is desired, R_1 is usually set at several ohms, and C_1, L_1, L_2 at zero. The elimination of L_2 is particularly important unless C_1 (or C_2) is also made large. Before the sustainer bridge was attached it was found that the d.c. generator circuit had sufficient self-inductance without L_2 to make spark ignition of the continuous arc ineffective unless C_1 was made at least 12 μf.

With some settings, particularly when R_1 is large, there is a risk that the discharge, though normally intermittent, may suddenly become continuous because of some chance failure of the extinguishing sequence. In such cases an air draught blown across the gap is a useful expedient to ensure regular extinction.

In the case of the non-inductive or over-damped discharge, the arc current will approach the charging current asymptotically, and for self-extinction of such discharges, therefore, the charging current must be lower than the minimum stable arc current, i.e., about one ampere or up to two amperes with an air draught. With the more inductive discharges, however, the charging current can be much higher and is likely to be limited only by the power available or by the maximum load of the condensers or wiring.

Assuming the discharge has extinguished itself, the recovery of the charge on C_1 will proceed at a rate, and to a voltage higher or lower than the d.c. supply, depending on the constants of the

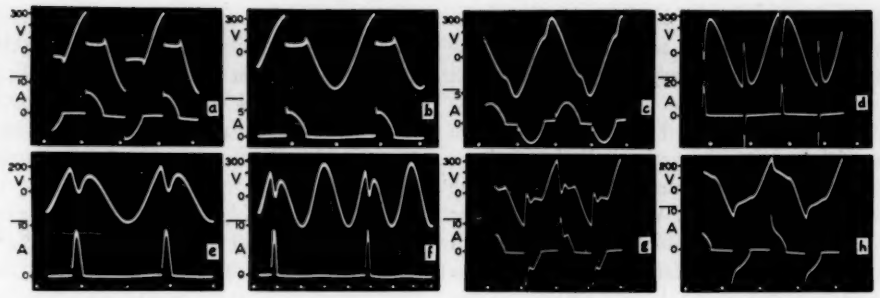

FIG. 4. Oscillograms from a.c. simple and condensed arc circuits. Tapping and units as for Fig. 3.

	a	*b*	*c*	*d*	*e*	*f*	*g*	*h*
C_1	—	—	—	16	32	32	16	32
L_1	—	—	168	2.5	7.5	7.5	7.5	—
R_1	2	1	2	1	2	2	2	20
A_2	3.8	2.0	2.1	2.9	2.8	2.6	4.0	3.0

circuit. With a purely resistive restraint on the charging current, an exponential recovery curve of the type shown in Fig. 3a and b may be expected, i.e., a fast initial rise followed by a flattening out to mains voltage. With appreciable inductance in the charging circuit, a damped oscillatory curve is followed, as in Fig. 3c, d and e, though it may be interrupted before the first maximum, as in Fig. 3f. The type of cycle obtained depends on the relation between frequency of ignition and the natural frequency of the charging loop.

In Fig. 3d the ignition point occurs at a trough in the recovery curve. When this is the case, an anomalous situation arises. The system behaves in a manner apparently contrary to Ohms Law, for a decrease in the control resistance R_3 leads to a fall in the current registered by A_1. The explanation is that R_3 acts as a damping resistance in the charging loop, and a lower degree of damping means a lower trough following the higher peak, i.e., the ignition voltage and arc current pulse are smaller and therefore the net d.c. charging current is lower.

The most usual type of cycle is the simple saw-tooth type shown in Fig. 3f. The larger the inductance L_2, the straighter becomes the recovery curve, i.e., the charging current becomes less affected by the voltage fluctuations of C_1, approaching a constant value equal to $(Vs-Vm)/R_3$, where Vs is supply voltage and Vm is the mean voltage of C_1. Since, when L_1 is large compared with R_1, Vm may be less than 100 volts (theoretical lower limit is arc-gap voltage), it is possible to obtain quite high powered condensed arcs of this type with a d.c. source of only 110 volts. For ease of initial ignition, however, and also for work with the more damped discharges when Vm is much higher (see Fig. 3g), it is believed that 250 volts is a desirable minimum supply voltage.

In the lower part of the recovery curve shown in Fig. 3h, a ripple will be seen, due to a backflow of charge from C_2 after the arc is extinguished. Although C_1 is carried down to a negative voltage by L_1, C_2 merely flattens out to a voltage equal to that across G_1 and R_1, and consequently may be at a substantially higher voltage than C_1 at the point of extinction and can temporarily contribute to the recharge. For the same reason it will be evident that the sustainer bridge does not assist reverse ignition; on the contrary, it acts in some degree as a suppressor of oscillations in the discharge.

Oscillatory discharges of the type shown in Fig. 3i and j are not considered desirable because the reversal tail is liable to be erratic in occurrence and the charging current unsteady. Such discharges occur most readily with combinations of high ignition voltages, low to moderate capacities, moderate inductances, and low resistances. With such settings it is observed that as R_3 is decreased the ammeter reading A_1 passes through an unsteady maximum at the point where the first reversal tail begins to appear. This is due to the recharging effect of

the reverse current. In spite of the arguments against it, experience has shown that, in some applications, good results are obtainable with an oscillatory discharge.

In Fig. 3k is illustrated a case of 50-cycle ignition, although sparks are supplied 100 times per second. Alternate sparks occur when the voltage of C_1 is near zero. With high capacities and inductance it is possible that ignition will fail until the second, third, or fourth spark. With the use of the original fixed gap at G_2 discharges can be maintained at these lower frequencies with appropriate settings of C_1 and L_1. At borderline settings, however, the frequency is apt to switch from one to another uncontrollably, and a synchronous interrupter in the ignition circuit is necessary to ensure regular ignition in such cases.

An oscilloscope, though practically indispensable for determining the ignition voltages and other exploratory work, need not be permanently attached to the unit, because in d.c. work, provided the discharges occur at constant intervals and reversal tails are avoided, the ammeter A_1 is the only electrical indicator required to enable repeatable discharges to be obtained at any setting of C_1, L_1, R_1.

With a.c. charging, complicated cycles such as those illustrated in Fig. 4 may be obtained. Figure 4a, b, and c represent simple uncondensed arcs, d, e, and f condensed arcs, and g and h mixed simple and condensed arcs. The ammeter A_2 is not a reliable indicator of discharge current when condenser C_1 is used, because it records the return current from C_1 to the mains as well as that contributing to the discharge. A_2 would be better located in the main discharge loop in such cases.

ARC PULSES AND SPECTROCHEMICAL CONSIDERATIONS

In the previous section charge and discharge are considered mainly in relation to the voltage cycles of the reservoir condenser C_1. The character of the actual current pulse occurring at the arc gap independently of the mechanism of its production is, however, the significant factor in spectrochemical work.

Four electrical factors determine the type of arc pulse obtained, *viz.*: C_1, L_1, R_1, V_1 (V_1 being the ignition voltage of C_1). With long period pulses the influx current A_1 during the discharge must also be taken into consideration. In general, V_1 is determined by the mean influx current, provided the frequency of ignition is fixed and complications such as reversal tails on the pulse are absent.

At the point of ignition the voltage at the gap drops to about 50 volts and is more or less independent of the current. With V_1 at 300 volts there remains 250 volts to be distributed over L_1 and R_1. It is evident that with small values of L_1 and R_1 initial currents of several hundred amperes could readily be attained. The theoretical value for the peak amperage of a spark is $VC^{\frac{1}{2}}/L^{\frac{1}{2}}$ (resistance neglected). Compared with the usual high voltage spark, the condensed arc can make up in the capacity factor in this formula what it loses in the voltage factor (e.g., 0.005 μf at 10,000 volts is equivalent to 8 μf at 250 volts). The low voltage discharge will, however, be more sensitive to small resistances. With ohmic impedance alone the initial current will be approximately $(V_1-50)/R_1$.

None of the oscillograms presented in this paper show discharge currents higher than 20 amperes. Peaks of over 300 amperes have, however, been observed with the oscilloscope (tapping across 0.5Ω), and much higher peaks could be attained if some attempt were made to reduce the minimum impedance of the discharge loop. No practical application in these laboratories has yet called for further extension on these lines, attention having been concentrated rather on the low current types.

The characteristics of the spectra obtained vary from the extremely spark-like type of the high current density, short-period discharge with its prominent ion lines, strong continuous background, and low analytical sensitivity, to the arc-like type of the low current density discharge with its strong neutral atom lines and high sensitivity. The superiority of the low density condensed arc over the continuous arc in giving more reproducible exposures arises mainly from the more regular distribution of burning area and lower heating rate of the electrodes. It is found, however, that the advantage of low heating cannot be pursued too far without losing sensitivity. The two main reasons for this are (a) in

many instances highest sensitivity can be attained only if the electrode reaches a temperature high enough to bring about preferential vaporization of the impurities; and (b) with the feebler discharges the relative strength of air band lines becomes excessive owing to the low concentration of metal vapor in the arc gap.

A comparison of the inductive, round-peaked pulses with the resistive type having a very sharp initial peak raises the question as to which form is preferable in spectrochemical analysis. From the operational point of view there are arguments for inductance in preference to resistance as the main control impedance in the discharge loop, since extinction is then more certain and regular, though a small amount of resistance is desirable to damp out reversal tails. Apart from this aspect, which is really concerned only with the mechanism of production, there appear to be definite advantages in having the peak current delayed, as in the inductive discharge. In this case the main arc energy is released after the pole spot of the electrode has been well established and preheated, and some metal vapor has migrated into the air gap. Therefore, more arc-like conditions and lower band line strength are to be expected than in the case of the early peaked discharges. Observations in practice support this view, for, in general, higher analytical sensitivities may be obtained with the inductive type of discharge.

APPLICATIONS

Some considerable work will be involved in making an exhaustive study of the properties and applications of the great variety of discharges possible with this unit. Although several techniques for various types of analysis have been developed, the selection of the optimum conditions in each case involves a lengthy survey. So many different combinations are possible with the four independent electrical variables that these, in addition to all the other variables in spectrochemical analysis, make the field of exploration a very complex one. A quantitative study of the influence of variations in the electrical circuit on some spectral properties of importance in zinc-base alloy analysis is the subject of a separate paper, and similar studies on aluminium- and copper-base alloys are in progress.

With most alloys the cathode provides the more useful vapor and at the same time is heated less than the anode. In such cases a technique using a flat surface on the sample as cathode and a pointed graphite rod as anode is generally the most convenient and effective. An exception is the analysis of steels for boron,[7] in which the sample is made the anode. Non-metallic specimens are also generally mounted on the anode.

Loose powders, because they are scattered off the electrode by intermittent discharges, are better treated by the continuous d.c. arc, but the simple a.c. arc has been found useful for some readily fusible non-metallic substances. Results of a high order of consistency have been obtained from an arc playing around the rim of a thin-walled graphite cup containing the sample, which soaks up the wick-like walls. This spark-ignited, low voltage a.c. arc would seem to be at least as effective as the high voltage self-igniting a.c. arc, and has the advantage that wider gaps and higher currents can be used without the large excess-power requirements and dangerous shock hazards of the latter.

[7] C. Corliss and B. Scribner, J. Research Nat. Bur. Stand. **36**, 351 (1946).

Color Variations in Glasses Containing Iron

JOHN W. FORREST, NORBERT J. KREIDL, AND TYLER G. PETT
Bausch and Lomb Optical Company, Rochester 2, New York

(Received January 12, 1948)

The variations of the color of iron glasses are due to the fluctuations in (a) concentration, and (b) oxidation-reduction equilibrium. In an experimental series, changes of these two variables were exaggerated. An increase in concentration caused a decrease in transmission and a shift to higher dominant wave-lengths (yellow), while reduction caused a decrease in transmission and a shift to lower dominant wave-lengths (blue). The changes in chromaticity were evaluated and applied to problems of control and specification. The Nickerson-Balinkin small color difference formula indicated a modification of existing specifications in transmission and dominant wave-length with tolerances equal in three color dimensions.

I. INTRODUCTION

THE control of the production of colored glasses should be greatly aided by applying the increasing knowledge of the chemical behavior of colorants in glass in conjunction with the modern methods of color notation and concepts of perception of color differences by the human eye. Certain colorants undergo no chemical changes under varying conditions, and as a result their spectral transmissions can be considered as following Beer's law, depending solely upon their concentration in the glass. For such substances, specifications can be simply written by stating the transmissions. In certain other systems the coloring agent may undergo chemical changes as a result of changes in concentration, oxidizing-reducing conditions, or some other cause. In such systems Beer's law does not apply, and it is necessary to formulate the behavior of the individual system. Iron oxide in a glass follows this latter behavior. The present study proposes to correlate in a brief and simple manner the chemical processes encountered in the preparation of iron oxide bearing glasses with chromaticity data, specifications, and tolerances.

For this purpose the variations observed in practice were greatly exaggerated in the synthesis of experimental glasses. The location in color space of these glasses was then applied to specifications, tolerances, and control problems in the smaller color space surrounding an idealized base glass.

II. COLOR OF IRON IN GLASS

The color observed most frequently in glasses containing iron is green. The rarer colors observed in extreme base glasses are not considered here.

Bluish hues are enhanced by:

(a) low concentration of iron, (b) reducing conditions (atmosphere, reducing agents), (c) long melting time, high melting temperature, and (d) base glasses rich in silica.

Conversely, yellowish hues are enhanced by:

(a) high concentration of iron, (b) oxidizing conditions (atmosphere, oxidizing agents), (c) short melting time, low melting temperature, (d) base glasses high in alkali.

The bluish hues were observed at least as early as the 18th century and correctly associated with an increase in the reduced ion Fe^{2+} by Zsigmondy[1] in 1893. Since Fe^{2+} alone is colorless in aqueous solutions, the interaction of Fe^{2+} with Fe^{3+} in certain concentrations, rather than complete reduction to Fe^{2+}, is believed responsible for the dark blue colors of solutions, minerals[2] and glasses.[3] Charcoal and aluminum are examples of the reducing agents used in practice in glasses exhibiting bluish casts.

The bluish hues observed after long melting periods and at higher melting temperatures are caused by the increasing shift of the equilibrium $Fe^{3+} \rightleftarrows Fe^{2+}$ towards Fe^{2+} at higher temperatures.[4]

The equilibrium also shifts in the direction of Fe^{2+} with decreasing concentration of iron.[5] In

[1] R. Zsigmondy, "Glass impervious to heat rays," Dingl. Polytech. J. **287**, 17, 68, 108 (1893).
[2] G. R. MacCarthy, "Colors produced by iron in minerals and sediments," Am. J. Sci. **12**, 16 (1926).
[3] H. Heinrichs, "The estimation of ferrous oxide in heat-protective glasses," Glastech. Ber. **5**, 154 (1927/8).
[4] J. C. Hostetter and H. S. Roberts, "Ferric oxide in glass," J. Am. Cer. Soc. **4**, 927 (1921).
[5] C. Andreason-Kraft, "Physical researches on soda-silicate glasses containing FeO and Fe_2O_3," Glastech. Ber.

the range between 0 percent and 12 percent Fe_2O_3 the relative content of iron oxide as FeO varies from 36 percent to 8 percent of the total.

These considerations are easily applied to the opposite effects of short melting times, low temperature, oxidizing atmosphere, and oxidizing agents such as arsenic and antimony oxides, particularly in the presence of nitrates which favor the yellowish hues caused by a shift of the equilibrium $Fe^{3+} \rightleftarrows Fe^{2+}$ towards Fe^{3+}.

In practice the complete reduction to Fe^{2+} has not been realized[6] and crystalline silicates of Fe^{2+} melt incongruently to form molten silicates of Fe^{3+} and free iron.[4]

According to Weyl,[6] the interaction between Fe^{2+} and Fe^{3+} to promote green to blue colors presupposes the presence of Fe^{3+} in what glass technologists call the network proper that is in the approximate role of silicon. This situation may explain why glasses high in alkali promote the yellow casts associated with Fe^{3+} which then is predominantly in the role of Si^{4+}.

However this may be, variations of the color of iron towards blue are promoted in glasses of constant synthetical composition by incidental drifts of the following types: reducing gases, erroneous decrease of antimony or arsenic, higher volatilization of arsenic or combustion of charcoal, etc., and variations towards yellow by the reverse errors.

It remains to see how these changes affect the spectral transmissions.

III. THE SPECTRAL TRANSMISSION OF IRON GLASS

The spectral transmissions of iron glasses of conventional base composition are characterized by a transmission maximum in the green and a gradual drop of transmission to absorption bands in both the ultraviolet and infra-red regions (Fig. 1).

In the family of the "reduced" glasses corresponding to a higher Fe^{2+}/Fe^{3+} ratio the infra-red band moves towards shorter wave-lengths and the transmission maximum moves in the same direction while it decreases in intensity. At the same time the absorption band in the near UV moves somewhat out of the visible range. The glass appears bluer (Fig. 1—Curve *B*).

Conversely, the opposite variations appear in the spectral transmission of oxidized glasses (Fig. 1—curve *C*).

In this study the principal oxidized glasses made were produced by increased concentration, (Fig. 1—curve *C*), in which case the transmission maxima became less, but it is probable that oxidation at constant concentration would produce maximum transmissions of higher values.

IV. EXPERIMENTAL PROCEDURE

Quantitative relations regarding the influence of concentration and oxidation-reduction shifts on the chromaticity of green sunglasses were obtained by the measurement of the chromaticities of glasses in which the chemical variations were much greater than in practice.

The concentration of iron was varied by a factor of 20, while practical variations caused by

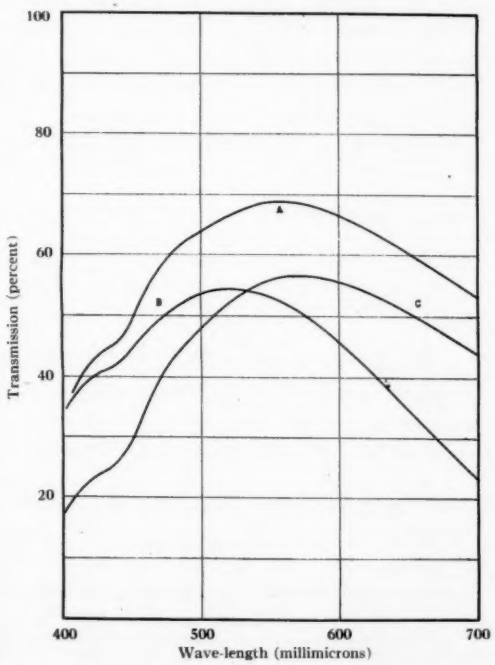

FIG. 1. Transmission curves of iron glasses: *B*—transmission curves of glass containing same Fe_2O_3 as *A*, but with added reducing agent; *C*—transmission curve of glass containing more Fe_2O_3 than *A*, hence being more oxidized.

9, 577 (1931); N. E. Densem and W. E. S. Turner, "The equilibrium between ferrous and ferric oxides in glasses," J. Soc. Glass Tech. **22**, 372 (1938).

[6] W. Weyl, "Colored glasses, II. Color of glasses produced by various coloring ions, Fe," J. Soc. Glass Tech. **27**, 265 (1943).

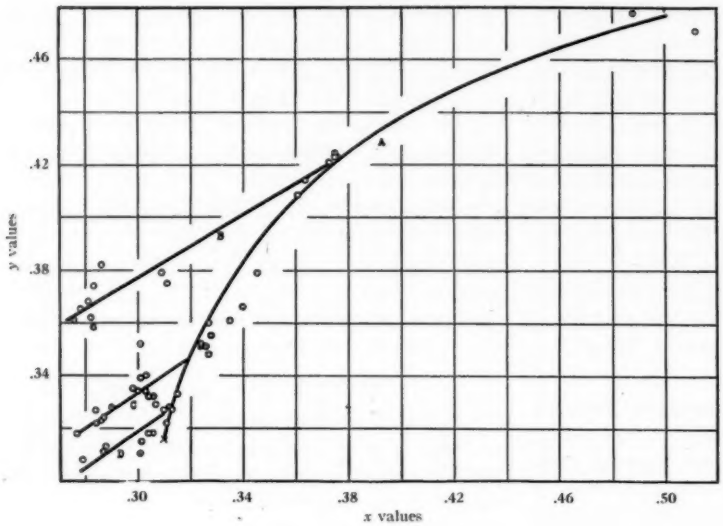

FIG. 2. Chromaticities of iron glasses (I.C.I. space): *A*—chromaticities obtained by varying concentration, without adding oxidizing or reducing agents—higher concentrations at upper right; *B-C-D*—chromaticities obtained by reducing glasses containing 1.67 wt. percent, 0.84 wt. percent and 0.42 wt. percent, respectively, of added Fe_2O_3.

batch errors, raw materials, etc., must be much smaller than 10 percent. The amount of reduction was measured indirectly by the effect on color since the effective quantity of charcoal used as a reducer remains unknown. However, the magnitude of the effect of reducing and oxidizing agents used was more than ten times greater than the variation one would allow in production.

In a base glass of 0.800 mole of SiO_2, 0.200 mole of CaO, and 0.200 mole of Na_2O, amounts of Fe_2O_3 ranging from 0.005 mole to 0.04 mole were added. For the purpose of reduction carbon up to 0.32 mole was added, while for the purpose of oxidation As_2O_3 in amounts up to 0.08 mole was added. With the exception of a few reduced melts, which were made in a gas-fired furnace in a reducing atmosphere, the melts were made in an electric furnace. The melts, approximating 150 grams of glass, were melted in silimanite body crucibles, about 1 to 2 hours being used for filling and about 3 hours for fining. The temperature during the fining was held constant at 1400°C, and then reduced to 1350°C during the last half-hour before pouring. The poured samples were all annealed with the same annealing schedules.

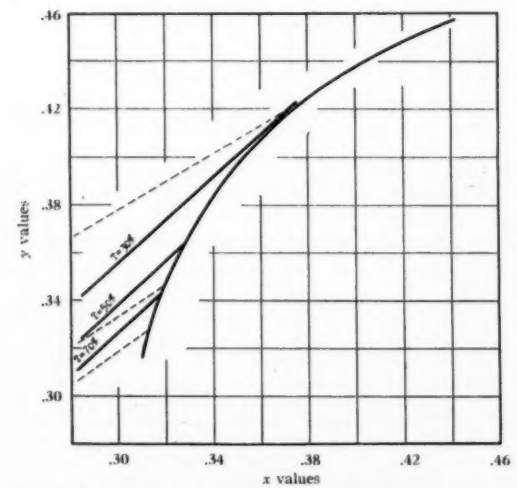

FIG. 3. Relation of chromaticity and transmissions of iron glasses: broken lines and curved line are the same as in Fig. 2; other heavy lines are iso-transmission lines.

Spectral transmission curves were made on a Hardy-General Electric recording spectrophotometer with ground and polished samples of the resultant glasses. Transmission curves were corrected to 2-mm and I.C.I. chromaticities and transmissions calculated with 10 selected ordinates.

From the standard I.C.I. chromaticities and transmissions, the Munsell value, hue, and chroma were obtained by means of the large charts available from the Munsell Foundation which were prepared according to the "Final report of the OSA subcommittee on the spacing of the Munsell colors."[7]

[7] J. Opt. Soc. Am. **33**, 385 (1943).

TABLE I.

Sample	Concentration Fe_2O_3 g Fe_2O_3 added per 100-g base glass	Oxidation conditions*	Transmission %	x	y
1987	0		90.0	0.311	0.316
1988	2.2	*N*	72.2	0.327	0.348
1990	8.9	*N*	9.0	0.488	0.478
2002	2.2	*R*	55.2	0.307	0.337
2003	4.5	*R*	29.3	0.362	0.409
2006	2.6	*N*	64.5	0.327	0.360
2007	2.9	*N*	63.1	0.335	0.361
2008	3.1	*N*	58.9	0.340	0.365
2009	3.3	*N*	53.6	0.346	0.379
2037	2.2	*R*	50.0	0.277	0.318
2059	3.6	*R*	29.0	0.310	0.364
2060	3.6	*R*	38.9	0.334	0.360
2061	3.6	*R*	31.7	0.302	0.352
2062	3.6	*R*	35.4	0.288	0.370
2063	3.6	*R*	26.0	0.283	0.374
2084	4.5	*R*	15.5	0.283	0.358
2085	4.5	*R*	13.6	0.275	0.362
2099	2.2	*O*	71.7	0.328	0.355
2100	3.3	*O*	57.7	0.354	0.386
2101	4.5	*O*	44.4	0.364	0.414
2107	3.3	*R*	12.8	0.426	0.449
2112	3.3	*R*	21.5	0.327	0.435
2113	2.2	*R*	42.7	0.283	0.392
2116	1.1	*N*	80.9	0.313	0.327
2117	1.1	*O*	81.7	0.315	0.333
2118	1.1	*R*	81.1	0.304	0.318
2119–1	1.1	*R*	71.1	0.287	0.311
2119–2	1.1	*R*	71.9	0.288	0.313
2120–1	1.1	*R*	68.4	0.279	0.308
2120–2	1.1	*R*	67.5	0.306	0.318
2264–1	0.26	*N*	89.3	0.311	0.320
2264–2	0.26	*N*	89.5	0.335	0.309
2265–1	0.52	*N*	86.6	0.311	0.321
2265–2	0.52	*N*	87.2	0.311	0.322
2266–1	1.1	*N*	81.7	0.315	0.329

TABLE I.—(*Continued*)

Sample	Concentration Fe_2O_3 g Fe_2O_3 added per 100-g base glass	Oxidation conditions	Transmission %	x	y
2266–2	1.1	*N*	81.5	0.310	0.327
2267–1	2.2	*N*	66.7	0.324	0.352
2267–2	2.2	*N*	67.6	0.324	0.351
2268–1	4.5	*N*	34.1	0.373	0.421
2268–2	4.5	*N*	33.9	0.375	0.324
2269	8.9		3.4	0.512	0.471
2270–1	0.26	*N*	91.2	0.309	0.323
2270–2	0.26	*N*	91.2	0.309	0.319
2271–1	0.52	*N*	87.2	0.312	0.322
2271–2	0.52	*N*	87.2	0.312	0.328
2272–1	1.1	*N*	60.5	0.312	0.328
2272–2	1.1	*N*	81.6	0.302	0.315
2273–1	2.2	*N*	66.3	0.326	0.351
2273–2	2.2	*N*	65.6	0.306	0.332
2274–2	4.5	*N*	31.3	0.376	0.428
2276–1	2.2	*R*	51.4	0.301	0.339
2276–2	2.2	*R*	56.4	0.300	0.334
2277–1	2.2	*R*	50.5	0.303	0.334
2277–2	2.2	*R*	50.2	0.298	0.335
2278–1	2.2	*R*	53.9	0.305	0.332
2278–2	2.2	*R*	50.7	0.303	0.340
2279–1	2.2	*R*	50.0	0.290	0.328
2279–2	2.2	*R*	53.1	0.287	0.324
2280–1	2.2	*R*	51.5	0.286	0.323
2280–2	2.2	*R*	51.1	0.287	0.324
2281–1	2.2	*R*	53.6	0.284	0.327
2281–2	2.2	*R*	53.5	0.284	0.322
2294	4.5	*R*	15.8	0.286	0.382
2295	4.5	*R*	16.8	0.311	0.375
2296	4.5	*R*	14.8	0.309	0.379
2297	4.5	*R*	15.7	0.278	0.365
2298	4.5	*R*	14.5	0.281	0.362
2299	4.5	*R*	13.9	0.281	0.368

* Note: *N* = nothing added, *R* = carbon added, *O* = As_2O_3 and NO_3 added.

Chromaticities were plotted against concentrations of iron oxide in the batch material (Fig. 2) and chromaticities were plotted against transmission (Fig. 3).

V. CHROMATICITY OF EXPERIMENTAL SERIES OF INCREASING IRON CONCENTRATION AND REDUCTION

The chromaticity variations with (a) iron concentration and (b) reduction at three iron concentration levels are shown in Table I and Fig. 2.

The increase in iron concentration resulted in the expected decrease in transmission accompanied by a shift of dominant wave-length towards the yellow. The dominant wave-length increased from $\lambda = 558$ for 0.21 wt. percent Fe_2O_3 to $\lambda = 581$ for 3.3 wt. percent Fe_2O_3, while the transmission decreased from 87 percent to 3 percent.

Reduction of any concentration of iron results in lower transmissions and a shift of dominant wave-length towards the blue. Because of the chemistry involved it is not possible to describe the quantity of reduction in terms of the reducing agent—charcoal—added. The continuity of the color shift and the maximum shift realized alone are significant. This maximum shift was for 0.42 wt. percent Fe_2O_3 from $\lambda = 565$ to $\lambda = 488$, with a

transmission shift from 82 percent to 68 percent. Similar shifts occur at other iron concentration levels.

In Fig. 3 the line of increasing iron concentration is seen to come down to lower transmission values, crossing lines of equal transmission; the lines representing reduction for different concentrations of iron approach lines of lower transmissions in the bluer greens.

The surface representing the locus of all glasses in a transmission-x-y space thus comes down in all directions from glass containing the smallest amount of iron unreduced. It also would continue to rise if lesser iron contents and stronger oxidation were considered.

VI. APPLICATION TO COLOR CONTROL

The diagrams reveal the causes of failure of a melt to meet color specifications and suggest the correction for subsequent melts. In the glass industry specifications have generally been given in terms of dominant wave-length and transmission. Consider, for example, that the specification presumes a glass at A of Fig. 4. If now a melt is obtained which is too dark and yet contains the proper amount of iron oxide, as point B of Fig. 4, it will be too blue. If the more obvious attempt should be made to correct the low transmission by omission of some iron oxide from the batch without a change in reducing conditions, the specified transmission would be reached at a dominant wave-length even farther from the original specification than the original melt. Such a correction leads along the line C of Fig. 4. The less obvious correction is a smaller amount of the reducing agent which will lead the melt along the line of constant iron oxide from B toward A. If several arbitrary attempts to correct with reduction and concentration are made, the color can drift considerably both parallel and oblique to the iso-concentration lines of Fig. 4.

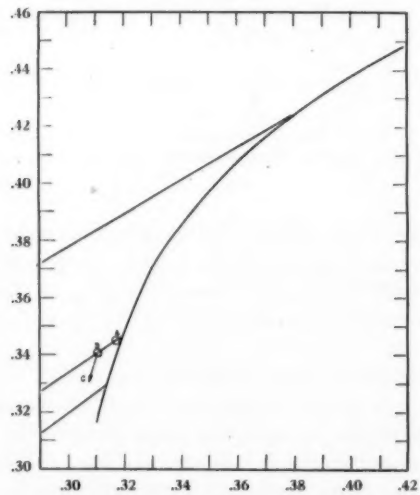

FIG. 4. Chromaticities of iron oxide glasses for various concentrations at various degrees of reduction; a melt occurring at point B will move in the direction C if correction is made by removing iron oxide from subsequent batches. It will move along the line of constant concentration toward A if the amount of reducing agent is decreased.

VII. APPLICATION TO SPECIFICATIONS AND TOLERANCES

(a) Conventional Specification

The knowledge of the real movements of "off-color" samples in color space suggests their consideration in the establishment of specifications and tolerances. Conventional specifications are generally in terms of dominant wave-length and transmission. Let us assume the specification $\lambda = 564 \pm 2$ mμ; $T = 80.8 \pm 2$ percent.

(b) Translation into Nickerson-Balinkin Isometric Space

In order to see whether conventional specifications simultaneously contain realizable glasses and exclude others equally distant from the specified color, the transformation of the specification to a space of equally perceptible distances is advisable.

Into this space may then be transferred the realm of realizable glasses and the conventional tolerances with the intention to correct the tolerance to include samples of equal color distance with those included now. Since for narrow transmission ranges chemistry limits realizable colors the general result can then be retranslated to simple specifications containing wave-length and another color parameter.

In this endeavor the limited knowledge on the perception of color differences in transparent materials imposes certain restrictions. However, valuable suggestions were derived from the tentative applications of Balinkin's[8] modification of

[8] I. H. Balinkin, "Measurement and designation of small color differences," Bull. Am. Cer. Soc. **20**, 392 (1941).

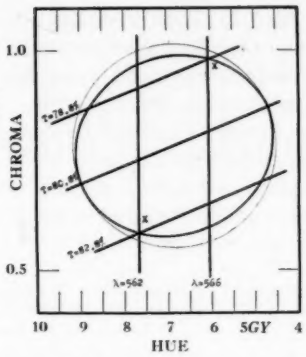

FIG. 5. A specification in Nickerson-Balinkin uniform color space; the specification of transmission and dominant wave-length has been shown in the Nickerson-Balinkin space. The sphere which has a radius of half the maximum color difference shown by the wave-length-transmission specification has been determined. The ellipse is the intersection of this sphere with the plane of the two lines $T=78.8$ percent and $T=82.8$ percent.

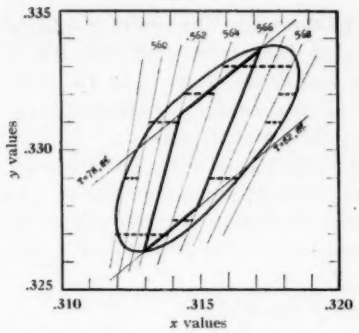

FIG. 6. Uniform color difference specification transposed to I.C.I. space; the polygon defined by the lines $T=78.8$, $\lambda=566$, $T=82.8$, and $\lambda=562$ is the original specification. The chromaticities enclosed by the curve are of acceptable glasses in terms of uniform color differences.

Nickerson's relation of small color differences in Munsell space. For the purpose of this presentation the Nickerson-Balinkin equation,

$$I=[(2\Delta H\cdot C/5)^2+(6\Delta V)^2+(\Delta C\cdot 20/\pi)^2]^{\frac{1}{2}},$$

(where the symbols: H, C, and V signify hue, chroma, and value, respectively) may be applied graphically in the simpler form:

$$I=[(2\Delta H\cdot C/5)^2+(6\Delta V)^2+(6\Delta C)^2]^{\frac{1}{2}}.$$

For the translation into this isometric Munsell type space the experimental glasses can be considered as having chroma 0.75. This equation defines a sphere in the modified Munsell color space within which the color difference of two colors is equal to or less than an amount $2I$. The experimental glasses approximate a surface, which for a limited color region is nearly a plane.

Figure 5 represents the intersection of the sphere and the plane of the iron glasses, lines of equal value (transmission), and the limits of the specification on the hue-chroma plane of Nickerson-Balinkin modified Munsell space.

According to the formula all points within the sphere have color differences from any other point in this sphere no greater than a maximum which can be computed as the diameter of the sphere. Two points (×, ×) on the specification apparently bear this maximum difference from each other. No other points in the sphere bear a greater difference, yet many are not included in the translated original specification. It would appear that all points within the sphere fulfill the intention of the specification.

Figure 6 shows the intersection of the sphere of equidistant colors from the specified mean and the plane of iron glasses retranslated into I.C.I. space.

The obvious specification to be derived from Fig. 6 is that any chromaticity which falls within the approximate ellipse is acceptable. In case such a complete variability of dominant wave-length is not desirable, the space can be broken up into several parts as shown by the lines of dominant wave-length and the broken lines. Such a specification would then read:

$\lambda=560$–562	562–564	564–566	566–568
$y\geqq 0.327$	0.327	0.3275	0.329
and $\leqq 0.331$	0.332	0.333	0.333

78.8 percent $\leqq T \leqq$ 82.8 percent.

If the original specification assumed in this work were a commercial one, it must be termed as too rigid in certain color directions and should be relaxed without greater color differences becoming evident in inspection or sales.

If, for purposes of simplicity, one insists on a specification of two dominant wave-lengths and two transmissions, this rigid specification is quite adequate. However, using different purities (as given by the y values) for different dominant wave-lengths in conformity with a Nickerson-Balinkin sphere many melts rejected under the assumed specification would be saved without

harm to the user. The use of a well established system of isometric color notation for transparent materials may thus be considered a practical or necessary prerequisite of setting specifications and tolerances.

The Nickerson-Balinkin space was used in this study because it seemed easiest to apply to the problem. However, several others have been proposed, particularly those of Judd[9] and of Adams,[10] and should be investigated by anyone attempting to set up a specification.

The glass industry could profitably use more data on small color differences in transparent materials. Present data are predominantly derived from reflecting surfaces. Such data may permit writing, *a priori*, a sensible specification which then may be simplified in the light of what can be chemically realized.

[9] D. B. Judd, "Specification of uniform color tolerances for textiles," Textile Research **9**, 253 (1939).

[10] E. Q. Adams, "X–Z planes in the 1931 I.C.I. system of colorimetry," J. Opt. Soc. Am. **32**, 168 (1942).

Book Review

The Microscope—Its Theory and Applications

J. H. WREDDEN. J. H. Churchill, Ltd., London, and Greene and Stratton, New York, 1948. Price 21 shillings or $4.25.

This is an elementary text covering the theory, construction, and use of the microscope, and containing a section dealing with specimen preparation.

The sections in which optical theory are discussed are weak. Many violations of the laws of optics occur in the figures (cf. Figs. 12, 24, 26, 32, 33, 35, 203, 204), and the text is often inaccurate. The description of spherical aberration as causing the field to look curved and out of focus at the edge is an outstanding example of this. Again, in discussing depth of focus, the physical optics involved are not brought to the reader's attention at all, and the author concludes with the remark: "Thus we see that 'depth of focus' is in reality a physiological misrepresentation of the actual condition and exists only in the imagination, anent which the accommodating power and acuteness of vision of the observer will play their part in determining its value."

In discussing the substage condenser and illumination systems the author follows the well beaten path of many older English writers in his insistence upon critical illumination. Köhler illumination is classified as a modification of critical illumination, popular for photomicrography, but not capable of producing the absolute maximum out of an optical system. The work of Max Berek, which refuted this notion, is not mentioned.

The author's sections dealing with specimen preparation, photomicrography, and the use of the microscope show his real field of excellence. His encouragement towards using unorthodox methods is commendable. The small "grinding microtome" and his use of this modified petrographic tool in the field of biology are interesting.

Two subjects of modern interest not mentioned are the electron microscope and the phase microscope.

JAMES R. BENFORD,
Bausch & Lomb Optical Company
Rochester, New York